RSC Advances

REVIEW

View Article Online
View Journal | View Issue

Cite this: *RSC Adv.*, 2021, **11**, 32158

Scholl reaction as a powerful tool for the synthesis of nanographenes: a systematic review

Rabab S. Jassas,[a] Ehsan Ullah Mughal,[*b] Amina Sadiq,[c] Reem I. Alsantali,[d] Munirah M. Al-Rooqi,[e] Nafeesa Naeem,[b] Ziad Moussa[f] and Saleh A. Ahmed[*egh]

Received 4th August 2021
Accepted 10th September 2021

DOI: 10.1039/d1ra05910f

rsc.li/rsc-advances

Nanographenes, or extended polycyclic aromatic hydrocarbons, have been attracting increasing attention owing to their widespread applications in organic electronics. However, the atomically precise fabrication of nanographenes has thus far been achieved only through synthetic organic chemistry. Polycyclic aromatic hydrocarbons (PAHs) are popular research subjects due to their high stability, rigid planar structure, and characteristic optical spectra. The recent discovery of graphene, which can be regarded as giant PAH, has further stimulated research interest in this area. Chemists working with nanographene and heterocyclic analogs thereof have chosen it as their preferred tool for the assembly of large and complex architectures. The Scholl reaction has maintained significant relevance in contemporary organic synthesis with many advances in recent years and now ranks among the most useful C–C bond-forming processes for the generation of the π-conjugated frameworks of nanographene or their heterocyclic analogs. A broad range of oxidants and Lewis acids have found use in Scholl-type processes, including $Cu(OTf)_2/AlCl_3$, $FeCl_3$, $MoCl_5$, $PIFA/BF_3–Et_2O$, and DDQ, in combination with Brønsted or Lewis acids, and the surface-mediated reaction has found especially wide applications in PAH synthesis.

[a]*Department of Chemistry, Jamoum University College, Umm Al-Qura University, 21955 Makkah, Saudi Arabia*

[b]*Department of Chemistry, University of Gujrat, Gujrat-50700, Pakistan. E-mail: ehsan.ullah@uog.edu.pk*

[c]*Department of Chemistry, Govt. College Women University, Sialkot-51300, Pakistan*

[d]*Department of Pharmaceutical Chemistry, College of Pharmacy, Taif University, P.O. Box 11099, Taif 21944, Saudi Arabia*

[e]*Department of Chemistry, Faculty of Applied Science, Umm Al-Qura University, 21955 Makkah, Saudi Arabia. E-mail: saahmed@uqu.edu.sa*

[f]*Department of Chemistry, College of Science, United Arab Emirates University, P.O. Box 15551, Al Ain, United Arab Emirates*

[g]*Research Laboratories Unit, Faculty of Applied Science, Umm Al-Qura University, 21955 Makkah, Saudi Arabia*

[h]*Chemistry Department, Faculty of Science, Assiut University, 71516 Assiut, Egypt*

Ehsan Ullah Mughal was born in Wazirabad, Pakistan, in 1978 and obtained his Master's degree from Quaid-e-Azam University, Islamabad, Pakistan, in organic chemistry. He obtained his PhD in 2013 from Bielefeld University, Germany, under the supervision of Prof. Dr Dietmar Kuck. For postdoctoral studies, he joined the group of Prof. Dr Xinliang Feng, Max Planck Institute for Polymer Research, Mainz, Germany. In 2015, he started his independent research group at the Department of Chemistry, University of Gujrat, Gujrat, Pakistan. His current research interests focus on the design and synthesis of bioactive heterocycles, synthetic flavonoids, transition metals-based terpyridine complexes, and their fabrication in DSSCs and organic functional materials for applications in organic electronics.

Saleh A. Ahmed was born in Assiut, Egypt in 1968 where is undertook undergraduate and postgraduate studies. He received his Bachelor and MSc from Assiut University, Egypt and PhD in photochemistry (photochromism) under the supervision of Prof. Heinz Dürr in Saarland University, Saarbrücken, Germany. He worked as postdoctoral fellow, senior researcher and visiting professor in France (CNRS fellow), Japan (JSPS fellow), Germany (AvH, DFG and DAAD fellows), Italy (TEMPUS fellow) and USA (Arab fund fellow). His current research interests include synthesis and photophysical properties of novel organic compounds, electronic devices and solar energy conversion, fluorophores with unique applications.

Undoubtedly, the utility of the Scholl reaction is supreme in the construction of nanographene and their heterocyclic analogues. The detailed analysis of the progress achieved in this field reveals that many groups have contributed by pushing the boundary of structural possibilities, expanding into surface-assisted cyclodehydrogenation and developing new reagents. In this review, we highlight and discuss the recent modifications in the Scholl reaction for nanographene synthesis using numerous oxidant systems. In addition, the merits or demerits of each oxidative reagent is described herein.

1. Introduction to nanographenes

Over the past decade, polycyclic aromatic hydrocarbons (PAHs) and graphene nanoribbons (GNRs) have gained increasing attention owing to their unique applications in various fields of materials chemistry. As such, they have been used in polymer films,[1] sensors,[2] electronic devices,[3] and photovoltaic studies, and have shown interesting optical and biological properties because of their microporous nature.[4–6] The construction of the aryl–aryl bond in the π-extended PAHs and GNRs is undoubtedly the most promising approach to further elaborate the structure of such molecules and comprises a novel and exceptional research endeavor to pursue. This approach has brought about a revolution in materials chemistry as it has rebuilt the typical synthetic routes as well as introduced new synthetic pathways for large organic compounds.

Graphene, an allotrope of carbon, can be described as a single layer scaffold of interconnected hexagonal benzene rings having sp^2-hybridized carbons and are arranged in the form of a honeycomb pattern. It is a 2D material[7] that constitutes the individual layers of graphite. In fact, nanographenes are limited to nanoscale segments of graphene, while PAHs are the distinct patterns of graphene. The basic structure of nanographene is similar to that of PAHs but they differ in properties from PAHs.[8] In recent years, nanographenes have attracted great attention in organic chemistry due to their high electron mobility and high elasticity.[9] Notably, the Scholl reaction is the most used synthetic methodology for the synthesis of PAHs and GNRs and has been repeatedly used over time ever since it was introduced up to the present day. The most recent form of nanographenes is graphene nanoribbons (GNRs), which is prepared through surface chemistry mediated gold-catalyzed Scholl reaction.

2. Scholl reaction

In 1910, Roland Scholl, a Swiss chemist, found that aromatic moieties can undergo carbon–carbon bond formation in the presence of strong Lewis acids, such as neat aluminum chloride, at elevated temperatures.[10,11] Expanded polycyclic arenes became accessible under such harsh conditions.[12–14] Firstly, Scholl proposed the chemical syntheses of PAHs using the above-mentioned conditions. Later, this oxidative cyclization transformation was named as the "Scholl reaction".[15] In principle, it is an acid-catalyzed oxidative condensation of aryl groups that results in new C–C covalent bonds. The reaction has been extensively utilized for a intramolecular oxidative cyclodehydrogenation of various polybenzenoid hydrocarbons. An intermolecular reaction is a reaction between two or more reactant molecules. In some reactions, two pathways are possible: one *via* an intramolecular reaction (reacting groups both within the same molecule) and one *via* an intermolecular reaction (reacting groups in different molecules). Generally, intramolecular reactions are entropically favored. A representative example is depicted in Fig. 1a (intramolecular oxidative aromatic coupling) and 1b (intermolecular oxidative aromatic coupling).

In this review, we will focus on key achievements in the field of intermolecular and intramolecular oxidative aromatic coupling w.r.t various oxidants that have appeared in the literature.

3. Mechanistic pathways of the Scholl reaction

Oxidative aromatic coupling and the Scholl reaction, both discovered more than 100 years ago,[16–19] have not lost their appeal to organic chemists in the last decade despite the appearance of many modern C–H activation protocols and C–C bond-forming reactions. These reactions are often the methods of choice for the synthesis of large π-extended scaffolds as well as smaller benzenoid or heteroaromatic compounds possessing biaryl linkages. Recent findings on the skeletal rearrangement of polycyclic aromatics under oxidative and acidic conditions are envisioned to help the development of these Scholl reactions into a more useful and versatile method for synthesizing polycyclic aromatics based on rational design. Undoubtedly, the utility of Scholl reaction is the greatest in the construction of nanographenes[20a–e] and their heterocyclic analogues.[21] Indeed, in some cases, more than 100 C–C bonds can be formed in one synthetic operation from suitable precursors, furnishing truly amazing PAHs. There is no other reaction known in the literature capable of duplicating this result for a discrete molecule (excluding not a polymer). However, despite the ubiquitous

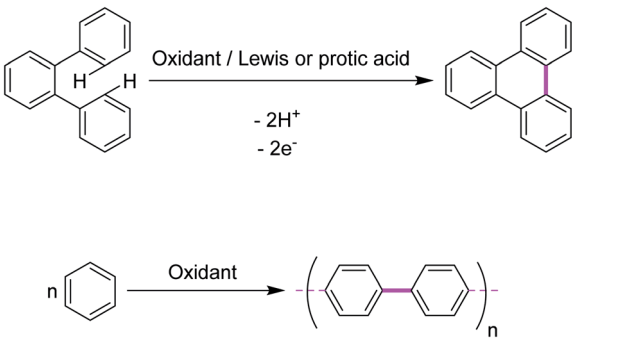

Fig. 1 (a) C–C bond formation between the two aryl units (intramolecular) through the Scholl reaction. (b) C–C bond formation between the two different aryl units (intermolecular) through the Scholl reaction.

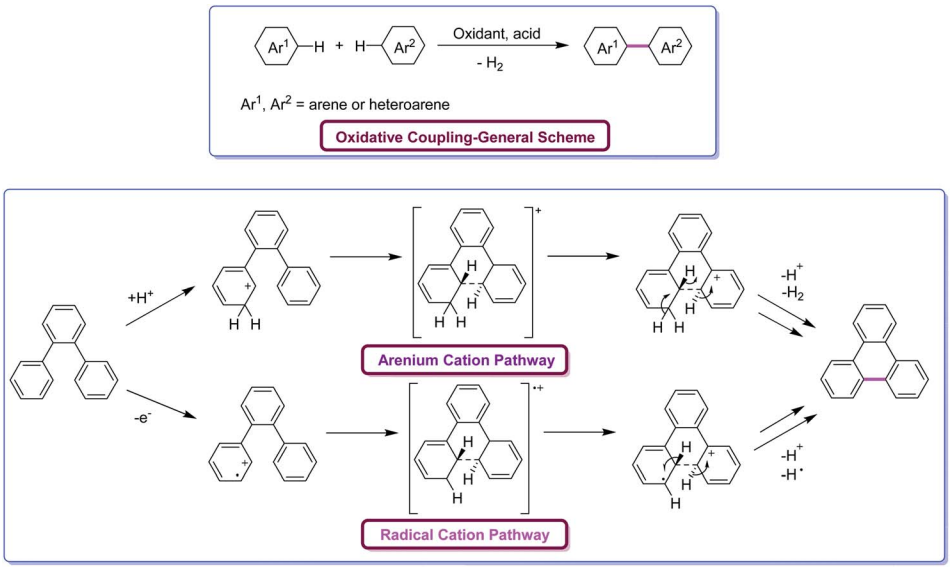

Fig. 2 Oxidative coupling of arenes through the two alternative possible pathways under Scholl reaction conditions.[24]

applications of the Scholl reaction, the ability to foresee when and how this reaction will occur is still lacking. Indeed, the complexity of the dehydrogenative coupling reaction is strongly related to the fact that it works with stunning efficiency in some cases but fails in others.

Mechanistically, the Scholl reaction mostly proceeds through electrophilic aromatic substitution process (Fig. 2). The reaction is facilitated by the presence of electronically activating substituents on the aromatic rings.[22] At the beginning, the mechanism of Scholl reaction was not entirely recognized. Later, Kenner and Baddeley[23a] proposed two possible mechanisms for this reaction. Kenner, along with Baddeley, firstly reported a radical cation-based mechanism while, later on, Baddeley[23b] suggested that the reaction proceeds *via* a mechanism involving the arenium cation as the intermediate. In both the cases, H_2 is eliminated as a result of cyclodehydrogenation driven by the oxidant and the catalyst, and a new C–C bond is formed, giving rise to new aryl rings. The exact mechanism of the Scholl reaction is not definite and still controversial. The chosen mechanistic pathway depends upon various factors such as the reagent used, electronic and steric effects, as well as the substitution positions, among others. The dehydrogenation of aromatic nuclei is carried out in the presence of a Lewis acid. As a result, a condensed ring system is formed.[24]

Most recently, these controversial mechanisms of the Scholl reaction have been described by King[25] and Rathore[26] in their research articles. King and co-workers supported the arenium ion mechanism by reporting the synthetic pathway for hexabenzocoronene synthesis from hexaphenylbenzene *via* the Scholl reaction.[27] In particular, a highly efficient synthesis of hexa-*peri*-hexabenzocoronene (HBC) **2** was established through the oxidative intramolecular cyclodehydrogenation of hexaphenylbenzene **1** (Scheme 1); a wide variety of π-extended PAHs were obtained using tailor-made oligophenylenes as the precursors.[28a] Such PAHs, consisting of sp^2 carbon frameworks extending over 1 nm, can be regarded as the smallest possible nanographenes or graphene molecules.[28b,c] In the last decade, extended PAHs have thus attracted renewed synthetic interest and more interdisciplinary attention as structurally well-defined graphene molecules with great potential for future applications in nanoelectronics, optoelectronics, and spintronics.[28d–i]

Rathore and co-workers supported the radical cation mechanism by reporting the synthetic pathways for the synthesis of

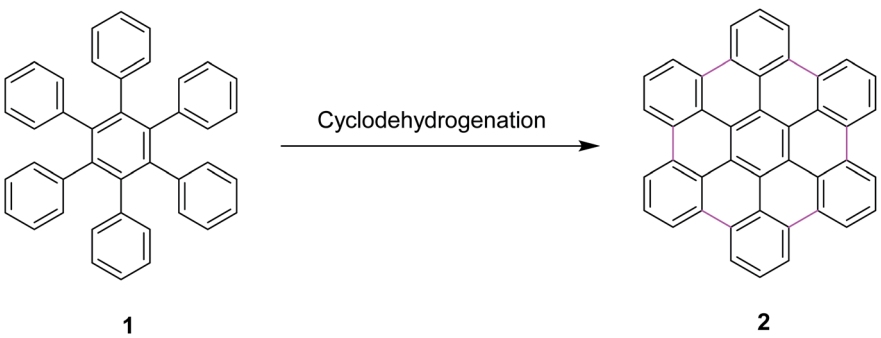

Scheme 1 Synthesis of hexa-*peri*-hexabenzocoronene through intramolecular oxidative cyclodehydrogenation.[28a]

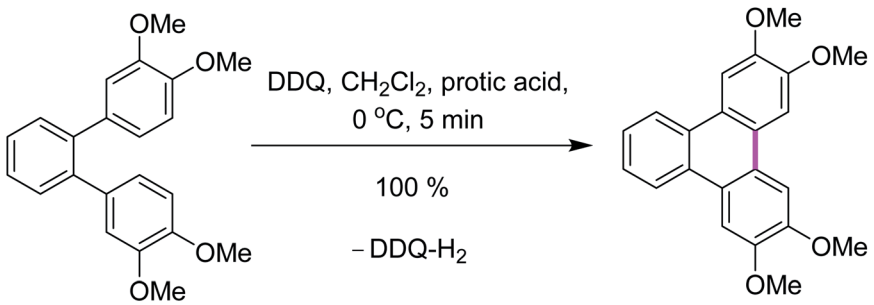

3 4

Scheme 2 Synthesis of tetramethoxytriphenylene using a combination of DDQ and protic acid.[29]

tetramethoxytriphenylenes **4** from *o*-terphenyl **3** by cyclodehydrogenation under either strong or mild conditions *via* the Scholl reaction using various oxidants (Scheme 2).[29] It is noteworthy that the Scholl reaction with the DDQ–acid oxidation system is equally effective with substrates undergoing both *intramolecular* and *intermolecular* aryl–aryl C–C bond formations. The efficient preparation of a variety of PAHs including tetramethoxytriphenylenes, ease of isolation of the synthesized products, and the ready regeneration of DDQ from easily recovered reduced DDQ–H_2 underscores the advantages of DDQ/H^+ for the Scholl reaction.[29]

4. Reagent modifications in the Scholl reaction

Over the last century, numerous reagent-mediated coupling reactions have been developed employing oxidizers such as iron(III) chloride, molybdenum(V) chloride, phenyliodobis(trifluoroacetate) (PIFA), and 2,3-dichloro-5,6-dicyano benzoquinone (DDQ) in combination with strong acids (*e.g.*, $MeSO_3H$).[30a–c] These elite reagents are highly regarded in reagent-mediated dehydrogenative coupling reactions since they replace highly toxic reagents based on thallium, mercury, or lead. The Scholl reaction can be accomplished using a variety of oxidants such as $FeCl_3$, $CuCl_2$ or $Cu(OTf)_2$ and $AlCl_3$, $Tl(O_2CCF_3)_3$ in CF_3CO_2H or BF_3–OEt_2, $Pb(OAc)_4/BF_3$–Et_2O in MeCN, triethyloxonium hexachloroantimonate ($Et_3O^+SbCl_6^-$), $SbCl_5$, and $MoCl_5$.

In this review, we have focused on the development of different reagent systems used in nanographene synthesis *via* the Scholl reaction. Firstly, we will provide a brief historical perspective to shed light on the Scholl reaction in its earliest phases and subsequent gradual evolution using these reagent systems. Then, we will comprehensively discuss the most advanced developments in nanographene synthesis to date. We will emphasize on the synthetic routes, improvements, merits, and demerits of some prominent reagent systems such as Cu salts, $FeCl_3$, DDQ, PIFA, molybdenum pentachloride ($MoCl_5$), palladium complexes, and gold along with various solvent systems. We will also concisely discuss some miscellaneous reagent systems such as PPA, HTIB, TTFA, VOF_3, CoF_3, $SbCl_6$, $AgSO_4$, and MnO_2 used for the Scholl reaction.

5. Synthetic strategies toward nanographenes by reagent-mediated Scholl reaction

5.1. $AlCl_3$ and Cu(II)-mediated Scholl reaction

Among numerous oxidants typically used for the construction of the new C–C bond in an oxidative manner, the most frequently applied is aluminum(III) chloride. The Scholl reaction was first mentioned as early as 1910, when Scholl and Mansfeld reported a clean conversion of quinone **5** to the π-extended quinone **6** by treatment with an excess of pure anhydrous $AlCl_3$ for 45 min at 140–145 °C, although no yield was given (Scheme 3).[31]

In order to further explore the reaction and optimize the yield, Scholl and co-workers performed multiple synthetic reactions. In 1910, Scholl proposed a potential mechanism for perylene **8** synthesis from naphthalene **7** using $AlCl_3$ at a high temperature of 180 °C; however, because of some decomposition, the yield of **8** was also poor. In 1913, the same reaction was repeated under modified conditions using 1,1′-binaphthalene **9** as the substrate. In this case, perylene **8** was synthesized from **9** using the same mechanism of the Scholl reaction at a lower temperature of 140 °C and this time, they obtained a better yield (Scheme 4).[32]

In 1941, Wiener and Mieg used the $AlCl_3/SO_2$ complex to promote C–C bond formation between two aryl groups.[33] Similarly, many other oxidants were used in combination with $AlCl_3$ but none of them provided the required targets with improved

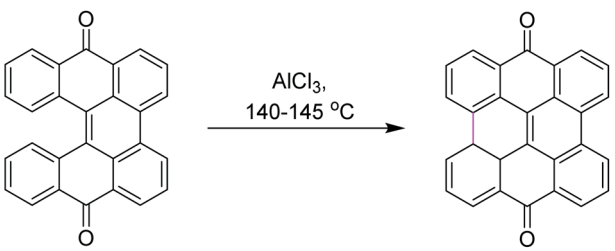

5 6

Scheme 3 Synthesis of quinones *via* the Scholl reaction.

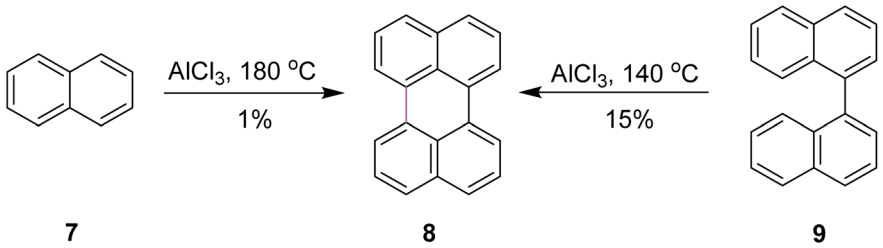

Scheme 4 Synthesis of perylene from naphthalene and binaphthalene.

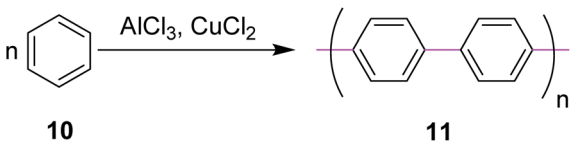

Scheme 5 Polyphenyl synthesis *via* the Scholl reaction.

yields. Hence, all these protocols were ruled out. In 1962, Kovacic and Kyriakis synthesized polyphenylene **11** from benzene *via* oxidative polymerization under $AlCl_3/CuCl_2$ conditions (Scheme 5).[34] They reported that monomer **10** can be polymerized smoothly in a catalyst–cocatalyst-oxidizing system to a solid product possessing the properties of *p*-polyphenylene. For example, in the presence of $AlCl_3$ (0.5 moles), water (1 mL), and $CuCl_2$ (0.5 moles), benzene (1 mole) was converted under mild conditions (36–37 °C) over a duration of 30 min to produce a brown solid of the target **11**.

As a further improvement, Vollmann proposed a better synthetic strategy than the previous methodologies, wherein the C–C bonds were constructed in the presence of an equimolar mixture of $AlCl_3$ and NaCl at a low vapor pressure (Scheme 6).[35] Since the early 1920s, this method has been applied in the industrial synthesis of many anthraquinone-derived dyes. This work was used until the 1970s.

Scholl and co-workers published numerous other examples following the preceding protocol. Until then, the organic substrate was baked along with $AlCl_3$. However, in 1971, they developed a new synthetic method for the dehydrogenative coupling of aromatic compounds by treatment with anhydrous aluminum chloride and co-catalysts. Mechanistically, the transformation bore close resemblance and was mainly based on the Friedel–Crafts reaction. In this method, tin(IV) chloride ($SnCl_4$) was used along with $AlCl_3$ to synthesize naphthotetraphene **17** from phenyltetraphene **16** in good yields (Scheme 7).[36]

In 1971, Wick utilized the $AlCl_3$–pyridine complex for the synthesis of compound **19** and compared it with the $AlCl_3$/NaCl complex system. He reported that the former complex system is superior to the latter (Scheme 8).[37] This new process also triggered the synthetic developments of aromatic hydrocarbon extension.

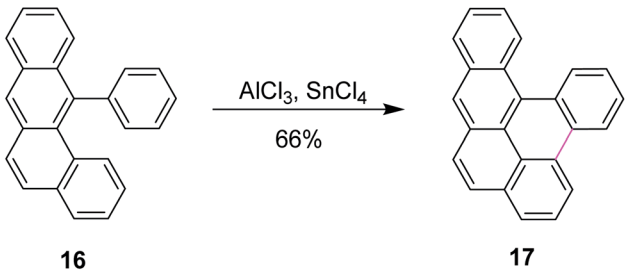

Scheme 7 Naphthotetraphene synthesis.

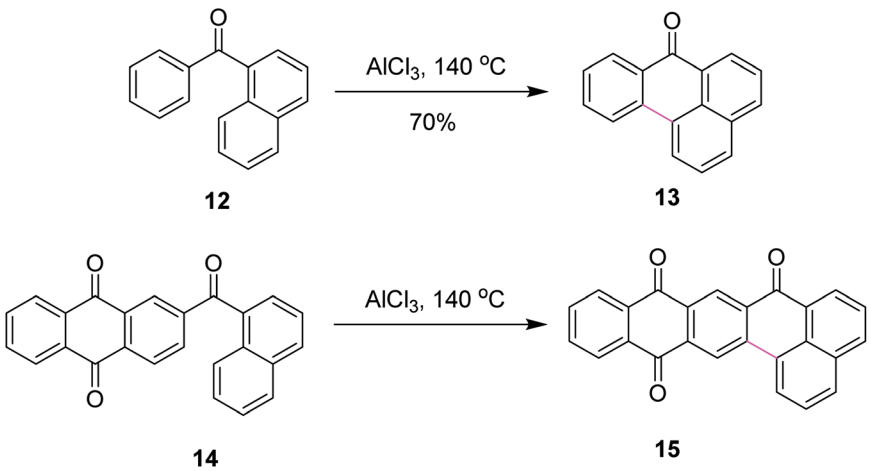

Scheme 6 C–C bond formation in anthraquinone-derived dyes.

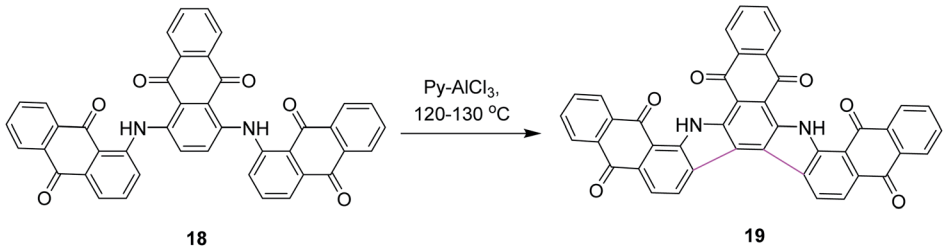

Scheme 8 Phthaloyl carbazole synthesis.

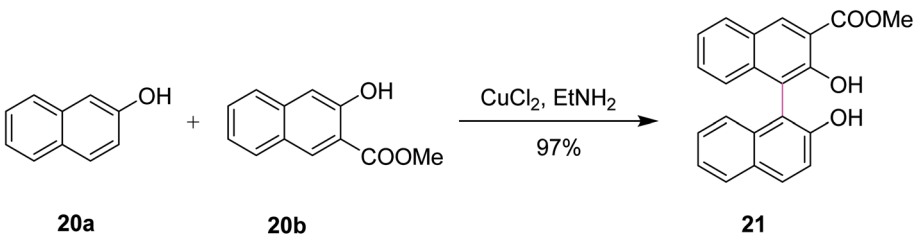

Scheme 9 Oxidative cross coupling of 2-naphthols.

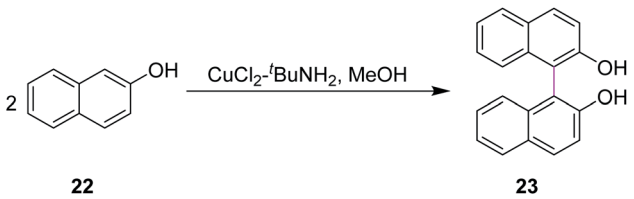

Scheme 10 Synthesis of enantiomerically pure binaphthol derivatives.

In 1990, Zavada and co-workers developed a method for the cross coupling of 2-naphthols **20a** and **20b** using an oxidant to selectively construct C–C bonds in binaphthyls such as **21**. The reaction was carried out in the presence of a Cu(II)–amine complex that provided 97% selective product depending on the substitutions, as depicted in Scheme 9. The reaction evidently proceeds through the radical-cation mechanism. The oxidative coupling of substituted 2-naphthols is now a well-established method for the preparation of l,l′-binaphthalene-2,2′-diols. Various oxidants such as $FeC1_3$, $K_3Fe(CN)_6$, and Cu(II)–amine complexes have been used so far to promote the coupling reaction. The authors described that Cu(II) mediated-coupling was more efficient as compared to Fe(III) and Mn(III)-mediated coupling. The work of Zavada also explored the cross-coupling reactions as the means to obtain unsymmetrical binaphthols selectively from differently substituted 2-naphthols instead of classical oxidative dimerization, which yielded symmetrical binaphthols.[38]

In 1992, Smrcina and co-workers reported a simple and effective method for the construction of symmetrically-substituted binaphthyl **23**. They developed a process for the mediated oxidative cross-coupling of 2-naphthol units such as **22**. They used $CuCl_2$/*t*-$BuNH_2$ in methanol to generate C–C bonds between two aryl rings, providing enantiomerically pure products, as presented in Scheme 10. 2,2′-Dihydroxy-1,1′-binaphthyl **23** is an established and highly potent chiral ligand, both enantiomers of which have been utilized in a variety of synthetic reactions to induce chirality. In most cases, the chemoselectivity was good and the cross-coupled products were obtained in good to excellent yields.[39]

Similarly, Kovosky and co-workers (1994) worked on the selective cross coupling of 2-naphthol **24a** and 2-naphthylamine **24b** to yield binaphthyl **25** (Scheme 11). This reaction was carried out in the presence of the highly efficient $CuCl_2$/*t*-$BuNH_2$ system that provided the product with good yield and exclusive chemoselectivity. They performed these cross-coupling reactions with a chiral complex of Cu(II), which resulted in enantioenriched/enantiomerically enriched binaphthyls.[40]

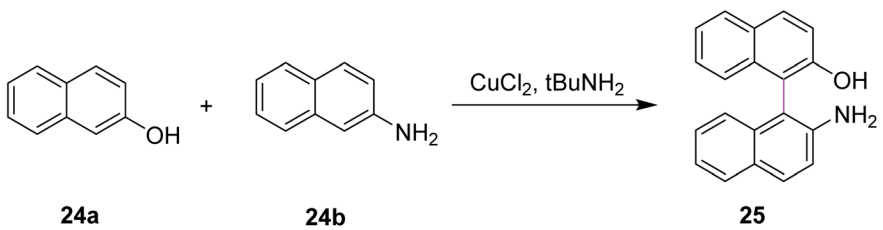

Scheme 11 Selective cross coupling induced by $CuCl_2$.

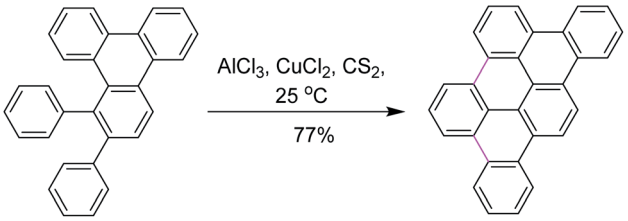

Scheme 12 Planar polycyclic aromatic hydrocarbon synthesis.[41]

In 1995, Müllen and co-workers introduced new conditions for the oxidative condensation of precursor **26** utilizing $AlCl_3$/$CuCl_2$/CS_2 at ambient temperature (Scheme 12).[41] This method is quite feasible for the synthesis of a large number of PAHs. The presented cycloaddition–cyclodehydrogenation sequence offers a new and surprisingly simple approach to obtain planar aromatic hydrocarbons. However, the $CuCl_2$/$AlCl_3$ oxidizing system is associated with certain limitations. For example, this reagent leads to the increased formation of chlorinated and partially dehydrogenated side products in addition to the desired products. On the other hand, the use of $FeCl_3$ only yielded partially-cyclized products.

In 2002, the same group reported an improved oxidizing system, in which they replaced $CuCl_2$ by copper(II) trifluoromethanesulfonate salt and thus developed a synthetic method to prepare the largest flat PAHs so far utilizing $AlCl_3$/$Cu(SO_3CF_3)_2$/CS_2 (ref. 42) oxidant system, concluding that the successful synthesis of PAH **29** from oligophenylene **28** represents an important step toward improved graphite model structures. It shows, on the one hand, the efficiency, but on the other hand, also the limits of the synthetic concept employed regarding the planarization of large soluble oligophenylene precursors by the multiple cyclodehydrogenation to PAHs. Due to the extremely low solubility of **29** in all solvents, the successful cyclodehydrogenation could not be proven by conventional spectroscopic methods. Nevertheless, the formation of such planar nanographene was confirmed by mass measurement using MALDI-ToF mass spectrometry. This protocol prompted the scientific community to design and synthesize the large π-extended nanographenes with tailored dimensions and electronic properties (Scheme 13).

In 2006, Müllen and co-workers developed a new synthetic route for oxidative cyclodehydrogenation to construct terylene **31**, a higher homolog of perylene, over multiple steps. They utilized $AlCl_3$ in chlorobenzene at 80 °C as a mild oxidant to develop the new hexagonal ring in compound **30** (Scheme 14). Here, $AlCl_3$ is in fact a non-oxidizing Lewis acid. This implies oxidation by air at high temperatures. Iron(III) chloride ($FeCl_3$) was also used as the oxidant and provided less chlorinated derivatives as the by-products, although it resulted in a pentagonal ring instead of the hexagonal ring in compound **30**.[43]

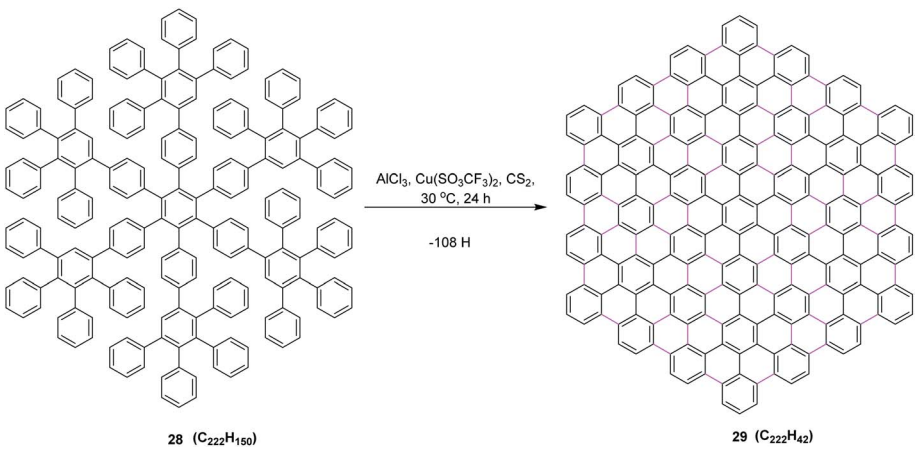

Scheme 13 Oxidative cyclodehydrogenation of oligophenylene to the PAH.[42]

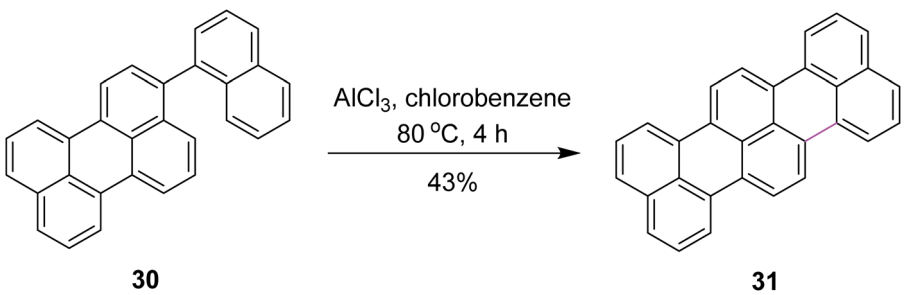

Scheme 14 Terylene synthesis *via* $AlCl_3$.

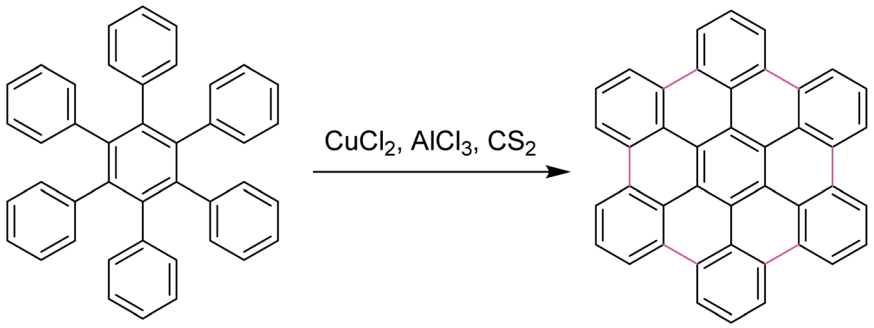

Scheme 15 HBC synthesis by the Scholl reaction.[44]

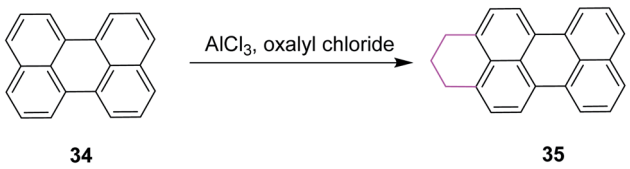

Scheme 16 Arene–arene coupling by the Scholl reaction.[45]

In 2006, King and co-workers proposed a facile pathway for intramolecular Scholl reaction for reactive phenylbenzenes using $CuCl_2/AlCl_3/CS_2$ as an efficient catalytic system. They also disclosed a possible mechanism using different oxidants such as PIFA, $MoCl_5$, $FeCl_3$, and $CuCl_2$. The $CuCl_2/AlCl_3/CS_2$ complex for the synthesis of hexabenzocoronenes (HBC) **33** is shown in Scheme 15. According to thermodynamic assumptions, PIFA and $MoCl_5$ proved to be more efficient than $CuCl_2$ for the Scholl cyclization of phenylbenzenes. Moreover, $CuCl_2$ was not soluble in CS_2, which indicated that oxidation occurred on the $CuCl_2$ surface.[44]

In 2010, Wu and Jiao introduced a synthetic methodology for the preparation of polycyclic aromatic near-infrared (NIR) dyes using Scholl reaction as the key step. They implemented oxidative coupling for C–C bond formation in annulated perylene **34** to construct a partially saturated hexagonal ring in perylene **35** by treating the substrate with oxalyl chloride and $AlCl_3$ (Scheme 16). The resulting product was passed through multistep reactions and finally converted into a bisquaterrylene dye.[45]

In 2011, Groth and co-workers introduced a new bottom-up strategy for the synthesis of large PAHs by the Scholl reaction. The $AlCl_3$/NaCl complex was used for the cyclodehydrogenation of perylene **36** to construct giant quaterrylenes **37** (Scheme 17). This reagent system was the most common method used at that time for the Scholl reaction due to its easy availability and low cost. The main factor that controlled the oligomerization trend was temperature. The process of oligomerization was more controllable at a high temperature.[46]

Later on, encouraged by a previous work reported on the Scholl reaction, Kuck and Mughal (2012) introduced a method to merge tribenzotriquinacene (TBTQ) with HBC, generating a cycloheptatriene ring by the Scholl-type reaction (Scheme 18). They constructed the bowl-shaped nanographene **42** utilizing $AlCl_3/Cu(OTf)_2/CS_2$ as an effective oxidant system for the intramolecular cyclodehydrogenation step. This oxidant system proved more efficient than $FeCl_3$ as it provided the complete condensation product and eliminated all other side reactions. The cycloheptatriene ring was constructed by the incorporation of the 1,2-benzene unit in the rigid diphenylmethane units of the TBTQ-scaffold.[47a] This reaction was repeated several times under different conditions. However, each attempt gave a mixture of partially reacted products and the starting material. Unfortunately, the complete removal of 48 hydrogen atoms to give the target compound **40** turned out to be unsuccessful and still presents a great challenge. Increasing the reaction time and amount of the reagents did not alter the results; rather, complex mixtures of the products were obtained. The concept to use TBTQ derivatives that bear three oligophenylphenyl **41** residues in the C_3-symmetrical orientation at the outer periphery (C-2, C-6, and C-10) of the TBTQ core appeared promising despite the limitations encountered in this work. In conclusion, for the first time, one of the three 3D-bays of the TBTQ scaffold was bridged

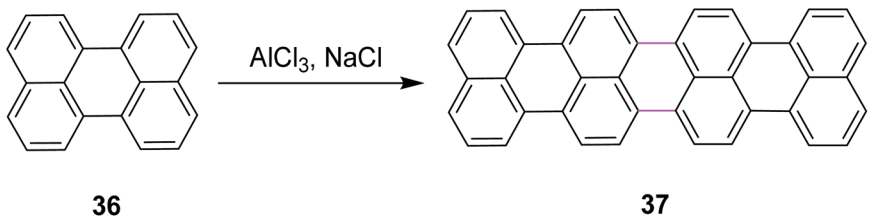

Scheme 17 Synthesis of quaterrylenes *via* the Scholl reaction.[46]

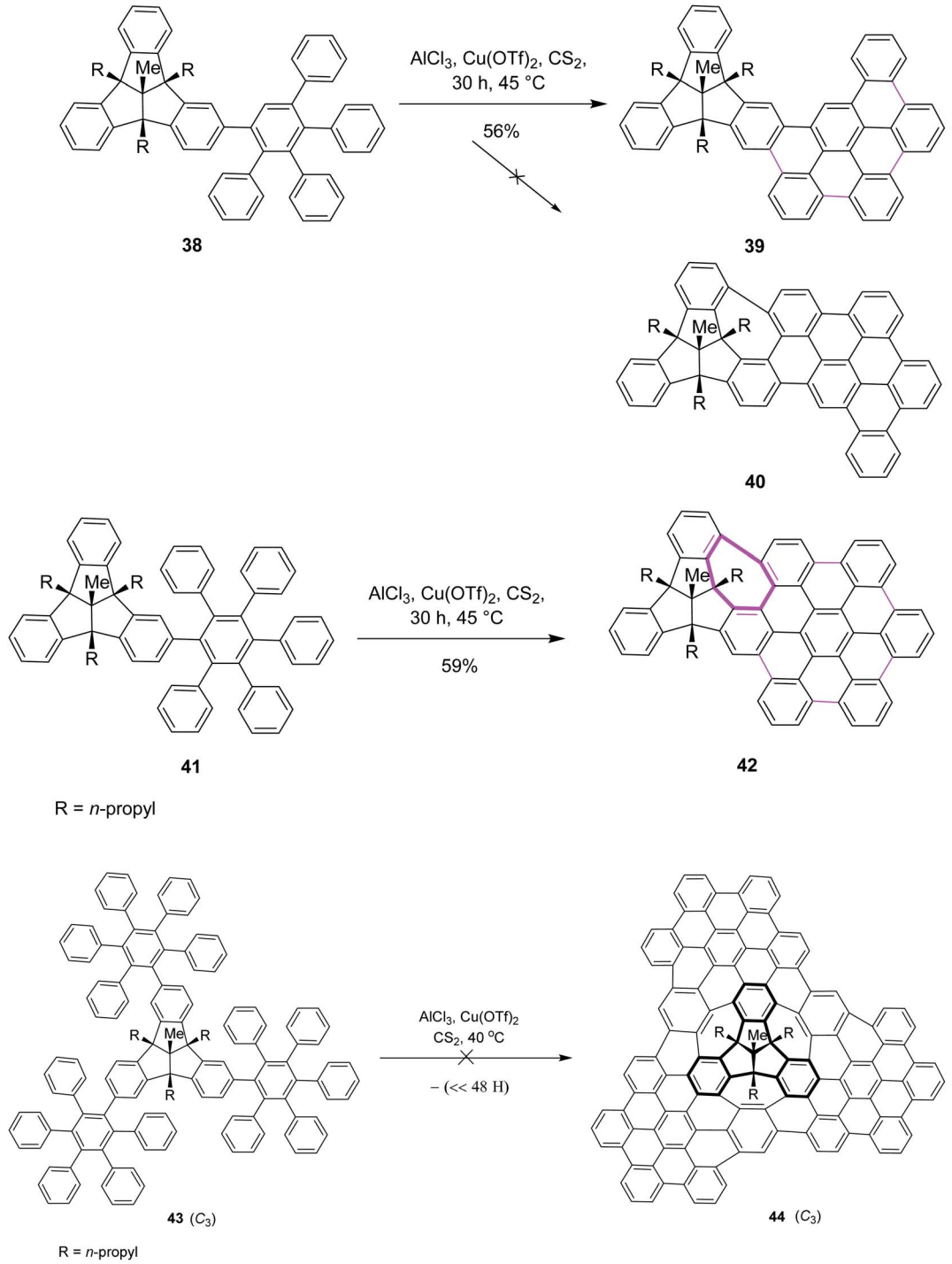

Scheme 18 Synthesis of oligophenylphenyl–TBTQ derivatives by the Scholl reaction leading to the condensed and threefold TBTQ hydrocarbons.

efficiently through a 1,2-benzeno unit, resulting in the generation of a seven-membered ring bearing PAH **42** within the quasi-planar fused carbon skeletons of TBTQ and hexa-*peri*-hexabenzocoronene. Encouraged by the abovementioned results, we attempted the threefold extension of compound **43** in order to access the bowl-shaped graphene-like structure **44** (Scheme 18). This reaction was repeated several times under different conditions. However, each attempt gave a mixture of partially reacted products and the starting material, as revealed by MALDI mass spectrometry. Increasing the reaction time and amount of the reagents did not alter the results; rather, complex mixtures of products were obtained. Probably the poor solubility of the intermediates or particular crowdedness of the starting material are major obstacles in the complete

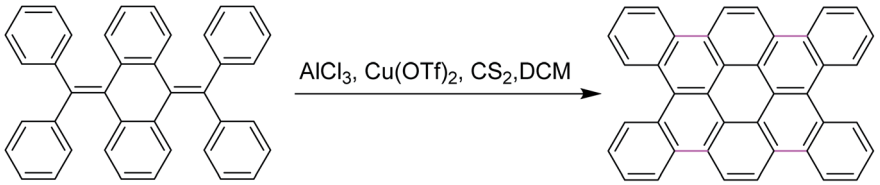

45 46

Scheme 19 Tetrabenzocronene synthesis by the Scholl reaction.[48]

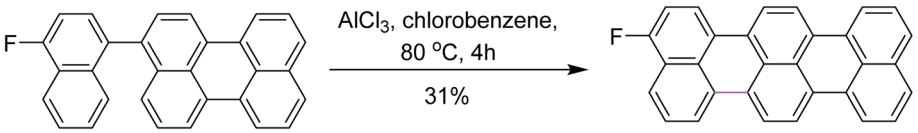

47 48

Scheme 20 $AlCl_3$-mediated cyclodehydrogenation for C–C bond formation.

intramolecular oxidative coupling, requiring the removal of 48 hydrogen atoms of precursor **43** to form target compound **44** (Scheme 18).[47b] Therefore, the synthesis of the bowl-shaped graphene-like structure **44** by adapting the above-discussed synthetic plan remains an open challenge to date.

In 2012, Tao and co-workers developed a new protocol for the construction of contorted tetrabenzocoronene **46** by the Scholl reaction. They utilized the $AlCl_3/Cu(OTf)_2/CS_2$ complex for the cyclodehydrogenation of bis-olefin **45** to construct the C–C bonds of tetrabenzocoronene (Scheme 19). They also used $FeCl_3$ as the oxidant for the same reaction but it gave a mixture of the desired product **46** and the chlorinated by-products. Therefore, $Cu(OTf)_2$ proved to be a comparatively better oxidant.[48]

In 2015, Gourdon and co-workers proposed a novel pathway for the formation of 3-fluoroterrylene **48** from perylene **47** (Scheme 20). The resulting product was recognized as a molecular nanoprobe for single-electron optical sensing. The reaction pathway involved the $AlCl_3$-mediated Scholl reaction to form a C–C bond between the two functionalized aryl vertices. The authors used other reagents along with $AlCl_3$ and presented a selectivity comparison using ^{19}F NMR spectroscopic characterization, where $AlCl_3$ proved to be more efficient in constructing the hexagonal ring and DDQ promoted the more efficient construction of the pentagonal ring.[49]

In 2016, Agranat and co-workers described the regioselectivity in the Scholl reaction of 1-benzoylpyrene **49**. The reaction was carried out under the Scholl reaction conditions, *i.e.*, $AlCl_3$/NaCl at high temperature to obtain fine yield of the product **50** and **51** from ***Z*-49** (Scheme 21). The reaction followed the arenium ion mechanism for C–C bond formation, which proceeded through a lower energetic barrier *via* the Scholl reaction in acidic conditions, as demonstrated by the quantum mechanical calculations. This reaction proved to he highly regioselective as only one product was formed out of the four expected products.[50]

In 2018, Huang and co-workers introduced a method for the synthesis of microporous organic polymers (MOPs) using the Scholl reaction to promote the key C–C coupling reaction. During this process, two aryl hydrogens were removed from adjacent phenyl rings by treating reactant **52** with anhydrous $AlCl_3$ in chloroform to construct a new aryl–aryl bond in product **53** (Scheme 22). This C–C bond formation between two aryl groups generated diversity in the functional group and the molecular geometry of MOPs, which gave rise to different properties in MOPs such as rigidity and cross-linked network that eventually led to high microporosity.[51] The methodology provides a new route for the fabrication of microporous organic

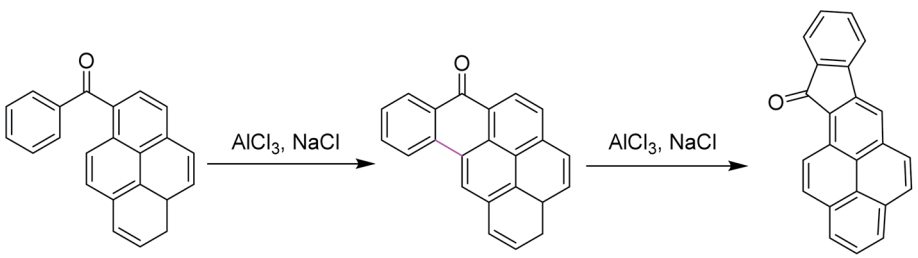

49 50 51

Scheme 21 $AlCl_3$-mediated intramolecular Scholl reaction.[50]

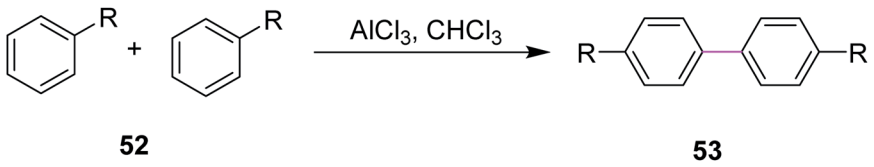

52 53

Scheme 22 Scholl coupling reaction *via* $AlCl_3$.[51]

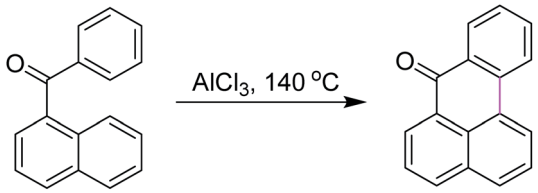

54 55

Scheme 23 $AlCl_3$-mediated Scholl reaction of benzoylnaphthalene.[52]

nanotubes for various potential applications including energy storage, adsorption, separation, and catalysis.

In 2019, Agranat and co-workers designed a protocol for C–C bond formation between two aryl systems using excess of $AlCl_3$/NaCl at elevated temperature (140–220 °C). This reaction involved Scholl cyclization of different benzoylnaphthalenes **54** to synthesize 7*H*-benz[de]anthracen-7-one **55** (Scheme 23). This type of reaction could be extended further into the synthesis of PAHs. This reaction was recognized as similar to the Friedel–Crafts acylation that was carried out in the presence of PPA. $AlCl_3$ promoted the Scholl reaction, whereas PPA promoted the Friedel–Craft acylation.[52]

In 2020, Jimenez and co-workers reported a method for the cyclodehydrogenation reaction of 2-substituted binaphthyls **56a** and **56b** to afford *bay*-substituted perylenes. Using $AlCl_3$ as the Lewis acid and high temperatures, the two new products **57a** and **57b** bearing NH_2 and $N(CH_3)_2$ groups at position 2 of the perylene ring were synthesized (Scheme 24).[53] Under these conditions, the authors were also able to obtain perylene **57c** from ternaphthalene in 39% yield after two cyclodehydrogenation reactions in a single step. According to these analyses, within this experimental condition ($AlCl_3$/NaCl, 170 °C), substrates **56a** and **56b** can generate the σ-complex to initiate the reaction and consequently produce intramolecular cyclization. The attempts to promote the formation of a radical cation using $FeCl_3$ or a strong oxidant such as DDQ did not yield the expected products.

In 2020, Miao and co-workers presented their work, where they stitched nitrogen-containing aromatic units **58** *via* easily maneuverable $AlCl_3$-mediated Scholl reaction in a single operation. The mild reaction conditions in this strategy feature moderate temperature and short time. As a result, a highly stable nitrogen-containing porous organic framework (POF) **59** was constructed, as described in Scheme 25. $AlCl_3$ was used as a catalyst due to its lower toxicity, high stability, and high cross-linking ability. POF was then used to capture radioactive volatile iodine by reversible capture.[54]

It is concluded that $AlCl_3$ proved to be a better oxidant due to its better oxidizing ability as compared to the other reagents. Its reduction potential value is −1.667 V.

5.2. $FeCl_3$-mediated Scholl reaction

Iron(III) chloride ($FeCl_3$) simultaneously acts as the oxidant and as the Lewis acid in the Scholl reaction. Previously, $FeCl_3$ was utilized in the Scholl reaction because of its ready availability and eco-friendly nature. Many substituted triphenylenes **61** were synthesized from benzene derivatives **60** through cyclotrimerization using $FeCl_3$ as the oxidant to construct the C–C bonds (Scheme 26).

Mattmer and co-workers (1994) used a mixture of $FeCl_3$ and conc. sulfuric acid (H_2SO_4) for the synthesis of triphenylene.[55] This procedure provided a good yield but its workup was a little strenuous and hazardous to the environment. To overcome this problem, Cooke and co-workers synthesized a triphenylene in 1999 by replacing the abovementioned oxidant system with $FeCl_3/Al_2O_3$. This process provided quite good yield, which is a safe and environmentally friendly synthetic route for performing the cyclotrimerization of dialkyloxy benzenes **60** to produce triphenylene derivatives such as **61**.[56]

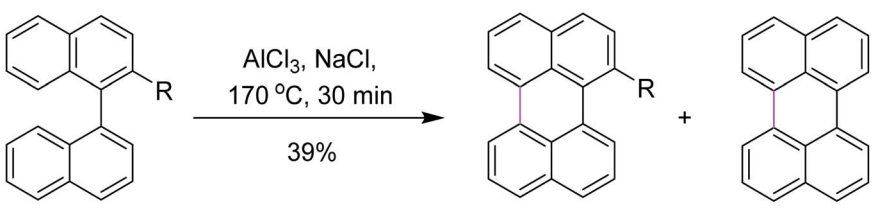

56a R = NH_2
56b R = $N(CH_3)_2$

57a R = NH_2
57b R = $N(CH_3)_2$
57c

Scheme 24 Synthesis of perylene *via* the Scholl reaction.[53]

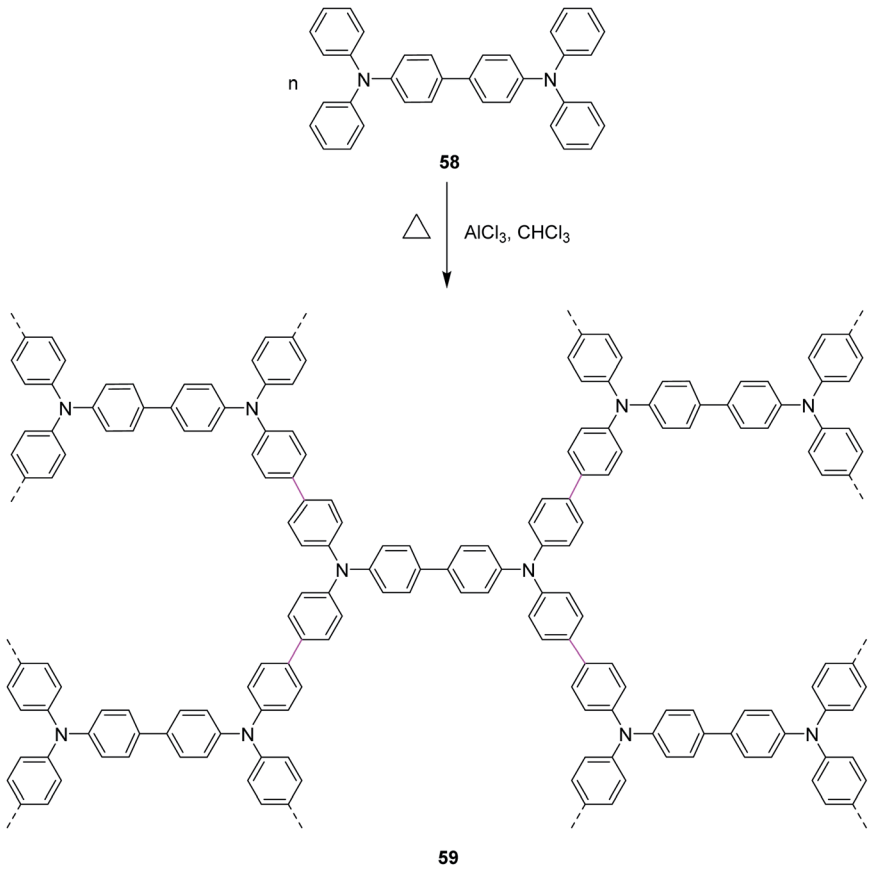

Scheme 25 POF synthesis by the $AlCl_3$-mediated Scholl reaction.[54]

Bushby and co-workers, in 2006, used $FeCl_3$/methanol in dichloromethane (DCM) for triphenylene synthesis. They experimentally proved that this oxidant complex was much better many other oxidant complexes such as $FeCl_3/Al_2O_3$, $MOCl_5$, and $VOCl_3$.[57]

Similarly, Bai and Lin (2011) synthesized triphenylene in the presence of anhydrous $FeCl_3$. This method involved a more efficient and selective procedure for the solvent-free oxidative cyclodehydrogenation of arenes. This coupling reaction was cheap and an environmentally friendly "*Green Chemistry*" method due to the elimination of expensive and hazardous solvent systems. The product obtained by this method was soluble in organic solvents.[58]

In 2011, Yang and co-workers developed a synthetic protocol for the synthesis of binaphthyls **63** utilizing $FeCl_3/K_2CO_3$ in dichloroethane (DCE) *via* Scholl cyclization. Naphthylamines **62** were subjected to oxidative coupling for the construction of C–C bonds in binaphthyl diamines (Scheme 27). The group used

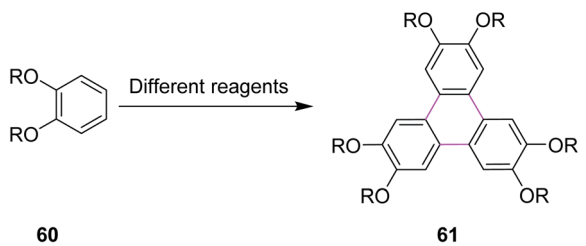

60 **61**

R = CH_3, $(CH_2)_4CH_3$, $(CH_2)_5CH_3$ *etc.*

Reagents

1. $FeCl_3/H_2SO_4$[55]
2. $FeCl_3/Al_2O_3$[56]
3. $FeCl_3$/Methanol,DCM[57]
4. Anhydrous $FeCl_3$[58]

Scheme 26 Triphenylene synthesis employing $FeCl_3$.

62 **63**

R = alkyl, aryl

Scheme 27 Binaphthyl synthesis by $FeCl_3$ catalysis.

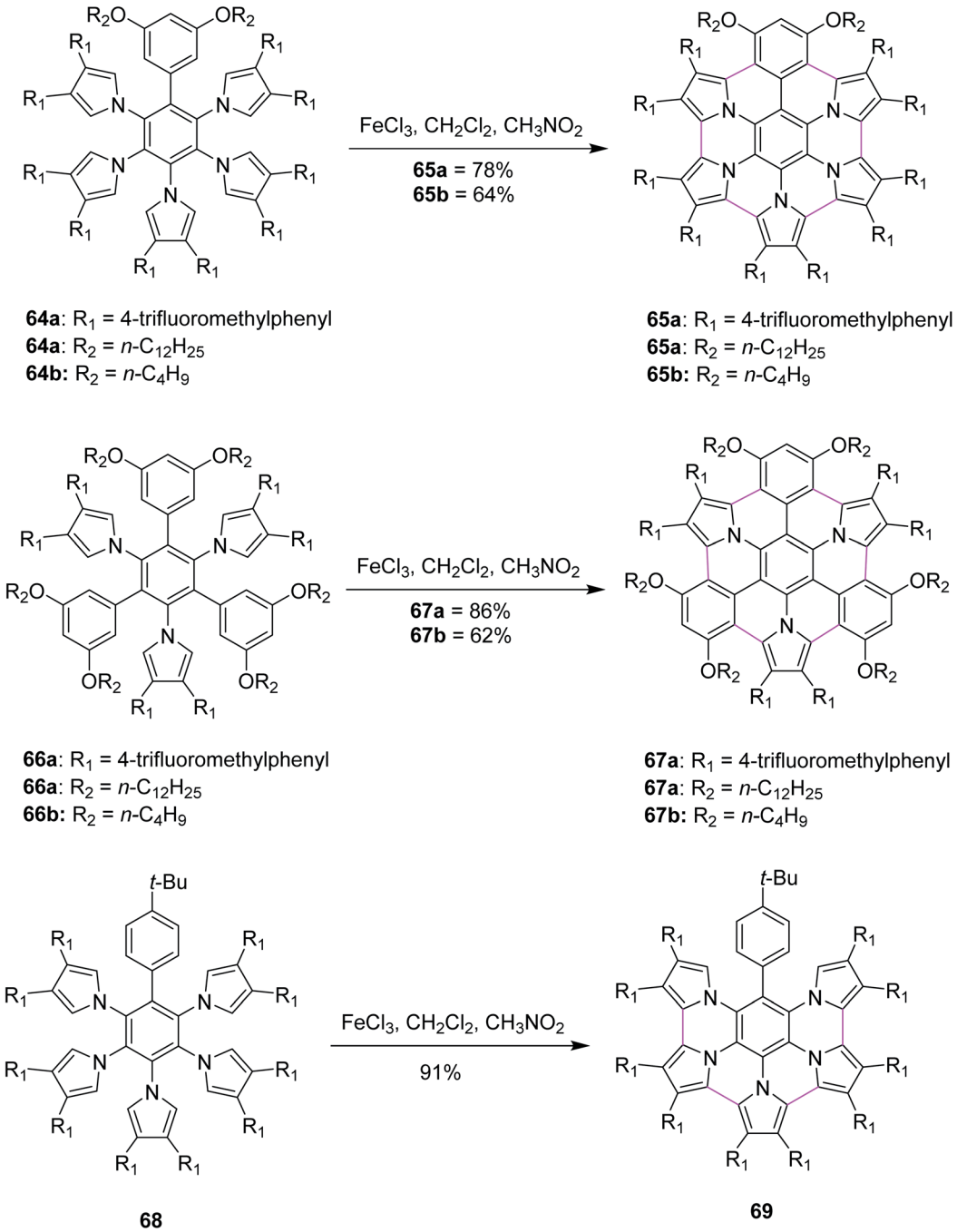

Scheme 28 Synthesis of pyrrole-fused azacoronenes employing $FeCl_3$.

$FeCl_3$ as the oxidant owing to its properties as a promoter for the oxidative coupling of electron-rich arenes and more importantly, is non-toxic, less expensive, environmental benign, and easily commercially available. K_2CO_3 was used as the base for catalyzing the reaction as it neutralizes the additional HCl produced during this process. The reaction is dependent on the nature of the solvent under these reaction conditions. In the presence of DCE as the solvent, maximum yield was obtained.[59]

Heteroatom-doped graphenes constitute a new class of materials that possess properties and functions different from those of the parent graphene. In 2013, Müllen and co-workers devised a method for the synthesis of pyrrole-fused azacoronene (**65a,b**, **67a,b** and **69**) *via* the oxidative cyclodehydrogenation of the corresponding hexaarylbenzenes (**64a,b**, **66a,b**, and **68**). Bottom-up organic synthesis can provide structurally-defined heteroatom-doped graphene fragments with perfect control of not only the size, periphery, and substituents but also of the doping concentration and position. Final planarization with $FeCl_3$ offered targets (**65a,b** and **67a,b**) in good yields (60–86%). Notably, the 3,5-dialkoxyphenyl group

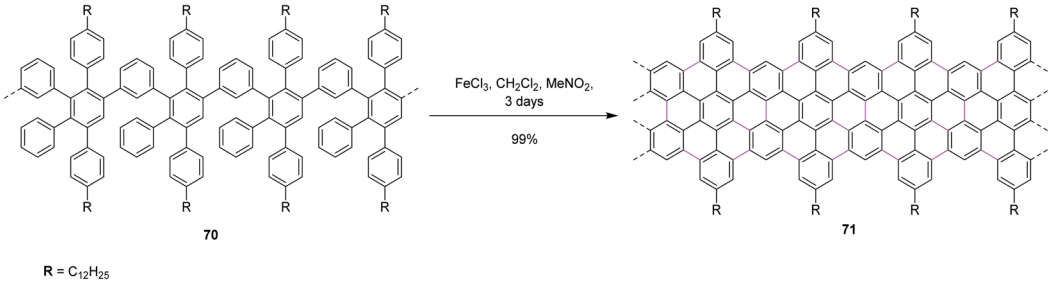

Scheme 29 Synthesis of graphene nanoribbons by the Scholl reaction.

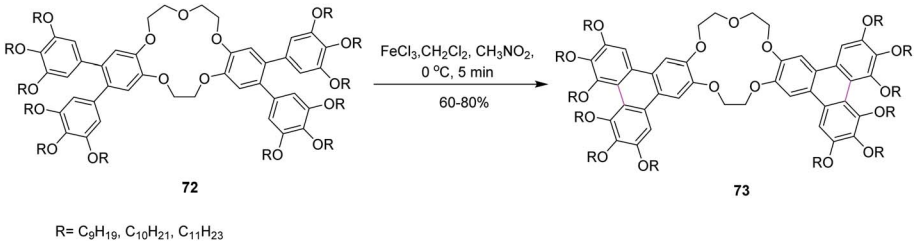

Scheme 30 Synthesis of sterically crowded *o*-terphenyl crown ether.

(**64a,b** and **66a,b**) appears to be required for the complete planarization of the azacoronene core/scaffold. However, when the Scholl reaction was performed with **68**, which possesses a 4-tertbutylphenyl group instead of a 3,5-dialkoxyphenyl group, partially fused compound **69** was obtained as the main product (91%) even though the completely fused structure was detected by MALDI. In line with their strategy to fuse hybrid aromatics, the further functionalization of PAHs would be beneficial for molecular electronics and spintronics with well-defined structures (Scheme 28).[60]

In 2014, Feng and co-workers switched their attention to apply the Scholl reaction for the intramolecular condensation of polyphenylene-based precursor **70** to furnish solution-processed GNRs **71** (Scheme 29). For the first time, they synthesized an AB-type Diels–Alder polymer to prepare GNR **71** with a "cove-type" edge structure and desired dimensions. The structurally well-defined GNRs can be prepared using a 'bottom-up' organic synthesis method through surface-assisted or solution-mediated cyclodehydrogenation reactions. In addition, non-planar polyphenylene precursors were first 'built up' from small molecules, and then 'graphitized' and 'planarized' to produce GNRs. Furthermore, C–C bond formation at undesired positions during the cyclodehydrogenation of **70** is hindered by the steric repulsion between the benzene rings and the bulky alkyl chains, ensuring the non-kinked and uniform structure of the resulting GNR **71**. Moreover, the insertion of various functional groups on the periphery of such GNRs is feasible and may prove to be valuable for the fundamental studies on graphene nanostructures, which can place specific functionalities on them and further enhance their processability to realize wider applications, such as in GNR-based nanocomposites.[61]

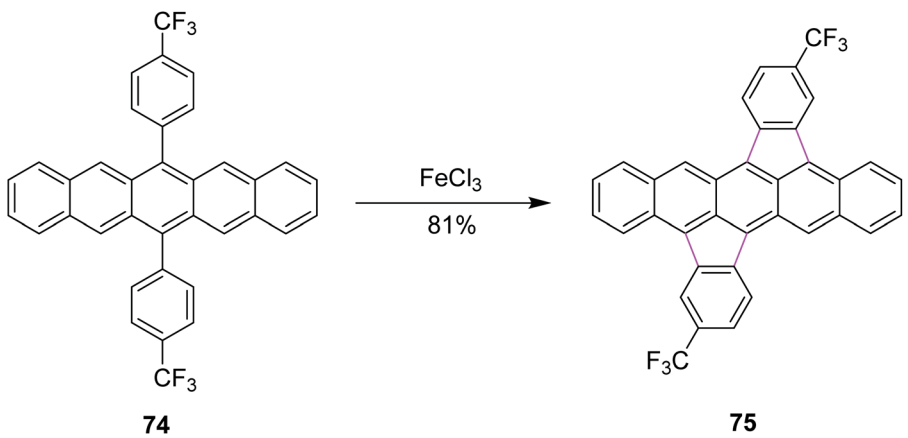

Scheme 31 Synthesis of bisindeno-annulated pentacenes.[63]

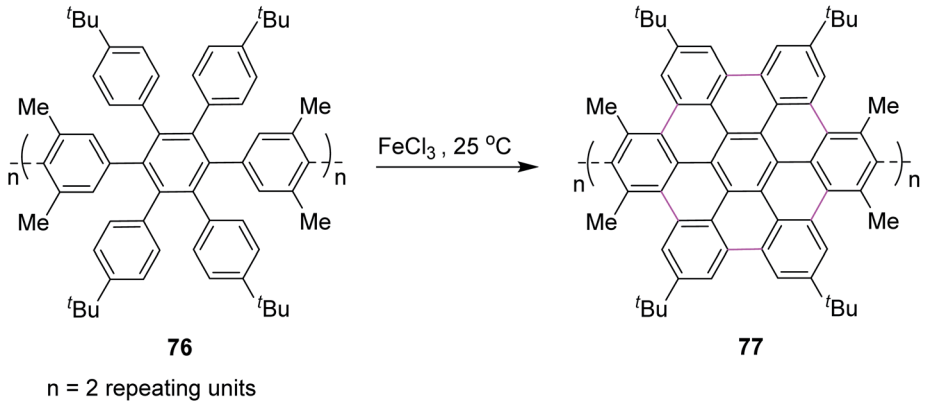

Scheme 32 Cyclodehydrogenation of polyphenylenes by $FeCl_3$.

In 2014, Laschat and co-workers presented a protocol for the synthesis of the sterically crowded *o*-terphenyl crown ether **73** using alkoxy substituents from tetrabromodibenzocrown **72** as well as boronic acids or borolanes by Suzuki coupling and consequently converted to triphenylenes applying the Scholl reaction (Scheme 30). Fifteen equivalents of $FeCl_3$ were used for Scholl cyclization in the presence of DCM. Sequentially, the product was dissolved in methanol for quick quenching. The resulting products demonstrated liquid crystalline behavior. The authors proposed that this type of harmonizing of the steric impact could be utilized as a scaffold for many other organic compounds.[62]

In 2015, Chi and co-workers reported a method for the synthesis of bisindeno-annulated pentacenes **75** using a facile $FeCl_3$-mediated Scholl reaction of regioselective nature from the pentacene precursor **74** (Scheme 31). $FeCl_3$ as the oxidant here selectively produced the transoid double cyclized product and in turn was used preferentially for such type of reactions. Notably, the high regioselectivity has been attributed to the high strain observed in the cisoid isomers. This combination of indeno-units intensely altered the chemical as well as the electronic properties of pentacene and the resulting products exhibited extraordinary photo-stability in solution. These compounds were used practically in electronic devices such as OFETs. This research offered broad conception to stabilize the π-conjugated systems, which are highly reactive in nature.[63]

In the same year, Nishiuchi and co-workers established a new post-construction method for the synthesis of GNRs and NGs. In this procedure, the large π-surface was formed using the $FeCl_3$-mediated Scholl reaction after attaining the cyclic structure (Scheme 32). In this method, graphene fragment **77** was constructed from hexaarylbenzene **76** through

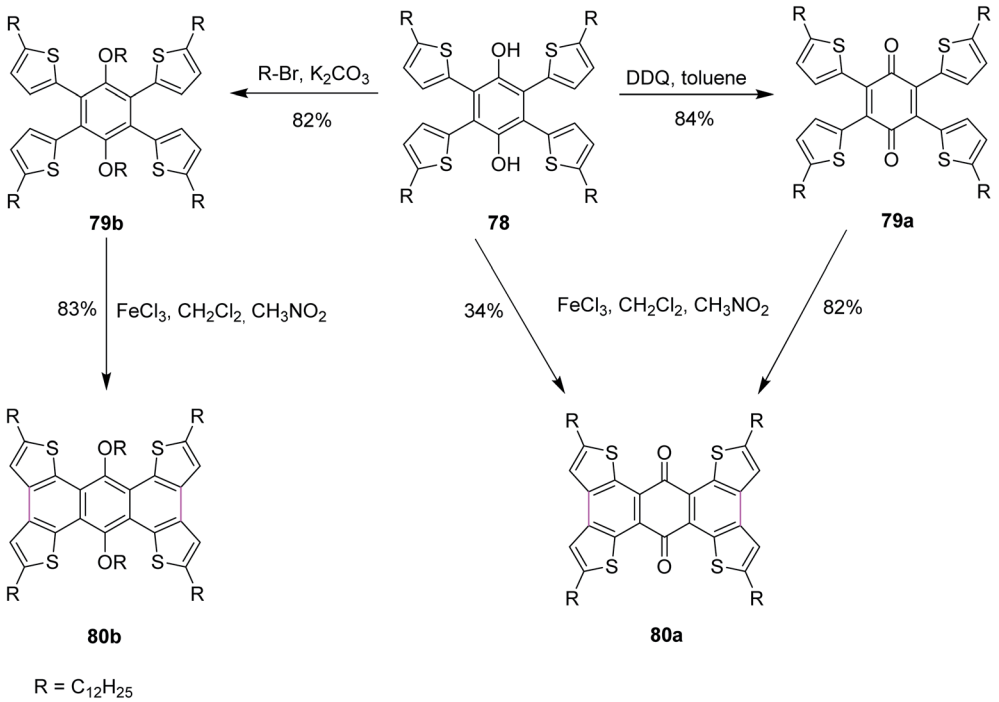

Scheme 33 Fused aromatic compound synthesis by the Scholl reaction.

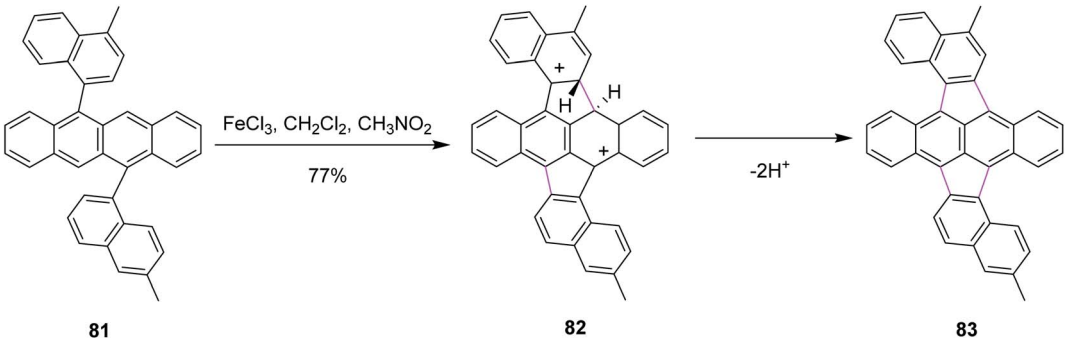

Scheme 34 Twofold Scholl cyclization by $FeCl_3$.

cyclodehydrogenation under $FeCl_3$-induced Scholl reaction conditions at ambient temperature.[64]

In 2016, Xu and co-workers described the three reaction pathways to synthesize benzoquinones and hydroquinone by following the Scholl reaction protocol. They used DDQ as the oxidant along with toluene in the first reaction pathway to give the intermediate product **79a**, which was then reacted with $FeCl_3$ to produce **80a** in 82% yield (Scheme 33). In a second reaction pathway, $FeCl_3$ was used directly to obtain product **80a** in 34% yield from substrate **78**. Lastly, in a third reaction pathway, target compound **80b** was obtained in 83% yield from reactant **78** over two steps, as described in Scheme 33. In their work, the authors also reported that the reaction center was located next to the carbonyl groups that influenced the Scholl reactivity. The direct oxidation of **78** with $FeCl_3$ to yield **80a** provided less yield (34%) due to the involvement of an active hydroxyl group hydrogen that could potentially initiate free radical reactions. Some by-products were observed in this reaction pathway. Therefore, an alternate pathway was used for the Scholl cyclization of **78** where it was treated with DDQ in the first step to generate an intermediate product **79a**, which was eventually converted to **80a**, giving much higher yield (82%). Similarly, the related product **80b** was obtained *via* intermediate **79b** in good yield (83%).[65]

In 2017, Murata and co-workers devised a protocol to induce unsymmetrical two-fold Scholl cyclization for the synthesis of pentagonal and hexagonal rings in the PAH systems such as 5,11-dinaphthyltetracene **81**. A $FeCl_3/CH_2Cl_2/CH_3NO_2$ reagent system was used for the Scholl cyclization. This reaction was selective as only one type of product **83** was obtained out of the three expected products (Scheme 34). The authors reported that the reaction mechanism of the Scholl cyclization in this type of synthesis was based on the formation of the di-cationic intermediate **82** instead of classical pathways that were based on radical cation or arenium ion formation. To avoid chlorination, they introduced a methyl group at each naphthyl ring. Hence, the choice of the reagent complex was also explained.[66]

In 2018, Borchardt and co-workers developed a solvent-free procedure for mechanochemical Scholl reaction. This procedure was introduced as a versatile graphitization tool for C–C bond formation. Several types of extensive ring systems such as hexabenzocoronene **85** from hexaphenylbenzene **84** were synthesized using this procedure (Scheme 35). Ball mills were used during this procedure to synthesize large-size nanographenes within a very short time due to the absence of extensive solvent systems and elimination of solubility limitation. $FeCl_3$ was used along with sodium chloride to obtain high yields in this process. High input energy from the ball mill and excess of $FeCl_3$ provided excellent yield with full chemical conversion. Furthermore, this pathway was safe to use and also avoided undesired by-product formation.[67]

In 2018, Merner and co-workers introduced a process for the π-extension of the benzenoid macrocycles **86** by the $FeCl_3$-mediated Scholl reaction. They converted a non-planar

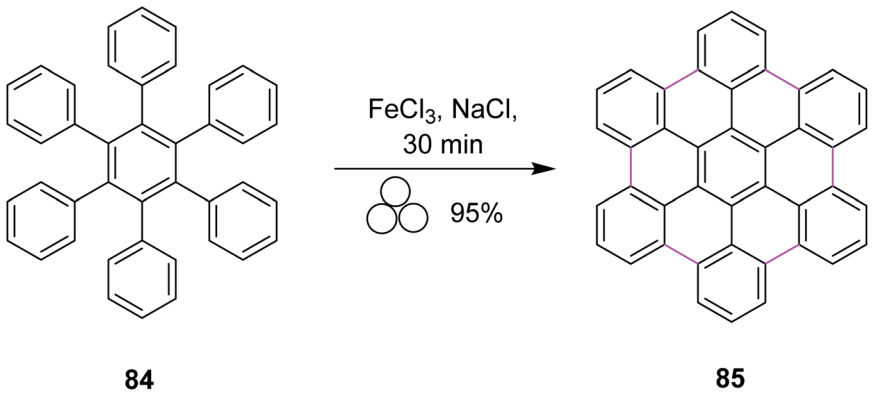

Scheme 35 Hexabenzocoronene synthesis *via* the Scholl reaction.

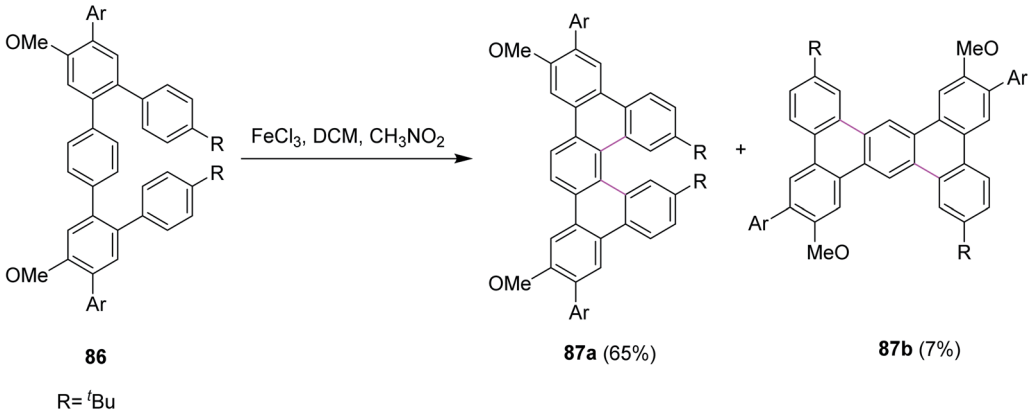

86

R= ^{t}Bu

87a (65%) **87b** (7%)

Scheme 36 $FeCl_3$-mediated Scholl reaction for π-extension.

benzenoid systems to a non-planar PAH system and subsequently subjected the latter to oxidation to promote cyclodehydrogenation. As a result, new hexagonal rings were formed, and the production of undesired products was also controlled. Two products **87a** (65%) and **87b** (7%) were observed during this reaction (Scheme 36). The reaction yield was quite high because of the suitable oxidant system and reduced the number of by-products.[68]

In 2020, Martín and co-workers synthesized a novel homo 3D nanographenes, featuring a cyclooctatetraene core. A concise and efficient bottom-up methodology was employed, during which 24 new C–C bonds were formed by means of the Scholl reaction. Nanographenes with 53 fused rings are realized, which exhibited good solubility in common organic solvents. The resulting saddle-like structures are electron-rich and show good chemical and electrochemical stability. Compound **88** subsequently underwent intramolecular cyclodehydrogenation mediated by $FeCl_3$ to generate **89** in moderate yields. Compound **88** was subjected to a further one-fold $FeCl_3$-mediated oxidative coupling in refluxing dichloroethane to produce compound **89**. However, under such optimized reaction conditions, **88** was interconverted into the fully coupled **89** (Scheme 37).[69]

Overall, it is concluded that $FeCl_3$ proved to be a better oxidant due to its excellent oxidizing capacity as compared to $AlCl_3$. Its reduction potential value is −0.409 V.

5.3. DDQ-mediated Scholl reaction

In 2009, Rathore and co-workers explored 2,3-dichloro-5,6-dicyano-1,4-benzoquinone (DDQ) as a new oxidant for performing the Scholl reaction with a variety of aromatic donor substrates. The reaction followed a radical cation mechanism to produce triphenylenes and hexabenzocoronene scaffolds under strong and mild conditions.[70] Biaryl synthesis has been particularly useful for the oxidative cyclodehydrogenation of a variety of substituted hexaarylbenzenes and *o*-terphenyls to produce the corresponding planar PAHs, for example, hexa-*peri*-hexabenzocoronenes (HBC's) and triphenylenes, respectively. The

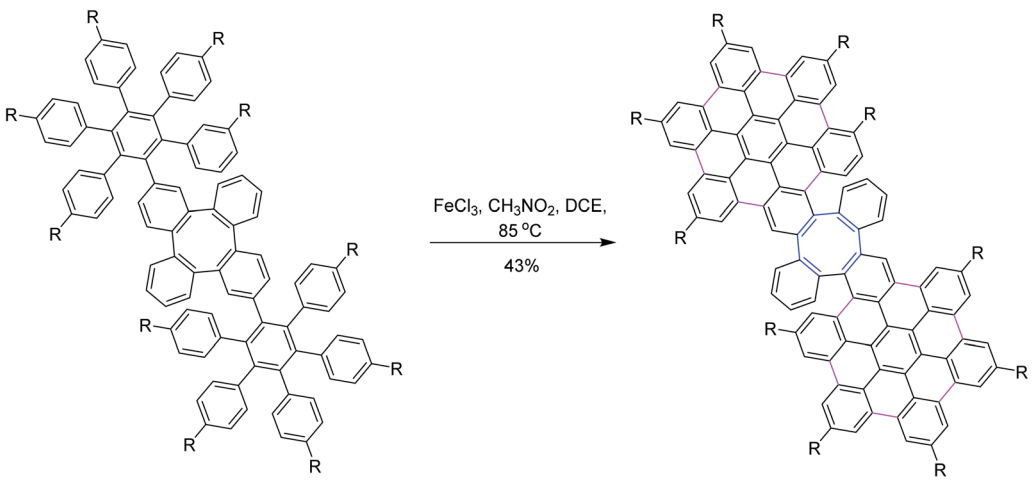

88

R = ^{t}Bu

89

Scheme 37 Nanographene synthesis by the Scholl reaction using $FeCl_3$.

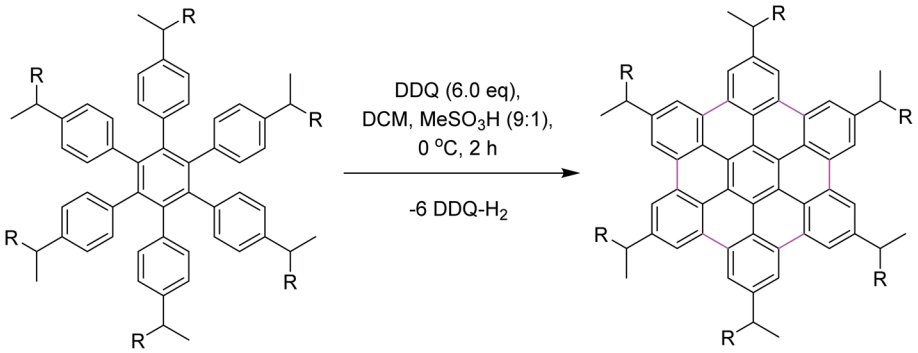

Scheme 38 Synthesis of soluble HBCs from hexaarylbenzene precursors.

usefulness of the DDQ–acid system for oxidative cyclodehydrogenation in the Scholl reaction was further validated by the formulation of soluble HBC's [**91a–c**] from hexakis (4-isoalkylphenyl)benzenes [**90a–c**], where six new C–C bonds were formed in one step to give graphitic products in excellent yields and high purity (Scheme 38).[70] The authors have demonstrated that the DDQ/H^+ oxidation system, which is known to oxidize a variety of aromatic donors with the oxidation potential as high as ~1.7 V to the corresponding cation radicals, can be effectively employed for the preparation of a variety of PAHs including graphitic hexa-*peri*-hexabenzocoronenes.[70]

In a follow-up study, Wong and co-workers (2012) developed a new set of reaction conditions for the oxidative cyclodehydrogenation of electron-poor polyphenylenes with various EWGs groups such as –Br and –F. Their coupling reactions to planar nanographenes was achieved using the DDQ–CF_3SO_3H oxidative system.[71] The –Br and –F substituted HBC derivatives (**93a–c**) were prepared from hexaphenylbenzene precursors (**92a–c**) on treatment with a combination of DDQ and CF_3SO_3H (Scheme 39). It is noteworthy that there are two proposed reaction mechanisms for the oxidative cyclodehydrogenation (Scholl) reaction, proceeding either through an arenium-ion or a radical-cation intermediate. In both the pathways, protic acids play a vital role in the progress of the reaction.

Consequently, Itami, Scott, and co-workers (2013) made major progress by achieving a concise two-step synthesis of grossly warped graphene molecule **96** (C_{80}) with five embedded seven-membered rings and one five-membered ring at the center. Starting from corannulene **94**, precursor **95** was obtained by Pd-catalyzed direct C–H arylation with arylboroxins, using *o*-chloranil as an oxidant for the intramolecular cyclization of precursor **95** that efficiently provided grossly warped graphene molecule **96** in good yields, overcoming the high steric demand to form five distorted seven-membered rings (Scheme 40).[72] Because of its highly non-planar structure, graphene molecule **96** showed good solubility in common organic solvents, and, surprisingly, graphene molecule **96b** with tertiary butyl groups could be dissolved even in hexane. The aforementioned studies proved the success of the current protocol, thus paving the way to synthesize the challenging heptagon-containing non-planar PAHs from polyphenylenes after condensing with the DDQ/H^+ oxidant system.

Inspired by the previous outcomes, in 2014, Müllen and coworkers explained the synthesis of the biphenylene-based condensed PAH **98** merged with two 8-membered and one 4-

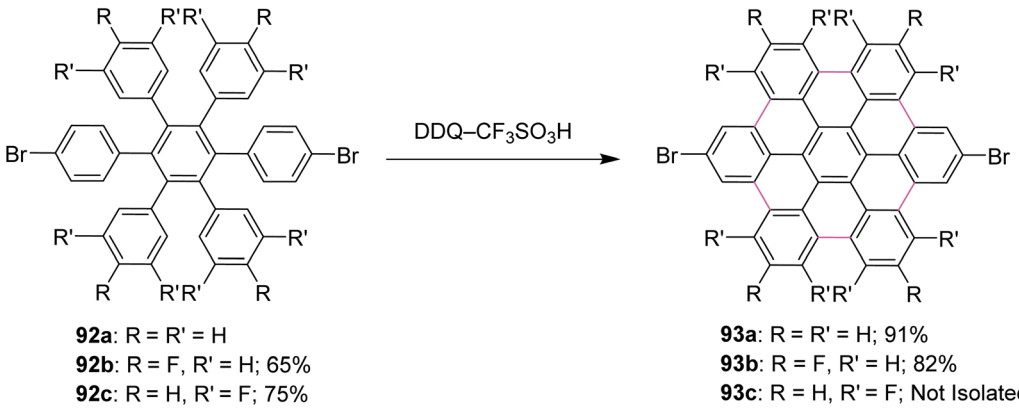

Scheme 39 Synthesis of a series of HBC derivatives containing EWGs *via* DDQ.

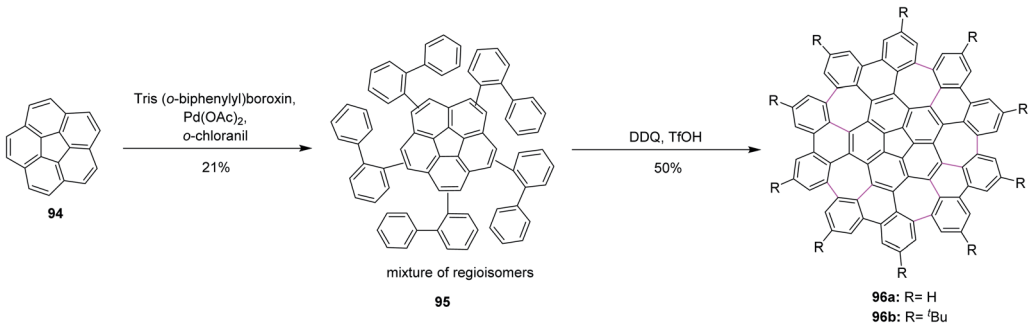

Scheme 40 DDQ-induced synthesis of grossly-warped graphene molecules.

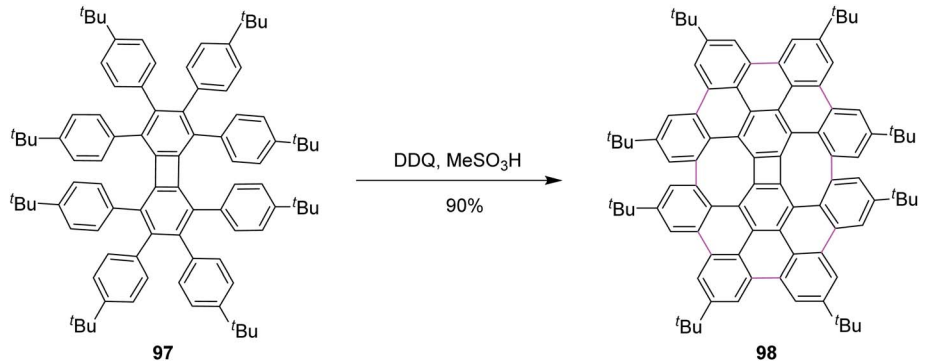

Scheme 41 Synthesis of biphenylene-based PAH by DDQ/$MeSO_3H$.

membered rings by the cyclodehydrogenation of the precursor octaarylbiphenylene **97** using a mixture of DDQ and $MeSO_3H$ (Scheme 41). The cyclodehydrogenation did not proceed any further, possibly due to the increased steric hindrance and selectivity, exclusively producing nanographene **98** in 90% yield.[73] Undoubtedly, this was also a breakthrough in showcasing the importance/value of DDQ as an oxidant in the field of nanographene synthesis. Moreover, the authors concluded that the isomeric graphene nanostructures were prepared to demonstrate a combination of four-, six-, and eight-membered rings in a single structure.

Miao and co-workers (2015) synthesized two new saddle-shaped polycyclic arenes having two heptagons delivered from saddle-shaped diketone **99a,b** (Scheme 42). The synthesis of the two novel saddle-shaped PAHs **101a,b** and **102a,b** with two entrenched heptagons was conducted by the oxidative cyclodehydrogenation of the precursors **100a,b** and **103a,b** using DDQ and CF_3SO_3H-initiated oxidation.[74] These findings further strengthened the importance of the DDQ/H^+ system in the insertion of a seven-membered ring in the nanographene structures, which could offer exciting electronic properties for applications in organic electronics.

In 2015, Mastalerz and co-workers developed a route for the synthesis of triptycene derivative **105** based on the tris-*ortho* terphenylene **104** (Scheme 43). They initially implemented Suzuki–Miyaura coupling to construct the basic scaffold of terphenylene from hexabromotriptycene, followed by the Scholl reaction in the presence of DDQ and CH_3SO_3H in DCM at 0 °C. This route provided high yield as compared to zirconium and stannylene routes. When the classical zirconium route was used for the same type of Scholl cyclization of terphenylene, no intermolecular oxidative coupling was observed.[75]

In 2016, Müllen and co-workers developed a novel synthetic strategy for bowl-shaped PAH containing two pentagons such as structure **107**, as shown in Scheme 44. They used the bottom-up strategy to construct C_{70} with two C_{34} subunits of fullerenes. Numerous reagents were utilized in this synthetic pathway due to its multistep process; however, the DDQ/CF_3SO_3H set-up was used in the fundamental step where pentagon rings were constructed in the presence of DCM by the Scholl reaction. DDQ provided highly selective 1,2-shifts of aryl groups in **106** during this synthetic strategy.[76] However, the main attempts were focused on the synthesis of buckminsterfullerene C_{60}. In contrast, the access to subunits of the C_{70} homologue remains challenging.

Kuck, Chow, and co-workers (2016) published, for the first time, the challenging approach for the attachment of three *o*-phenylene units **108a** at the bay regions of the C_{3v}-symmetrical hat-shaped polycyclic aromatic hydrocarbon bearing the tribenzotriquinacene (TBTQ) skeleton. The key step in their synthetic sequence includes three Scholl-type cycloheptatriene ring formation around the TBTQ core. Over the past years, they employed several oxidants to promote these oxidative cyclization reactions and were ultimately successful in fulfilling their goals, utilizing the DDQ/TfOH oxidant system. In this respect, they treated hydrocarbon **108a** with stoichiometric amounts of

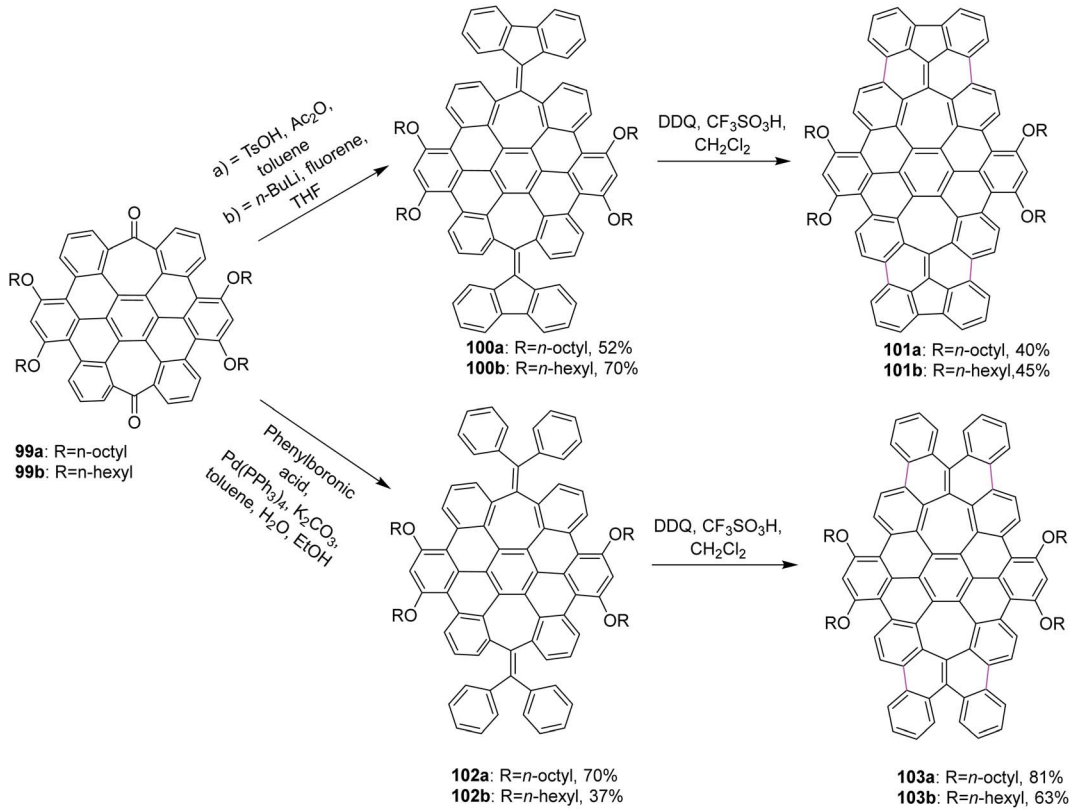

Scheme 42 Graphene syntheses with an embedded 7-membered ring by cyclodehydrogenation.

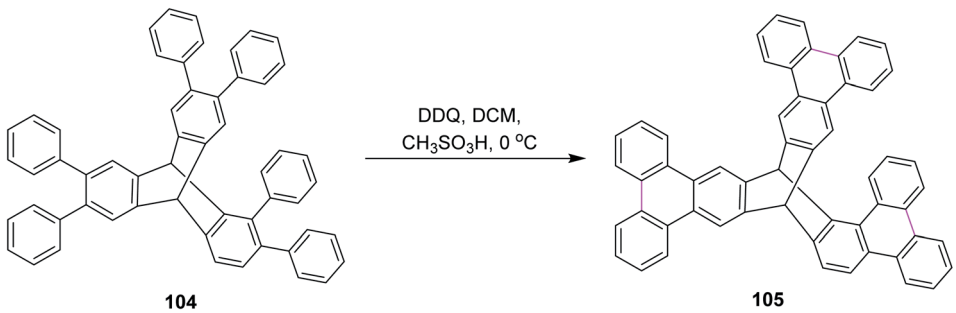

Scheme 43 Synthesis of triptycenes by DDQ.

DDQ and TfOH in DCM, as displayed in Scheme 45. These oxidative conditions produced intermediate product **108b** with incomplete cyclodehydrogenation in good yields. Obtaining multiple functionalization around the peripheral arene positions of TBTQ is itself quite challenging. Besides, upon increasing the amount of DDQ to 3.0 equivalents, they observed

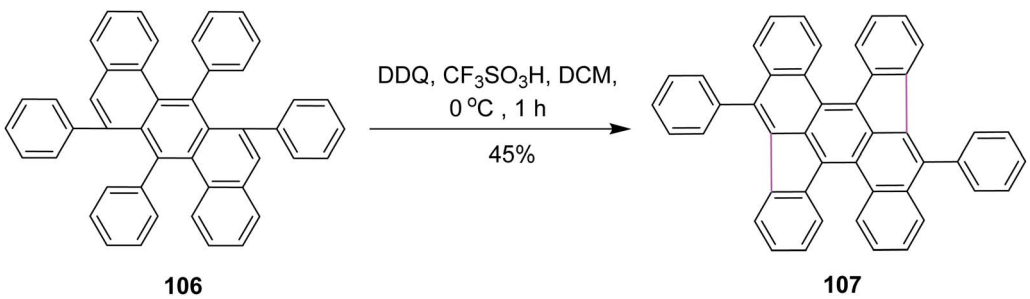

Scheme 44 Synthesis of fullerene pentagons with DDQ.

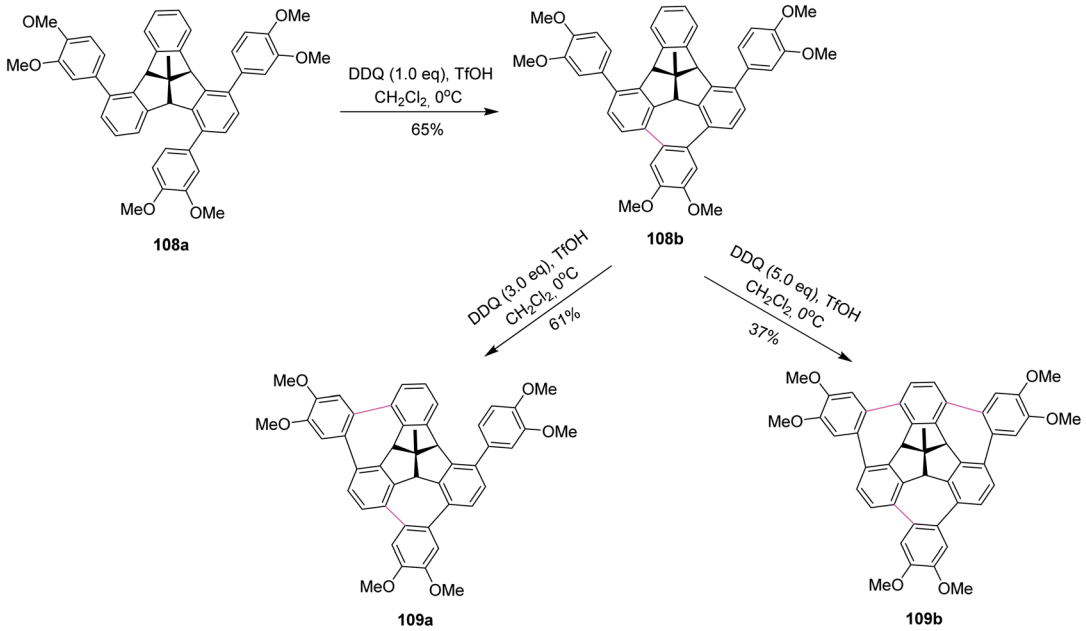

Scheme 45 DDQ-promoted oxidative cycloheptatriene ring formation around the TBTQ core.

the attachment of two 1,2-arylene units around the TBTQ core in the form of an unwanted product **109a** (Scheme 45) produced in moderate yield. Nevertheless, the desired target compound **109b** could be obtained in 37% yield using 5.0 equivalents of DDQ along with TfOH. Despite the relatively lower yield, TBTQ merged with three cycloheptatriene units represents a promising key intermediate for the construction of non-planar nanographene molecules bearing TBTQ as the central core.[77] These intriguing results opened the door for future design and to prepare organic functional materials based on the TBTQ motif.

In the following years, Kuck, Chow, and co-workers (2017) extended their research endeavors to apply the previously reported oxidative conditions (DDQ and TfOH) in the synthesis of cycloheptatriene-merged fenestrindane derivatives, as shown in Scheme 46. Promoted by DDQ/TfOH, the key step featured four Scholl-type cycloheptatriene formation steps, starting from the corresponding tetraarylfenestrindane derivatives **110** and **111** bearing electron-rich substituents. Consequently, the precursor hydrocarbons **110** and **111** were reacted with DDQ/TfOH in slight excess to produce a mixture of two-fold and four-fold cyclization reactions to afford the products **112a** (52%) and **113** (20%), respectively, in moderate yields (Scheme 46). In other attempts, the products of neither single nor triple cyclization were observed. With the peripheral –OCH_3 groups (**114**, **115**, and **116**) being available for further functionalization and C–C cross-coupling reactions, these molecules should provide access to various novel π-extended saddle-shaped nanographenes.[78]

In 2017, Tobe and co-workers proposed a procedure where a spiral-polycyclic hydrocarbon **117** was treated with DDQ/$Sc(OTf)_3$ in DCM at different temperatures. An unexpected skeletal rearrangement was observed instead of cyclodehydrogenation. The eight-membered ring rearranged into a seven-membered ring that was further converted into a six-membered ring **119** (Scheme 47). They also used $FeCl_3$ for the

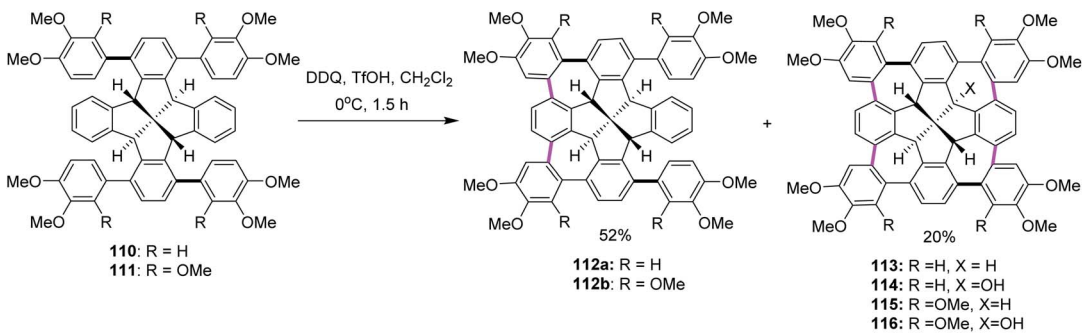

Scheme 46 DDQ-mediated Scholl-type oxidative cycloheptatriene formation; a fourfold bridging of the fenestrindanes core with the electron-rich aryl units.

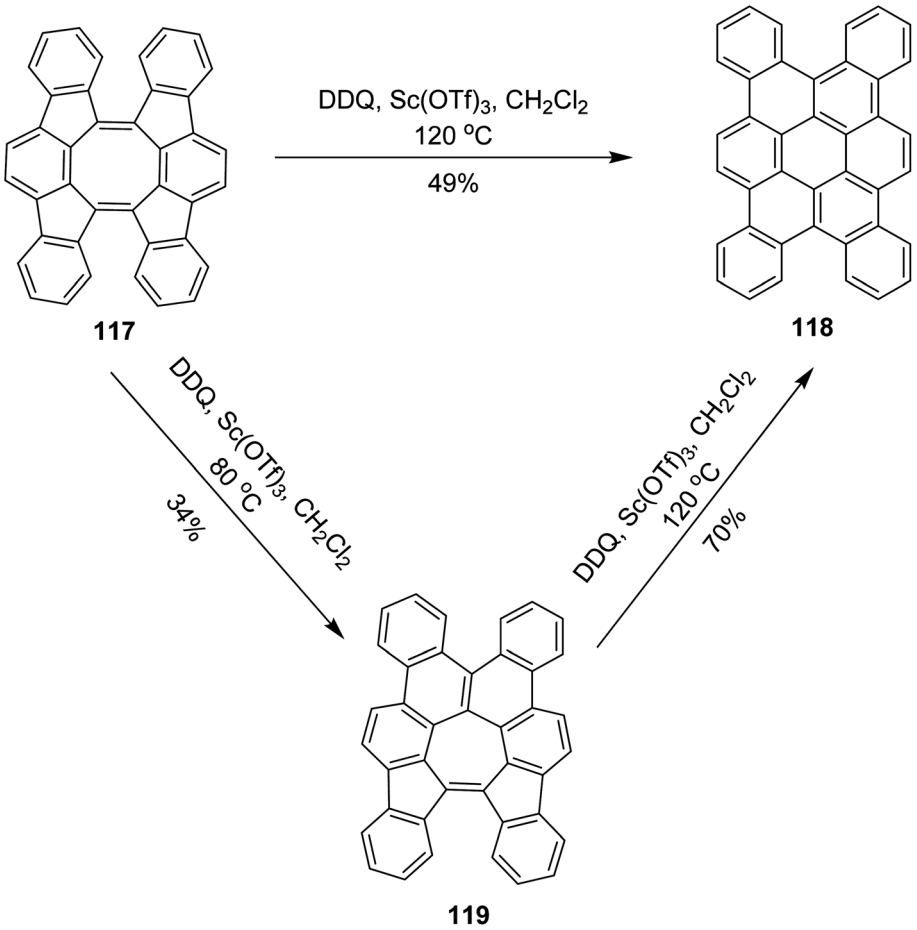

Scheme 47 Skeletal rearrangement of PAH by DDQ.

synthesis of **118**. $FeCl_3$ provided high yield as compared to DDQ.[79] The reaction of **117** with DDQ and $Sc(OTf)_3$ also gave **118**, whereas at higher temperature, tetrabenzocoronene **119** was obtained *via* 2-fold isomerization. Compound **118** adopts a twisted geometry to avoid intramolecular steric repulsions. It exhibits weak aggregation behavior in solution *via* the stacking of the π-conjugated framework. Theoretical calculations suggested that the activation barrier for skeletal rearrangements in cationic intermediates is lower than that of intramolecular bond formation for oxidative dehydrogenation reactions.

Narita and co-workers, in the same year, disclosed a new protocol for the synthesis of benzo-fused carbohelicene **121** by the regioselective cyclodehydrogenation of PAHs **120** (Scheme 48). DDQ, along with $TfOH/CH_2Cl_2$, was utilized in the Scholl cyclization step to construct π-extended C–C bond in carbohelicene. DDQ provided highly regioselective products with multi-

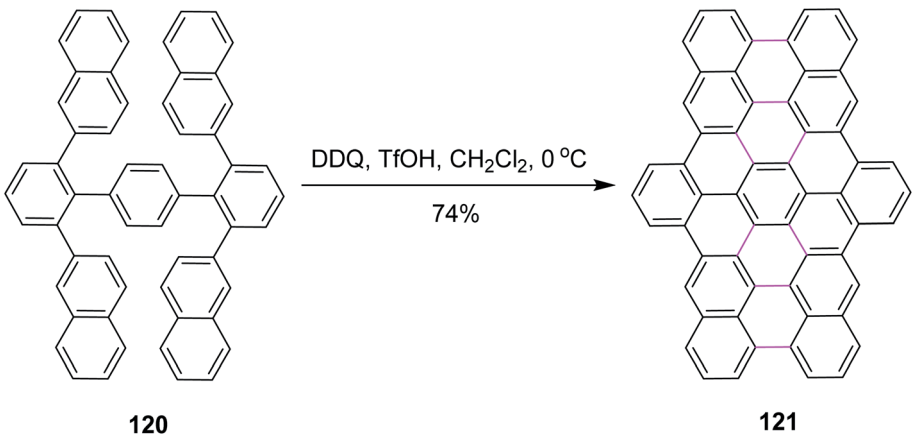

Scheme 48 Synthesis of benzo-fused carbohelicene by DDQ.

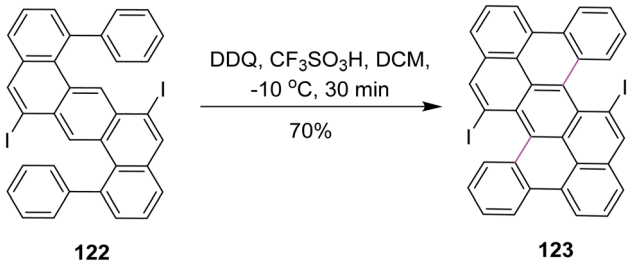

Scheme 49 Synthesis of tetracene *via* the Scholl reaction.

helical structures and promoted the selective formation of sterically-hindered double helicene in good yield.[80]

In 2018, Feng and co-workers developed a method for the development of zigzag-edged nanographenes. They performed oxidative cyclodehydrogenation of open-shell oligophenylenes and polyphenylenes such as **122** *via* the DDQ/CF_3SO_3H set-up in DCM to synthesize tetracenes. The reaction pathway was multistep and Scholl cyclization was the dynamic step to construct the π-extended arene rings in **123** (Scheme 49). DDQ here provided a good yield (70%) despite the high steric hindrance created by the iodine atoms. This approach offered access to the higher PAHs under mild conditions, yielding a novel electron-deficient tetracyano-circumanthracene with a full zigzag-edged structure.[81]

Recently, Kuck, Chow, and co-workers (2018) described the formation of porous and complex bowl-shaped TBTQ-based nanographenes (Scheme 49). Precursor **124** was synthesized over several steps from easily accessible starting materials[82] and was treated with different equivalents of DDQ–TfOH to promote the Scholl-type macrocyclization to produce the porous nanographene molecules **125–127** in different yields (Scheme 50). However, the authors concluded that to achieve threefold oxidative cyclization, 4.5 equivalents of DDQ and TfOH mixture were needed. The further extension of this cyclic porous nanographene **127** by Scholl's macrocyclization using DDQ/TfOH is still underway by researchers to prepare several novel PAHs.[82]

In 2020, Chalifoux and co-workers introduced a novel methodology for the construction of contorted nanographenes. It was a novel method for the development of contorted nanographenes other than typical planar nanographenes by ruthenium-catalyzed benzo-annulation of alkynes, followed by Scholl cyclization (Scheme 51) using bottom-up synthesis. The DDQ/CH_3SO_3H set-up in DCM was used as the oxidant for the introduction of a new arene ring. Here, DDQ provided the double annulated product **129** by the oxidative coupling of

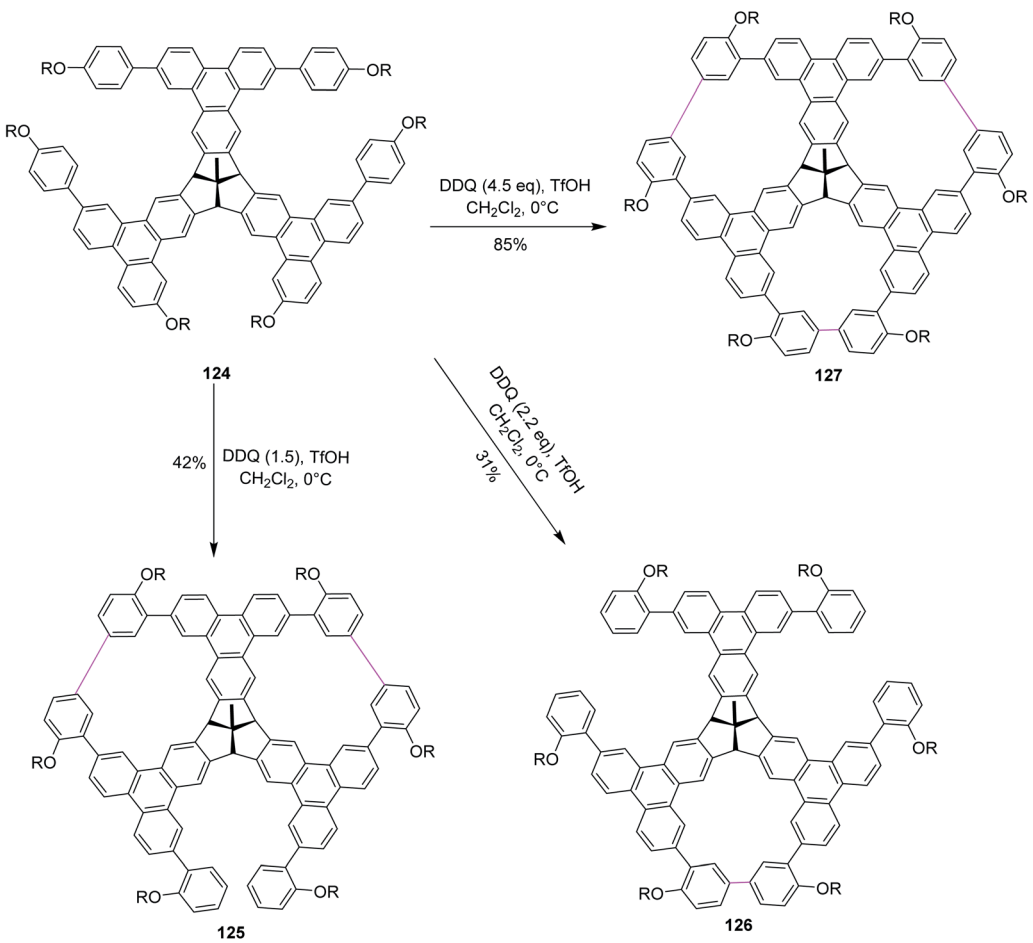

Scheme 50 DDQ–TfOH-promoted Scholl macrocyclization for porous nanographene syntheses.

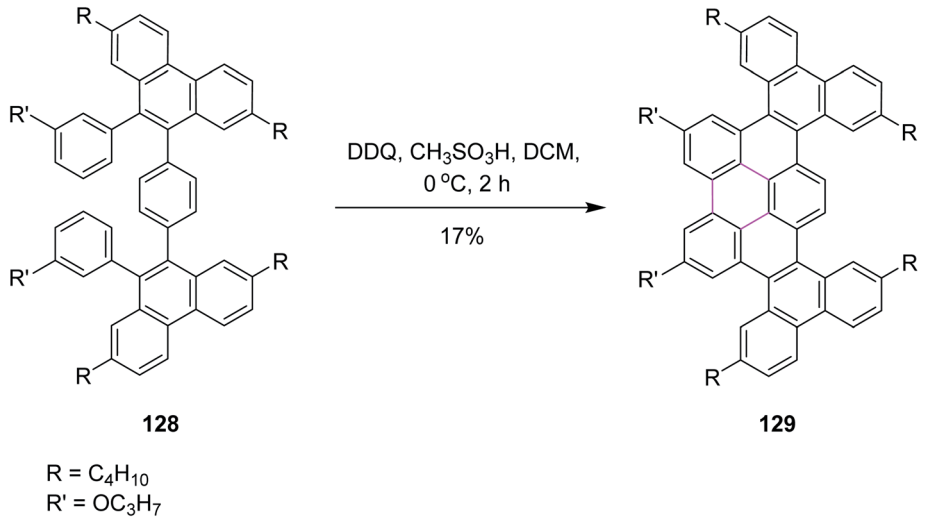

Scheme 51 Synthesis of nanographene unit *via* the Scholl reaction.

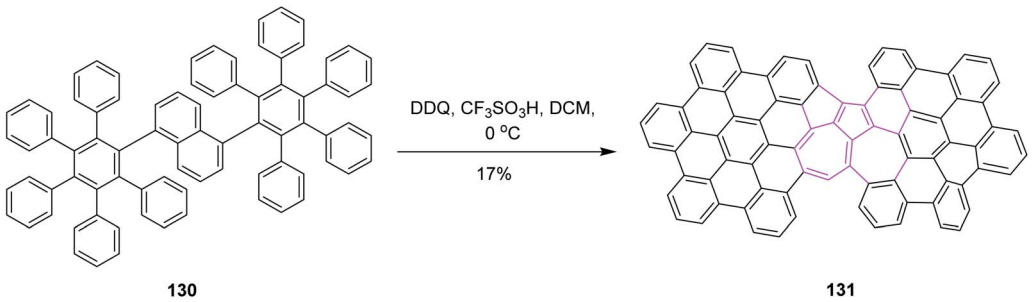

Scheme 52 Synthesis of azulene nanographene *via* the Scholl reaction.

isolated compound **128**. They also utilized $FeCl_3$ but DDQ provided the desired product selectively.[83]

In the same year, Chi and co-workers developed a synthetic pathway for azulene-embedded nanographenes **131** by implementing the Scholl reaction. The naphthalene rings of **130** were rearranged into azulene rings *via* DDQ and triflic acid in DCM, as depicted in Scheme 52. Hence, the incorporation of a non-hexagonal ring into a nanographene framework can lead to new electronic properties. Initially, they tested the approach with $FeCl_3$ in DCM but it only gave a complex mixture of products. However, DDQ was used preferentially to obtain the desired product regioselectively.[84] This research represents the first experimental example of the thermodynamically unfavorable naphthalene–azulene rearrangement and may lead to new azulene-based molecular materials.

Later on, Feng and co-workers (2020) prepared helical azulene-embedded nanographenes **133** from precursor **132**. They added three helical units in each nanographene. This was also a non-hexagonal addition of the rings. The synthetic pathway consisted of multiple steps and Scholl cyclization occurred in the presence of DDQ/TfOH in DCM. Here, DDQ provided the highest yield of the azulene-embedded compound *via* the oxidative coupling of diiodo-7,7′-bibenzochrysene **132** (Scheme 53). However, there was also a drawback associated

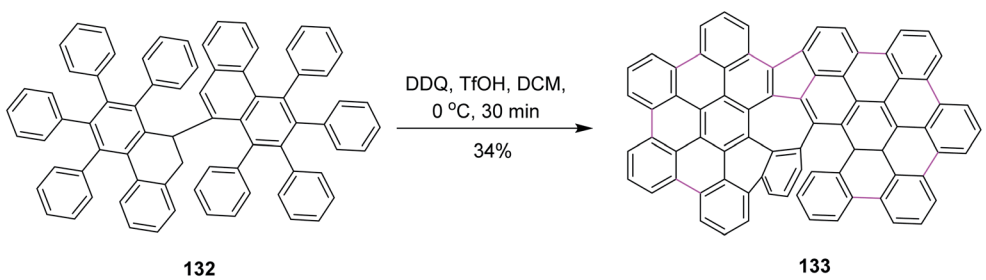

Scheme 53 Synthesis of helical azulene-based nanographene *via* the Scholl reaction.

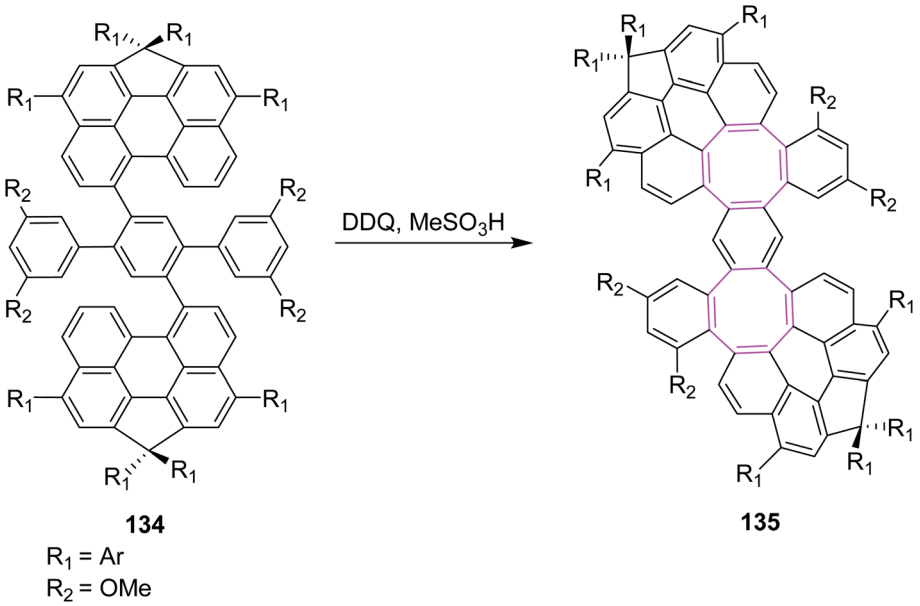

Scheme 54 Synthesis of eight-membered ring-embedded nanographene by the Scholl reaction.

with this type of cyclization as a lot of unidentified by-products were also formed.[85]

In 2021, Wu and co-workers (2021) described various conditions under the Scholl reaction to prepare nanographenes containing hexagonal and octagonal rings. Their procedure was mainly focused on the extension of graphene such as PAHs. They used $FeCl_3$ and DDQ in their reported procedure. The use of iron(III) chloride produced hexagonal rings while DDQ generated octagonal rings in compounds such as **135** *via* the oxidative cyclodehydrogenation of dibenzo-*peri*-hexacene **134** (Scheme 54). The DFT calculations suggested that the DDQ-mediated Scholl reaction occurred by the arenium ion mechanism, while the $FeCl_3$-mediated reaction took place *via* the radical cation mechanism to build the hexagonal ring. Thus, DDQ was preferably used to obtain eight-membered ring-embedded nanographene **135**.[86]

Recently, Miao and co-workers (2021) developed the zigzag nanobelts containing the wave-like arrangement of hexagonal aromatic rings. Hybrid cyclic arene oligomers **137** containing phenylene units were added to build nanographenes in the presence of the DDQ/TfOH set-up in DCM (Scheme 55). These hybrids and highly-strained nanobelts were part of the giant loop system of the polycyclic framework and comprise the advanced form of nanographenes. This area is still under development and offers ample room for future work. In the above study, the authors used both $FeCl_3$ and DDQ simultaneously. The use of DDQ provided impure product, while the use of $FeCl_3$ provided pure ones.[87a] The successful synthesis of these nanobelts demonstrates the power and efficiency of the Scholl reactions in synthesizing strained polycyclic aromatics. Previously, in 2019, Miao and co-workers reported the synthesis of carbon nanobelts from 2,5-di(benzyloxy)-1,4-benzoquinone in six steps by the π-expansion of the corresponding polyarylated carbon nanorings through the Scholl reaction.[87b]

Recently, Kuck, Chow, and co-workers (2021) disclosed the synthesis of TBTQ-based wizard hat-shaped π-extended nanographene **138** from the precursor polycyclic aromatic compound **138** through the Scholl type dehydrocyclization (Scheme 56). The key step involves the Scholl-type cyclodehydrogenation of precursor **138** upon treatment with the DDQ–TfOH/CH_2Cl_2 oxidative system to afford the unique non-planar PAH **139** in 38% isolated yield. This DDQ-induced

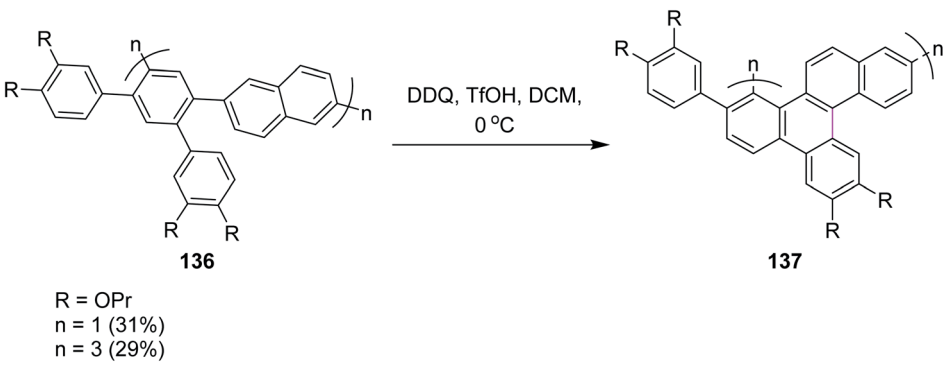

Scheme 55 Synthesis of graphene nanobelts *via* the Scholl reaction.

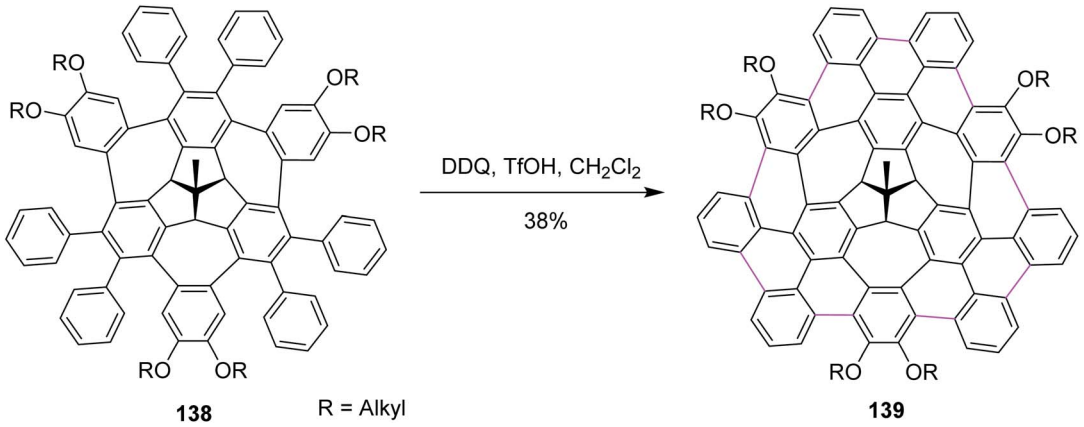

Scheme 56 Synthesis of the π-extended nanographene from the three-fold bay-bridged TBTQ derivative by DDQ/TfOH.

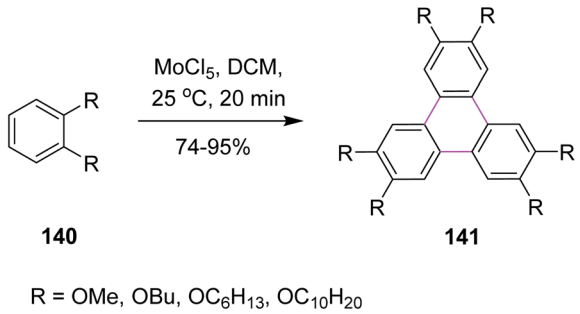

Scheme 57 Synthesis of substituted triphenylenes using $MoCl_5$.

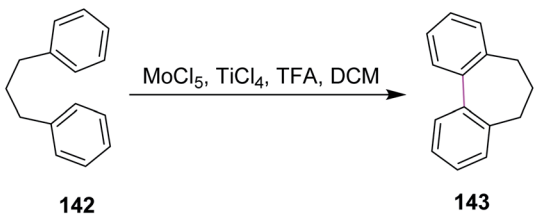

Scheme 58 Construction of a heptagonal ring using $MoCl_5$.

methodology has paved the way to design and synthesize electron-rich π-conjugated aromatics with the combination of five-, six-, and seven-membered carbocycles with interesting optical and electronic properties.[88]

From the abovementioned discussion, it is concluded that DDQ has excellent oxidant oxidizing capacity as compared to $FeCl_3$ and $AlCl_3$. Its reduction potential value is +0.50 V.

5.4. Molybdenum pentachloride ($MoCl_5$)-mediated Scholl reaction

Over the past two decades, molybdenum pentachloride ($MoCl_5$) was explored as an eco-friendly and efficient catalyst to perform the Scholl reaction. In this context, Kumar and Manickam (1997) developed a synthetic methodology for the synthesis of substituted triphenylene **141** *via* the oxidative trimerization of substituted benzene **140**. They constructed the C–C bonds using molybdenum pentachloride ($MoCl_5$) in DCM, affording the Scholl reaction, as depicted in Scheme 57. These sophisticated $FeCl_3$-based methods are useful for the preparation of low degree-substituted triphenylenes but are difficult to apply for large-scale production, while $MoCl_5$ was used for large-scale production. The reaction occurs under very mild conditions with or without an acid catalyst and in a very short time at room temperature. Moreover, the workup for this reaction was quite simple and provided high yield.[89]

In 2004, Kramer and Waldvogel proposed a novel protocol to prepare heptagonal ring-containing hydrocarbon **143** *via* the Scholl reaction. They utilized a combination of $MoCl_5$ and $TiCl_4$ in DCM to construct the seven-membered ring between two benzene rings from the precursor **142**, as shown in Scheme 58. The synthetic potential of $MoCl_5$ in oxidative cyclization is clear as it enabled the construction of a seven-membered ring. This type of reagent system gave typical moderate yields. The potential of $MoCl_5$ was enhanced significantly by Lewis acid additives such as $TiCl_4$. This reagent system provided comparatively high yields and proved to be efficient for this type of synthesis.[90]

In 2009, Waldvogel and co-workers devised a procedure for the preparation of thianthrene **145a** and **145b** by the oxidative coupling of the arylsulfides **144** with molybdenum pentachloride-

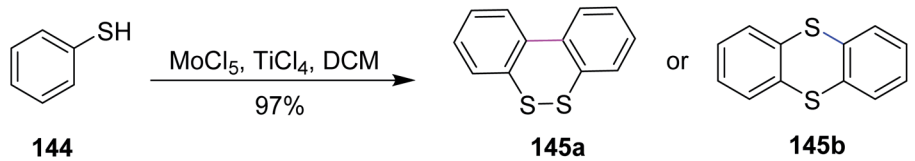

Scheme 59 Synthesis of thianthrene with $MoCl_5$.

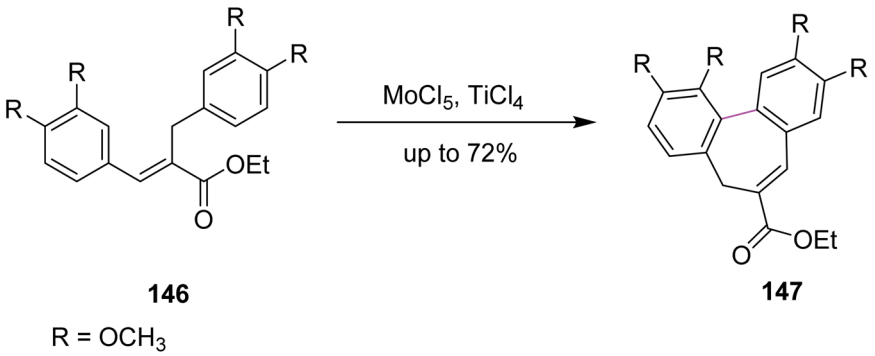

146

R = OCH_3

147

Scheme 60 Synthesis of metasequirin *via* $MoCl_5$.

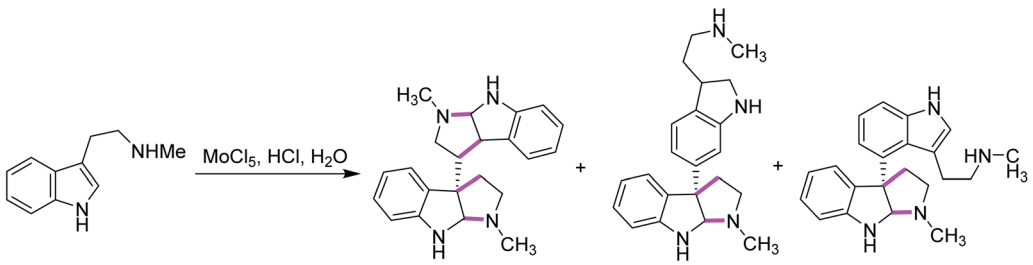

148

149a 7%

149b 4%

149c 12%

Scheme 61 Screening of the $MoCl_5$ oxidant for the oxidative dimerization reaction.

induced Scholl reaction (Scheme 59). In such types of reactions, a strong oxidizing agent was required to promote the insertion of the sulfur–arene bond. Therefore, $MoCl_5$ was used for this synthetic pathway, which features one-electron oxidation and successfully accomplished Scholl cyclization in the presence of $TiCl_4$ (Lewis acidic additive).[91] Hence, the oxidative treatment of 1,2-diaryldisulfides using $MoCl_5$ or mixtures thereof with $TiCl_4$ gives quick access to thianthrenes in moderate to excellent yields. Due to the cationic exchange of the aryl moiety, the cross-coupling of mixed disulfides does not proceed cleanly.

In 2011, Waldvogel and co-workers followed the same synthetic pathway for the synthesis of product **147**. They employed $MoCl_5$-mediated oxidative coupling to construct the C–C bond in **146** by the Scholl reaction, as described in Scheme 60. Due to the presence of multiple functional groups, $MoCl_5$ was used as a strong oxidizing agent and was shown to tolerate these functional groups to achieve the particular substitution pattern on the aryl groups. The authors successfully produced selective heptagonal rings bearing the carboxymethyl moiety without oxidizing any other functional group in good yield (72%).[92] Notably, the insertion of the carboxymethyl moiety on the seven-membered ring can only be achieved by the $MoCl_5$/$TiCl_4$ mixture.

In 2013, Ishikawa and co-workers presented a direct bio-inspired dimerization reaction, in which the amine-free tryptophan derivatives **148** were used in the presence of an aqueous acidic medium to give dimeric compounds having different

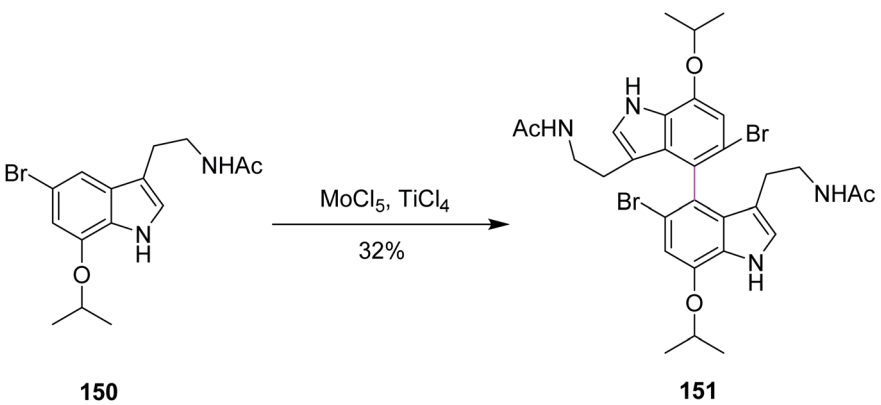

150

151

Scheme 62 Biomimetic synthesis of dendridine.

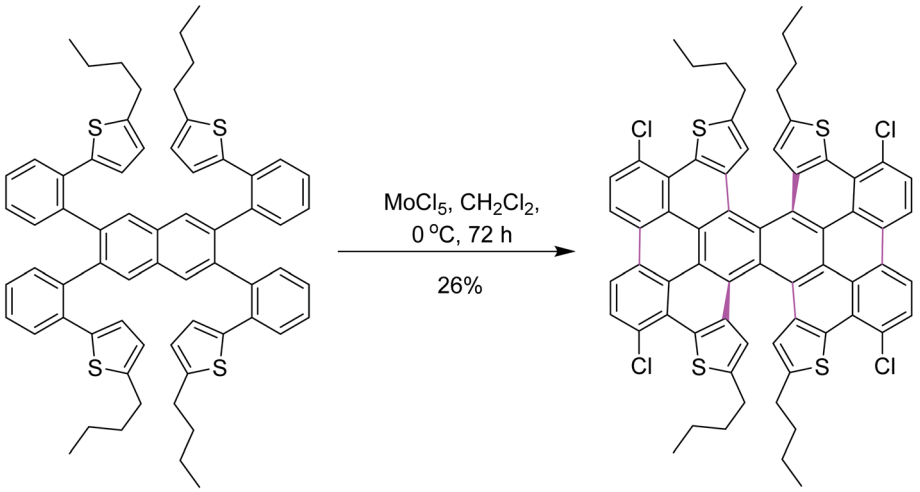

152 153

Scheme 63 Formation of π-extended dithia[6]helicene.

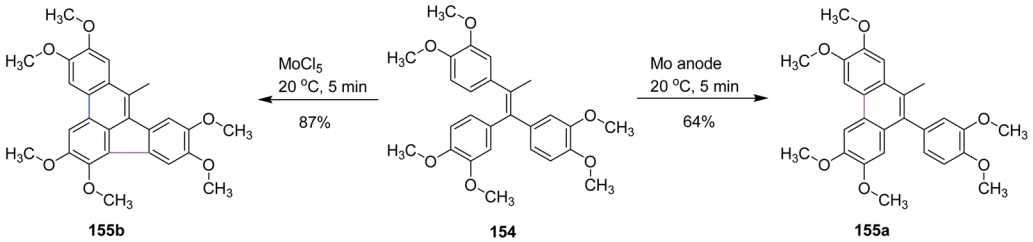

155b 154 155a

Scheme 64 Oxidative coupling of olefin.

symmetries. Different oxidants were utilized where $MoCl_5$ showed quick decomposition when mixed with simple N_b-methyltryptamine in aq. HCl solution and gave two symmetrical compounds, *i.e.*, chimonanthine **149a**, a naturally occurring compound, naseseazine **149b**, and one unsymmetrical dimeric compound **149c** (Scheme 61).[93]

In 2015, Sperry and Boyd proposed a mechanism for the biomimetic synthesis of dendridine **151** involving the intermolecular Scholl-type oxidation reaction of 7-isopropoxytryptamine with $MoCl_5$, following the desired *para–para* coupling. Various oxidants were used initially for this synthetic route but none except $(BuO)_2$ and $MoCl_5$ provided the dimeric product. The 7-isopropoxy substituent **150**, when treated with $MoCl_5$ (generating a radical cation to form the C–C bond) and $TiCl_4$ (a Lewis acid), produced 4,4′-bistryptamine **151** in an impressive ~32% yield while some non-symmetrical compounds appeared as the minor product (Scheme 62). Therefore, $MoCl_5$ was preferred over other reagents.[94]

In 2017, Itami and co-workers worked on different parameters to form novel π-extended double [6]helicene and a dithia[6]helicene having unique 2D structure; here again, the Scholl reaction was carried out with $MoCl_5$. For this purpose, naphthalene derivative **152** was treated with 20 equiv. of $MoCl_5$ in DCM, resulting in the formation of tetrachlorinated π-extended PAH **153** (26% yield), where reduced amounts of the oxidant did not give any fruitful results (Scheme 63). $MoCl_5$ resulted in the production of twisted isomers in this synthetic pathway.[95]

In 2019, Waldvogel and co-workers studied some intramolecular cyclization reactions by comparing them with conventional reagent-mediated coupling reactions. They used olefin **154** as a substrate as it produces five- and six-membered ring-containing compounds, as illustrated in Scheme 64. Surprisingly, different results were obtained under different conditions as under the anodic conditions, the only observed product was a six-membered ring **155a** formed in 64% yield, while the $MoCl_5$-mediated reaction formed product **155b** containing both rings in 87% yield. This method proved to be important because electrochemical intramolecular coupling with high yield was observed with $MoCl_5$ reagent.[96]

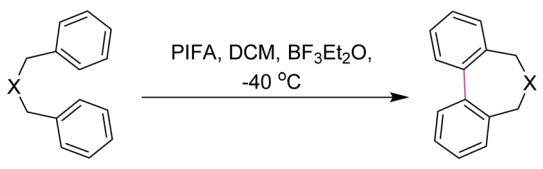

156 157

X = O, N, S

Scheme 65 Oxidative coupling of benzyl ethers with PIFA.

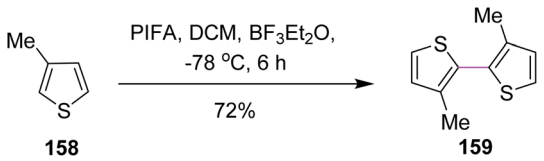

158 159

Scheme 66 Oxidative coupling of bithiophenes with PIFA.

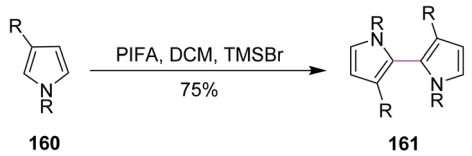

160 161

R = Aryl

Scheme 67 Oxidative coupling of bipyrroles.

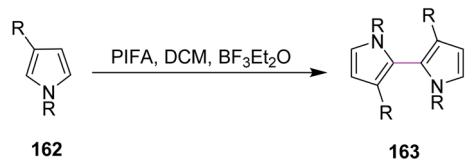

162 163

R = Hex

Scheme 68 Oxidative coupling of bipyrroles.

5.5. Phenyliodinebis(trifluoroacetate) (PIFA)-mediated Scholl reaction

In 1998, Kita and co-workers employed the oxidative coupling of arene derivatives **156** by the Scholl reaction using a unique oxidation agent such as PIFA. This hypervalent iodine reagent PIFA induced the intramolecular oxidative coupling reaction of the biaryls to generate seven-membered rings in biphenyls **157** (Scheme 65). Notably, the previously used reagents comprised of heavy and toxic metals, which did not give satisfactory products. Therefore, PIFA was proved to be superior to metals for performing the Scholl reaction.[97]

Kita and co-workers (2003) followed the same protocol of PIFA oxidative coupling for the synthesis of the bithiophenes/dithienyl derivative **159**. The substituted thiophenes **158** were subjected to the PIFA/$BF_3 \cdot Et_2O$ complex to generate the C–C bond between the two aryl units (Scheme 66). The reaction featured the selective and direct oxidative coupling reaction of alkyl thiophene derivatives without any activation of the thiophene monomers using the PIFA–$BF_3 \cdot Et_2O$ reagent system.[98]

In 2006, Kita and co-workers synthesized bipyrroles by the oxidative coupling of substituted pyrroles **160**. They utilized PIFA/TMSBr in DCM to construct the C–C bond of bipyrroles **161** under the Scholl reaction (Scheme 67). Palladium salts were used previously for the oxidative coupling of pyrroles. However, Pd salts produced many unwanted by-products during this reaction. Hence, the reagent system was shifted toward the direct coupling strategy using PIFA.[99]

In 2009, Kita and co-workers used the same earlier approach for bithiophenes and bipyrroles synthesis using the PIFA/BF_3-$\cdot Et_2O$ complex for the Scholl reaction as an extension of their previous work. The group synthesized compound **163** from pyrrole **162** (Scheme 68). The authors favored PIFA over other reagents due to its high reactivity and the possibility to recycle iodine. In addition, PIFA is a valuable reagent for the oxidative coupling of heterobiaryls.[100]

In 2013, Shafir and co-workers performed direct dehydrogenative coupling reaction under Kita's conditions using hypervalent PIFA–BF_3. The oxidative arylation of simple

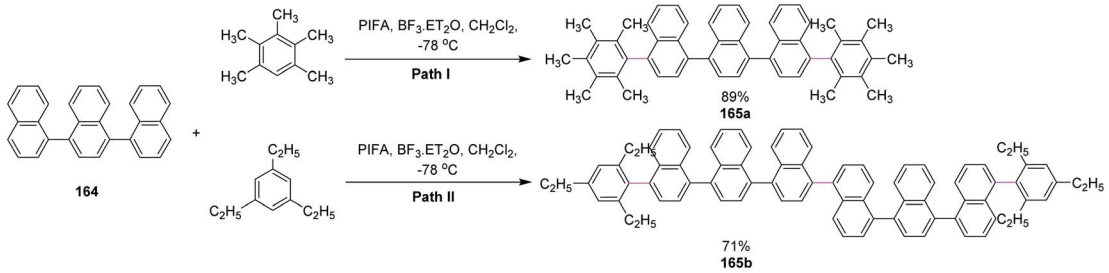

Scheme 69 Oxidative arylation of ternaphthyls.

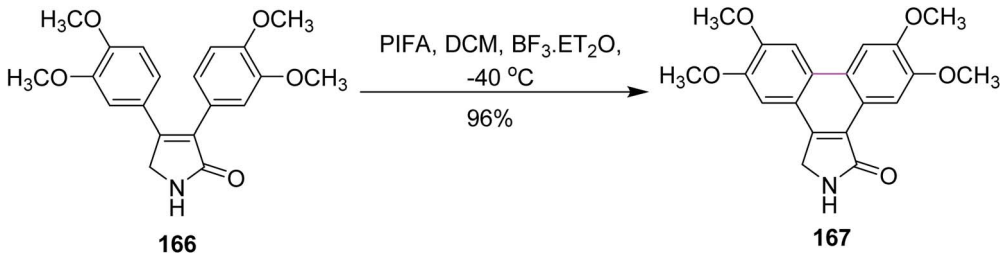

166 167

Scheme 70 Oxidative cyclization using PIFA–$BF_3 \cdot ET_2O$.

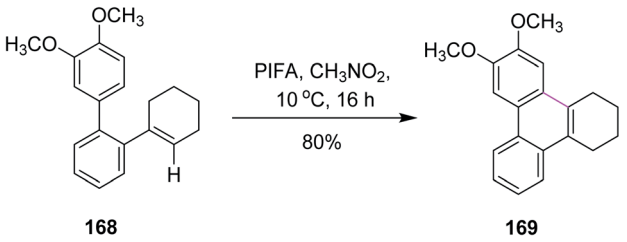

Scheme 71 A controlled oxidative intramolecular arene–alkene coupling reaction.

ternaphthalene **164** Nap_3 with pentamethylbenzene (path I) and triethylbenzene (path II) was achieved using the PIFA/$BF_3 \cdot Et_2O$ reagent system and produced excellent yield of the double arylation products **165a** and **165b**, respectively; however, such results were not observed for bulkier arenes as they lowered the reaction efficiency (Scheme 69).[101]

In 2014, Pelkey and co-workers synthesized dibenzo[*e*,*g*] isoindol-1-ones following the Scholl-type cyclodehydrogenation pathway with the PIFA reagent. They investigated the effect of different methoxy groups, which were substituted on 3,4-diaryl-3-pyrrolin-2-one substrates. Thus, substrates bearing one 3,4-dimethoxyphenyl group afforded 60–90% product yield while those bearing two 3,4-dimethoxyphenyl groups as in **166** gave **167** in 96% yield and substrates without such a moiety did not give desired product in yields higher than 50% (Scheme 70). The PIFA-mediated oxidative cyclization offered both symmetrical and unsymmetrical products in good yield and the reagent system was favored due to its facile and mild oxidative transformations.[102]

In 2016, Breder and co-workers established a mechanism for the synthesis of substituted phenanthrene analogs by selective oxidative intramolecular arene–alkene coupling (a Scholl-type reaction). They used different iodine(III)-mediated reagents such as PIFA, (diacetoxyiodo)benzene (PIDA), and *N*-chlorosuccinimide (NCS) to achieve this goal. While the addition of PIDA into 2,3,4,5-tetrahydroterphenyl derivative **168** did not setup the required reaction, PIFA (1 equiv.) at 10 °C produced product **169** in 80% yield in the presence of CH_3NO_2 (Scheme 71). PIFA, in this case, offered more consistent chemical conversion and isolated products in high yields.[103]

In the same year, Pelkey and co-workers prepared benzocarbazoles and an indolocarbazole using 3-aryltetramic acid as the substrate and the BF_3–PIFA reagent system. The respective fused carbazole **171** (83%) was obtained by the Scholl-type reaction by reacting 4-indolylpyrrolone **170** in the presence of PIFA and $BF_3 \cdot Et_2O$ (Scheme 72). A similar method was applied to the synthesis of indolocarbazole **173**, which was obtained in 69% yield through the oxidative cyclization of **172** (Scheme 73).[104]

In 2017, Li and co-workers devised a novel strategy to produce highly conjugated acenes, an important material to be used in electronics and optical devices, through two pathways, namely, Kita-coupling and Scholl type oxidative cyclodehydrogenation. Firstly, the precursors for acenes **175a** and **175b** were formed using ter-**174a** and quaternaphthyls **174b** and mesitylene under mild oxidation conditions (PIFA/$BF_3 \cdot ET_2O$ in CH_2Cl_2). Then, the prepared precursors **175a** and **175b** were subjected to reaction with $FeCl_3$ (oxidant and Lewis acid) to form promising products **176a** and **176b** in good yields (Scheme 74).[105]

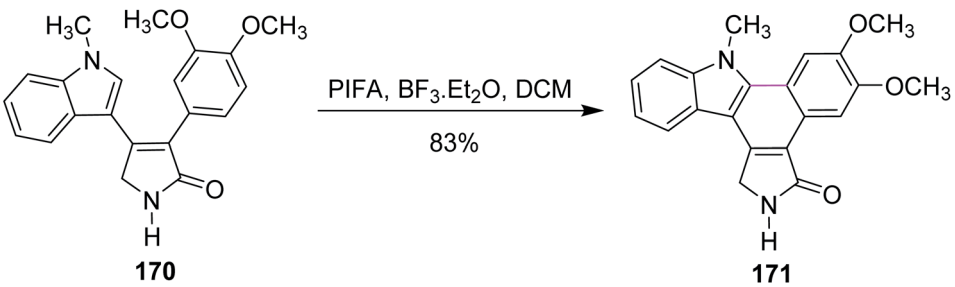

Scheme 72 An example of benzocarbazole synthesis.

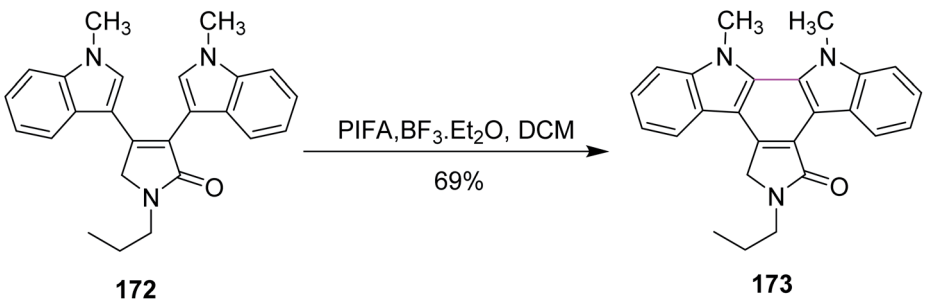

Scheme 73 Indolcarbazole synthesis.

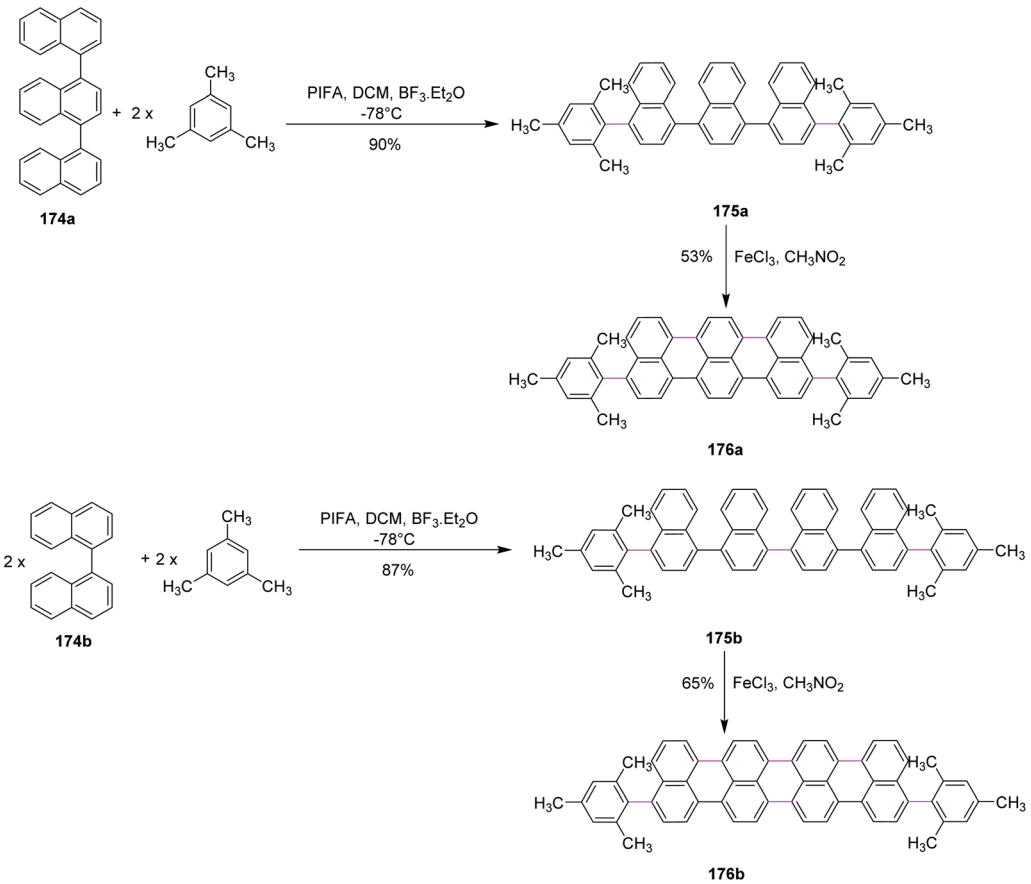

Scheme 74 Synthesis of highly conjugated acenes.

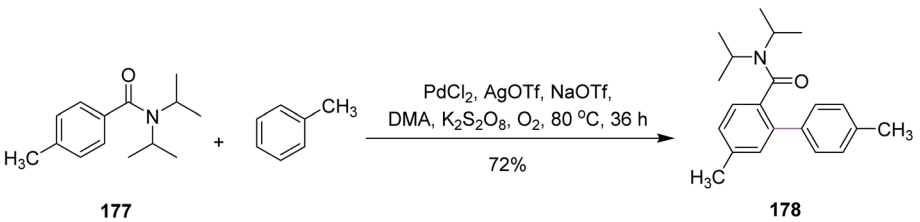

Scheme 75 Oxidative coupling of a tertiary benzamide with toluene.

5.6. Palladium- and chloranil-mediated Scholl reaction

In 2015, Guan and co-workers introduced new conditions comprising of a mixture of palladium (Pd) and chloranil to carry out the intermolecular Scholl reaction. They reported a variety of *para*-substituted biaryl units **178** synthesized from the coupling of tertiary benzamides **177** with arenes through palladium-catalyzed oxidative coupling reaction using dipotassium peroxodisulfate as the oxidant (Scheme 75). This was a potentially favored approach toward the selective arylation of mono-substituted arenes with high yield due to easily accessible reaction conditions. Due to the mild conditions and the easy availability of substrates and oxidant, this method could

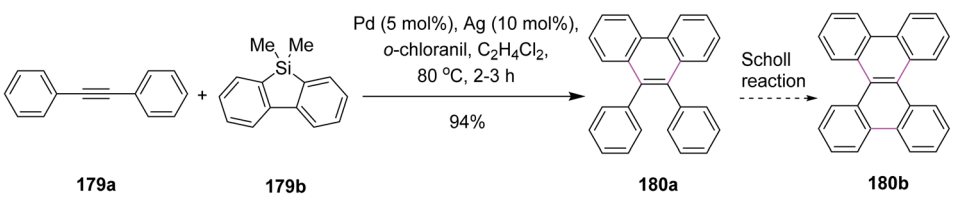

Scheme 76 Pd catalyzed APEX of PAHs.

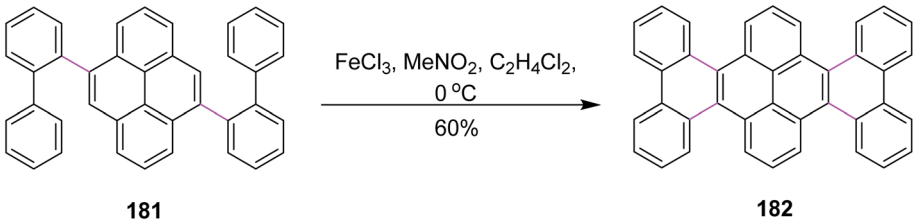

Scheme 77 π-extension of perylene by the Scholl reaction.

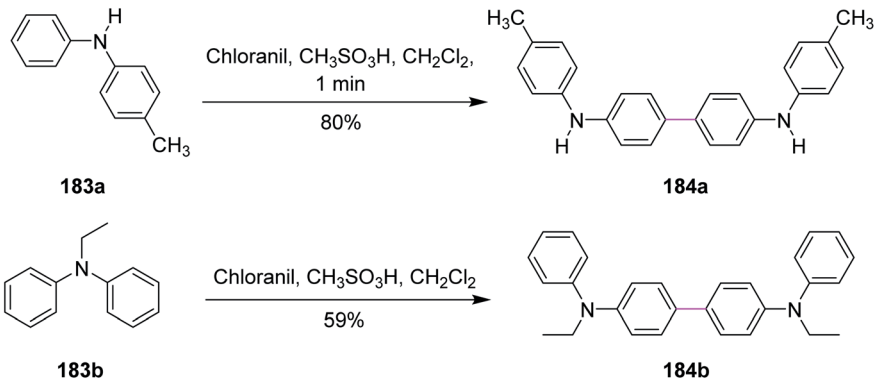

Scheme 78 Oxidative coupling of secondary and tertiary aromatic amines under the Scholl reaction.

potentially provide a practical approach for the synthesis of *p*-substituted biaryl compounds.[106]

In 2017, Itami and co-workers proposed a synthetic pathway for the annulative π-extension (APEX) of alkyne **179a** *via* Pd/*o*-chloranil catalysis. The regioselective APEX of PAHs could provide structurally uniform nanographenes such as **180b** by the Scholl reaction (Scheme 76). $CuCl_2$ was initially used for this purpose but it proved to be ineffectual. On the other hand, Pd promoted this reaction more efficiently. This reagent system expanded the APEX reaction considerably. In addition, the double APEX reaction of alkynes was also established as an efficient route to obtain sterically-hindered diphenanthrylenes.[107]

In the same year, Itami and co-workers developed a protocol for nanographene synthesis by the Scholl reaction. The APEX reaction was carried out in the presence of *o*-chloranil to produce compound **181**. Subsequently, this precursor was subjected to SR in the presence of $FeCl_3$ to furnish hexabenzotetracene **182** in good yield (Scheme 77). Metallic Pd catalyzed the regioselective construction of clover-shaped nanographenes in this method.[108]

In 2017, Venkatakrishnan and co-workers revealed a specific type of intermolecular oxidative C–C coupling of arylamines **183a** and **183b** for the formation of benzidines or naphthidines **184a** and **184b**, respectively, using the quinone-based organic reagents, *i.e.*, chloranil, instead of using any metal-containing oxidant. The aim was to learn about the chemistry of both the reaction mechanism and the preferred oxidative dimerization of substituted arylamines (either secondary or tertiary). The synthetic perspective (Scheme 78) showed that the methodology worked not only for substrates with various functional groups but also for ones with sterically hindered reactive sites.[109]

5.7. Other miscellaneous reagents for the Scholl reaction

In 1980, Taylor and co-workers developed a new synthetic approach for the regiospecific oxidative coupling of substituted benzenes **185**. The reaction was carried out in the presence of thallium trifloroacetate (TTFA) under Scholl reaction conditions to synthesize substituted biaryls **186**, as shown in Scheme 79. The authors reported that TTFA provided better yield as compared to $FeCl_3$ and $Hg(OCOCF_3)_2$ for biaryl synthesis while $Pb(OCOCH_3)_4$ provided either equal of better yields than TTFA. Thus, this reagent was selected and used preferentially over all other reagent systems to prepare, in particular, biaryls in good yields.[110]

In 1994, Wegner and co-workers devised a protocol for oxidative biaryl coupling using vanadium oxyfluoride to construct the C–C bonds by the Scholl reaction. The new hexagonal ring in compound **188** was formed between two substituted aryl rings of the benzil derivatives **187** mediated by the $VOF_3/BF_3 \cdot Et_2O$ complex in DCM with excellent yield (Scheme 80). Such oxidizing agents such as vanadium oxyfloride and other transition metal oxides were innovative and effective

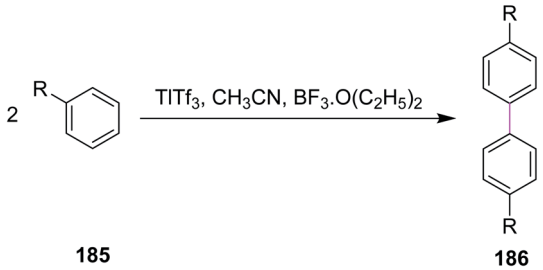

Scheme 79 Biaryl construction *via* Scholl reaction with $TlTf_3$.

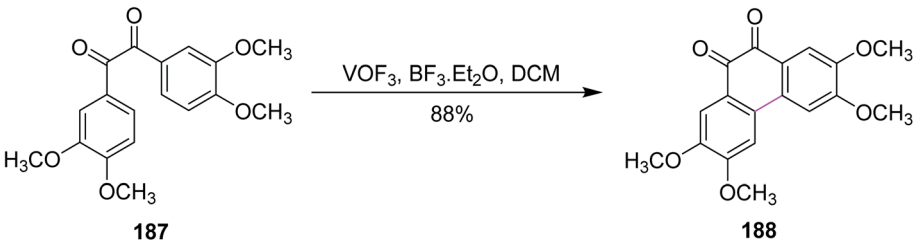

Scheme 80 Biaryl coupling with vanadium oxyfloride.

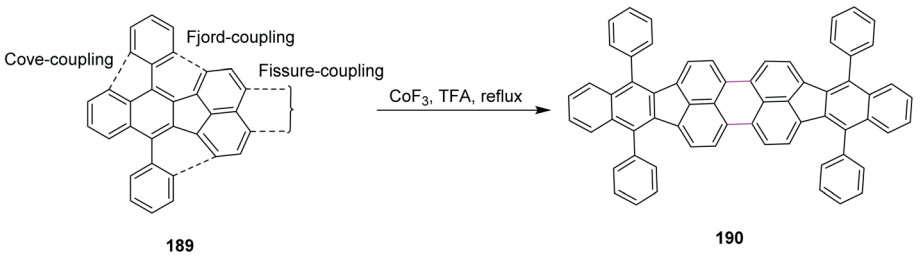

Scheme 81 PAHs extension with CoF_3.

means for intermolecular coupling, which are frequently utilized in the synthesis of various substituted benzils. The group used two oxidants simultaneously for this reaction, namely, thallium oxide and vanadium oxyfloride. The latter reagent gave the highest yield.[111] Substituted benzils and phenanthrene-9,10-diones constitute the key precursors for ligands in the field of discotic metallomesogens or polymeric mesogens.

In 1996, Bard and co-workers disclosed a new procedure for the synthesis of dibenzo-tetraphenylperiflanthene **190** by the CoF_3-induced Scholl reaction. The C–C bonds of PAH **190** were constructed in floranthene **189** by fissure coupling in TFA (Scheme 81). The notable advantages associated with the procedure involving the CoF_3/TFA reagent system is the flexible and short pathway for the synthesis of a wide range of non-benzenoid aromatics prone to dehydrogenation to highly fused systems by fissure, fjord, and core couplings.[112]

In 1998, Kochi and co-workers expanded the role of hexachloroantimonate in the oxidative coupling of naphthalene derivative **191** to generate the substituted binaphthyl **192** (Scheme 82). This reagent system provided the selective oxidation of aromatic donors (ArH) and permitted the easy synthesis and isolation of the pure biaryl product, successfully avoiding the chlorinated by-products.[113]

In 1999 and 2001, Kumar and Varshney introduced a synthetic pathway for the oxidative trimerization of substituted benzenes **193**. They synthesized unsymmetric triphenylene **194** using vanadium oxytrichloride in DCM and following the Scholl reaction, as shown in Scheme 83. $VOCl_3$ was the only liquid reagent used in the oxidative cyclization reaction and is soluble in common organic solvents. Therefore, handling the reaction under anhydrous conditions for large-scale synthesis was quite facile. It is noted though that some side products were also observed during this reaction.[114,115]

In 2008, Kita and co-workers developed a C–C bond formation reaction for phenols **195**. The reaction employed the H_2O_2/anhydrous acid complex for an iodoarene-catalyzed reaction to construct the seven-membered ring **196** by Scholl cyclization, as shown in Scheme 84. This metal-free reagent system provided an environmentally-benign synthetic pathway. An outstanding issue was that strong oxidizing agents could oxidize the iodoarenes to the iodine (I_2) at a low temperature. To circumvent this drawback, TFAA-modified with H_2O_2 was used during the spirocyclization of phenols to obtain high yields of novel aryl systems.[116]

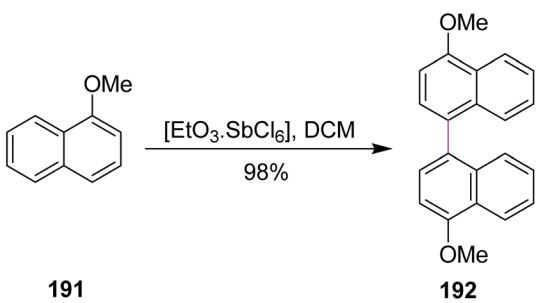

Scheme 82 Biaryl coupling *via* the Scholl reaction.

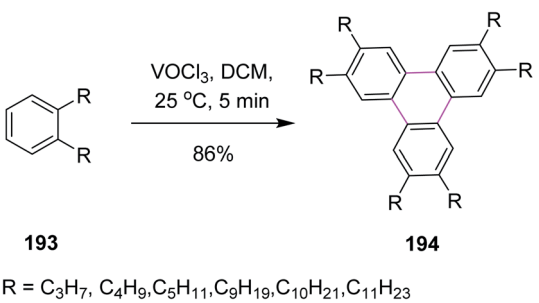

Scheme 83 Synthesis of triphenylenes with vanadium oxytrichloride.

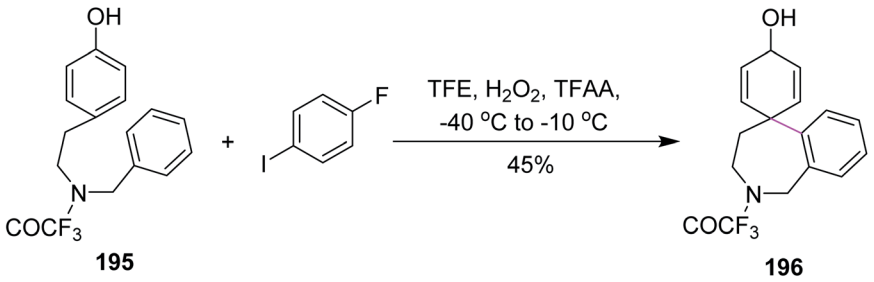

Scheme 84 Synthesis of the heptagonal ring by iodoarene using the Scholl reaction.

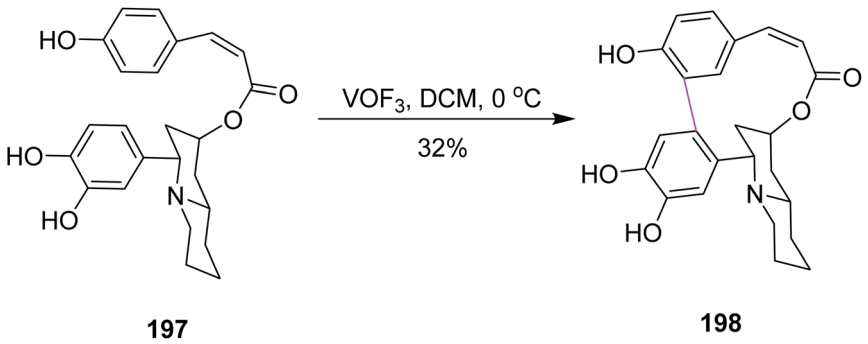

Scheme 85 Synthesis of decinine with vanadium oxyfloride.

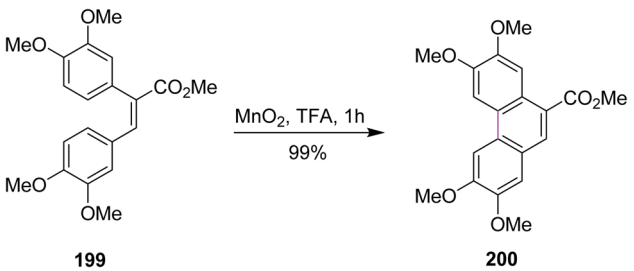

Scheme 86 Synthesis of phenanthrene with MnO_2/TFA.

In 2009, Yang and co-workers described the methodology behind the oxidative biaryl coupling of esters **197**. They reported the atropselective synthesis of decinine **198** using vanadium oxyfloride following non-phenolic oxidative Scholl cyclization, as depicted in Scheme 85. Decinine consisted of a macrocyclic ring, a quinolizidine ring, and a biphenyl moiety. The strained 12-membered macrocyclic ring that connected the two aryl rings was constructed by oxidative cyclodehydrogenation. VOF_3 played a key role in realizing the total synthesis of racemic decinine.[117]

In 2010, Wang and co-workers revealed a novel methodology for the oxidative coupling of polycyclic aromatic hydrocarbons *via* manganese dioxide-induced Scholl reaction. The phenanthrene **200** was synthesized using the MnO_2/acid system for the coupling of stilbenes **199** (Scheme 86). They used readily available manganese oxide as a mild oxidizing agent to create intermolecular and intramolecular C–C bonds in unfunctionalized arenes in the presence of protic acid. Excellent yields were obtained with less tedious experimental work.[118]

In 2010, Kita and co-workers developed a protocol for the regioselective oxidative coupling of thiophenes **201** by the Scholl reaction. Bithienyls **202a** (64%) and **202b** (>5%) were synthesized in the presence of HTIB- and HFIP-activators, as shown in Scheme 87. The typical metal oxidants were replaced with hypervalent iodine reagent (HTIB) to provide the regioselective products. This particular approach was a novel, selective, facile, and direct route for the coupling of thiophenes to obtain

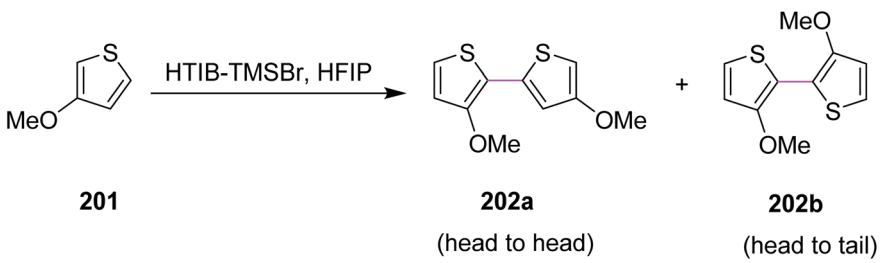

Scheme 87 Bithiophene synthesis by HTIB-activators.

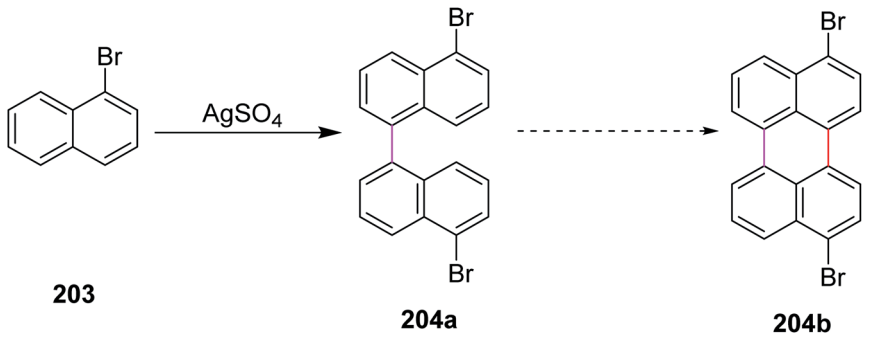

Scheme 88 C–C coupling of naphthalene units with $AgSO_4$.

bithiophenes.[119] On the basis of this strategy, a novel direct method for the synthesis of head-to-tail bithiophenes using hypervalent iodine(III) reagents has been developed.

In 2017, Leszczynski and co-workers reported a synthetic approach for the oxidative coupling of aromatic hydrocarbons **203** using silver sulphate as a novel reagent for intermolecular Scholl cyclization to construct C–C bonds between two aryl groups in **204a** (Scheme 88). The chemical transformation of precursor **204a** into the coupled product **204b** is still challenging. This synthetic methodology was economical and cost-effective. $AgSO_4$ could simply be regenerated electrochemically from $AgHSO_4$ (side-product). This particular coupling technique does not provide high yield and still requires further optimization.[120]

In 2020, Borchardt and co-workers introduced a novel and alternative reaction strategy to synthesize nanographenes, for example, hexabenzocoronene **206**. They used a combination of elemental copper and sodium chloride for the mechanochemical cyclodehydrogenation of hexaphenylbenzene **205** to generate six new C–C bonds in HBC **206** (Scheme 89). The procedure was carried out under solvent-free conditions in a ball-mill apparatus. This methodology proved to be more efficient, cheap, and easy compared to the previous ones. Using this method, other PAHs such as triphenylene were also obtained without any side products. Unlike $FeCl_3$, elemental copper did not give any chlorinated or dimerized products.[121]

Moreover, the researchers used electrochemistry to perform the Scholl reaction using several different substrates. Previously, the involvement of cation radical intermediates (formed by single electron oxidation) in oxidative C–C bond formations or biaryl syntheses has been carefully probed by Evrard,[122a] Rathore,[122b] and co-workers.

In 2021, Müllen and co-workers explored a one-step electrochemical method to synthesize unsubstituted PAHs, starting from twisted oligophenyl precursors and depositing their films with highly ordered and tightly packed structures. In this methodology, anodic oxidation was used in order to replace already existing chemical oxidizing agents used in the Scholl reaction for the formation of a new C–C bond between the two arene units. The electrochemical oxidative characteristics of the triangle-shaped precursor **207** and the ribbon-shaped precursor **209** (Scheme 90)[123] were first studied by cyclic voltammetry (CV) at a scan rate of 0.05 V s^{-1} using glassy carbon as a working electrode. The formation of π-conjugated discs of PAHs dramatically decreased the solubility, causing precipitation under the formation of homogeneous thin films in the neutral state. This electrochemical deposition method substantially simplifies the film-forming process and produces high quality thin PAH films with a controlled thickness and doping level. Furthermore, the group/authors enlarged the size to precursor **215** to produce PAH **212** (C-96). The envisaged product that formed at a potential of 1.65 V appeared to be incompletely cyclodehydrogenated. This behavior was contradictory to the formation of nanographenes **208** and **210**. Nonetheless, the complete dehydrogenation of precursor **211** into the flat disc **212** was achieved at a potential of 1.50 V. In fact, it is supposed that the large molecular size of precursor **211** increases the degree of charge delocalization over the large oligoaryl moieties and, in turn, the less reactive phenonium (or radical) cations hinder the intramolecular oxidative cyclodehydrogenation under mild conditions, which are some limitations associated with electrochemistry used *in lieu* of the oxidant in the Scholl reaction.

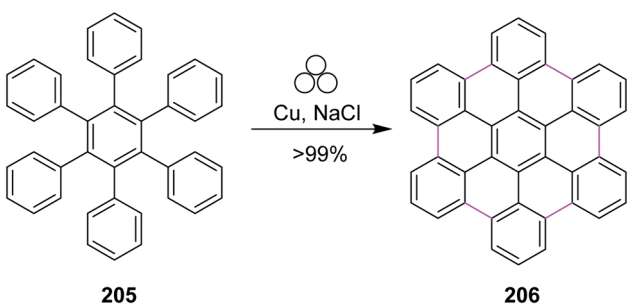

Scheme 89 Mechanochemical cyclodehydrogenation of hexaphenylbenzene by the Scholl reaction.

5.8. Surface-assisted synthesis of nanographenes under the Scholl reaction

The oxidative cyclodehydrogenation method is efficient for the synthesis of nanographenes and GNRs in solution. However, the bottom-up chemical synthesis of these graphene materials in solution suffers from the re-aggregation of graphitic structures during the cyclodehydrogenation of the polyphenylene precursors, which renders the further processing to regenerate single-layer graphenes immensely problematic.

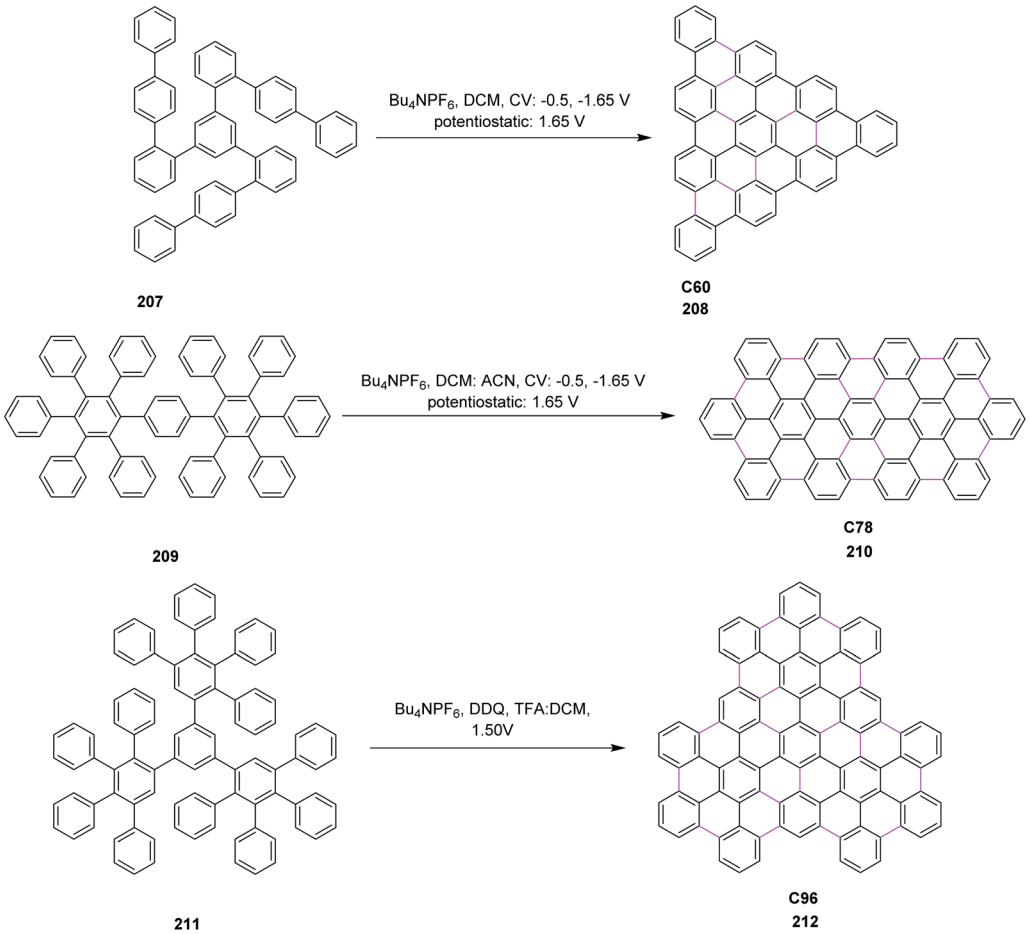

Scheme 90 Oxidative cyclodehydrogenation by electrochemical synthesis.

Recently, researchers involved in the chemical synthesis of nanographenes through the Scholl reaction have shifted their attention toward the use of new protocols aimed at the direct synthesis of graphene materials on the surface *via* the cyclodehydrogenation of pre-deposited or newly established precursors. This technique has proved to be robust and represents

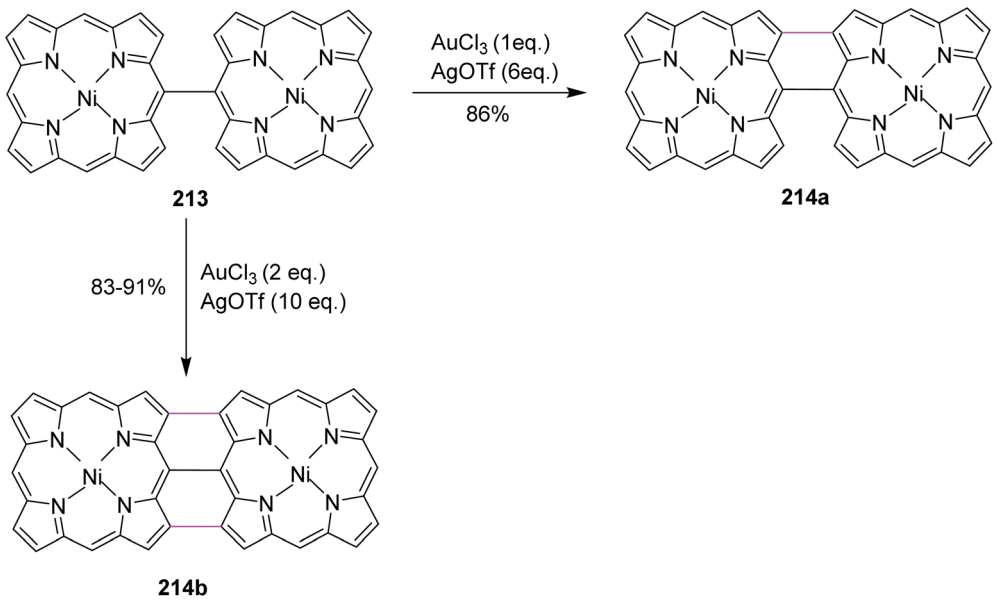

Scheme 91 C–C coupling of porphyrin units using Au(111).

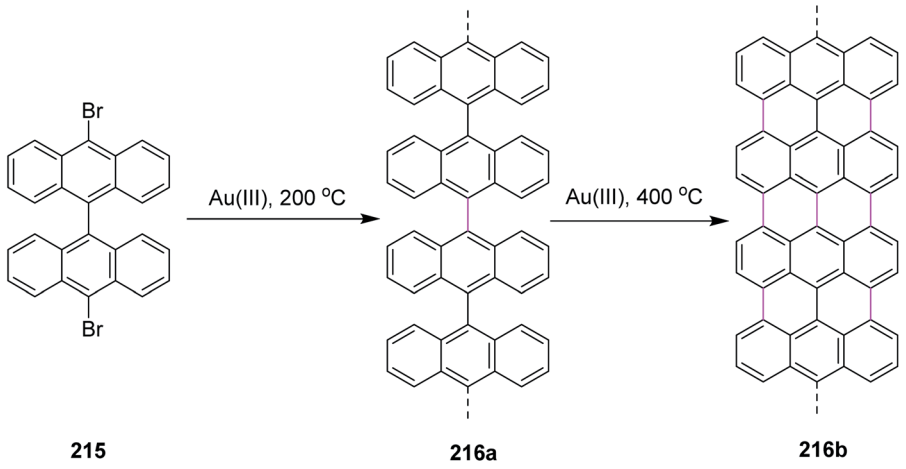

Scheme 92 Graphene nanoribbon synthesis on gold surface.

a promising route for the generation of structurally well-defined nanographenes for applications in electronic devices.

In 2009, Wegner introduced a novel synthetic methodology for the gold-catalyzed oxidative coupling of unfunctionalized aromatic compounds utilizing stoichiometric amounts of gold(111) for the construction of C–C bonds in porphyrin derivatives **213** by the Scholl reaction. Different equivalents of reagents gave different products **214a** and **214b**, as described in Scheme 91. The use of Au(111) during the pathway was convenient because precautions to remove moisture or air were not required. Moreover, oxidative coupling catalyzed by gold enabled the fast and effective construction of complex molecules.[124]

In the follow-up study, Cai and co-workers (2010) introduced a new strategy to construct graphene nanoribbons **216a** and **216b** from precursor **215** at a very high temperature. With a gradual increase in the temperature, the tendency to form the C–C bonds between two aryl groups also increased. The whole process shown in Scheme 92 was carried out on an Au(111) surface. The oxidative cyclodehydrogenation of the precursor monomer **215** was achieved by annealing it on the gold surface by the bottom-up approach. The presence of the gold surface fostered a significant increase in the length of the nanoribbons with ease.[125] In this case, gold offered an alternative to the oxidant used in the Scholl reaction. The polymerization of monomer **215** on the gold surface proceeded through two steps. This involved dehalogenation, followed by cyclodehydrogenation under the Scholl reaction.

In 2016, Ruffieux and Fasel developed a synthetic route toward cove-edged GNR **218b** employing 11,11′-dibromo-5,5′-bischrysene **217** as the monomer (Scheme 93).[126] Although a variety of GNRs with armchair-type edges have been prepared, GNR **218b** is the first GNR with the cove-edge structure. Short dimers and tetramers of GNR **218b** were separately synthesized in solution as the model compounds, and the single-XRD analysis of the tetramers revealed non-planar structures of such cove-edged GNRs with alternate "up-down" conformations of the peripheral benzene rings. The DFT calculations predicted a bandgap of 1.70 eV for cove-edged GNR **218b**. The successful bottom-up synthesis of atomically precise GNRs creates ample opportunities and challenges for the analysis of their physical properties (for example, the magnetism and charge/spin transport) and for the fabrication of GNR-based devices such as the proposed spin valves.

In 2017, Meunier and co-workers revealed a new approach for the on-surface formation of C–C bonds by the formal cycloaddition of the precursor monomer, which are halogen-functionalized at the *ortho* (2,3) positions of arenes **219a**. Choosing a 2,3-dibromotetracene precursor, the authors achieved the formation of tetracene linear dimers **220**, *cyclo*-trimers **221**, and X-shaped tetramers **222** (Scheme 94) under the Scholl reaction conditions.[127] This product variety is possible due to the availability of two different coupling scaffolds, namely, the formation of four-membered rings (cyclobutadiene units) *via* the [2+2] cycloaddition **220** and the formation of six-membered rings **221** and **222** *via* the [2+2+2] cycloaddition, respectively. *Ortho*-halogen functionalization and the resulting products provide new access to the emerging field of on-surface synthesis, and a prospective pathway to the synthesis of intriguing 1-D structures, such as biphenylene-bridged acene ribbons.

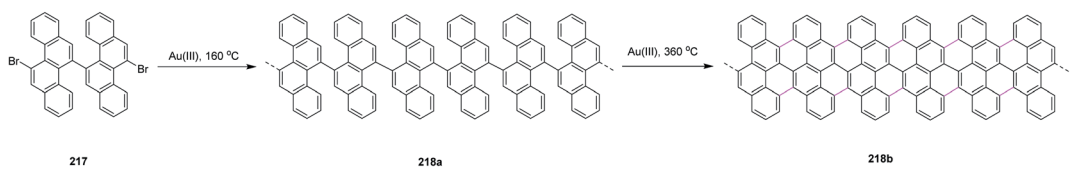

Scheme 93 Synthetic strategy for GNRs with zigzag edges by gold catalysis on the surface.

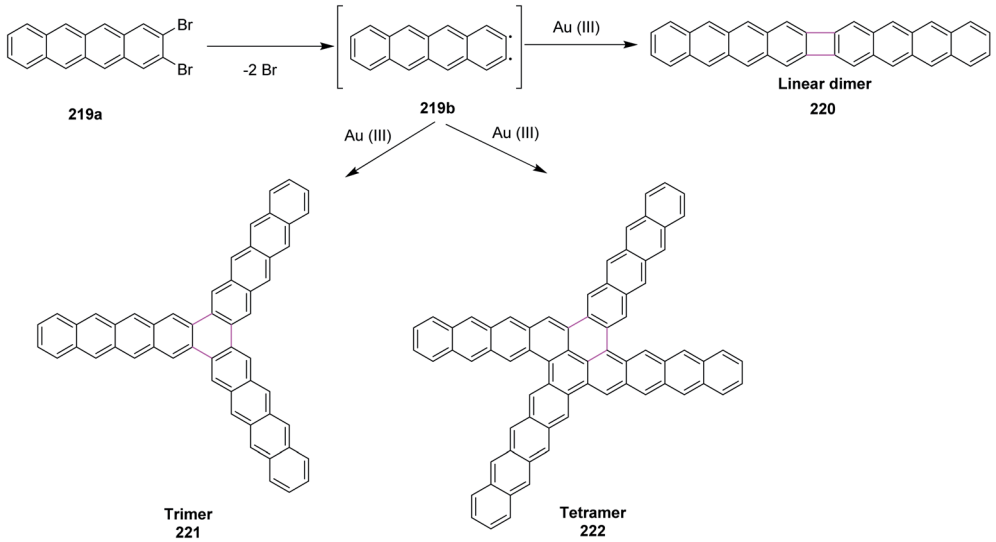

Scheme 94 On-surface cyclization of *o*-dihalotetracenes to four and six-membered rings.

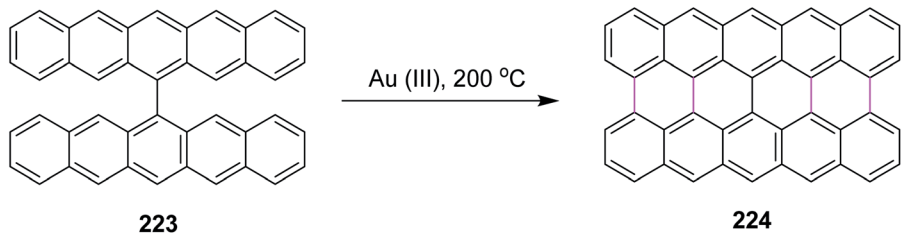

Scheme 95 Synthetic route toward *peri*-pentacene on the Au(111) surface.

In 2017, Feng and co-workers reported that *peri*-pentacene **224** could be obtained under ultra-high vacuum (UHV) conditions on an Au(111) surface by the thermally induced cyclodehydrogenation of the precursor 6,6′-bipentacene **223** (Scheme 95).[128] The fully cyclized *peri*-pentacene **224** was produced by annealing **223** at 200 °C for 30 min. The interaction of *peri*-pentacene with the free valences of the Au surface stabilizes this highly reactive molecule and prevents undesired radical-induced side reactions.

In 2017, Narita and co-workers revealed the on-surface synthesis of planarized heteroatom-doped (oxygen–boron–oxygen or OBO) *peri*-hexacene **226** by thermally annealing the substrate at 380 °C (Scheme 96).[129] Surface-catalyzed cyclodehydrogenation successfully transformed the double helicene **225** into the planar *peri*-hexacene **226.** Furthermore, the non-planar structure **225** underwent a conformational change upon the adsorption on surfaces, and 1D self-assembled superstructures were observed for both **225** and **226** due to the presence of OBO units along with zigzag edges. This work demonstrates a potential edge-heteroatom-doping strategy of the edges for fabricating tailor-made graphene nanoarchitectures and highlights the significance of on-surface chemistry to achieve an increased variety of nano-graphene structures.

In the follow-up study, Fasel and co-workers (2018) demonstrated that on-surface synthesis is a powerful route toward the fabrication of specific graphene-like nanostructures confined in 2D. This strategy was successfully applied to the growth of graphene nanoribbons **229** of diverse width and edge morphology. Particular attention was given to the role of

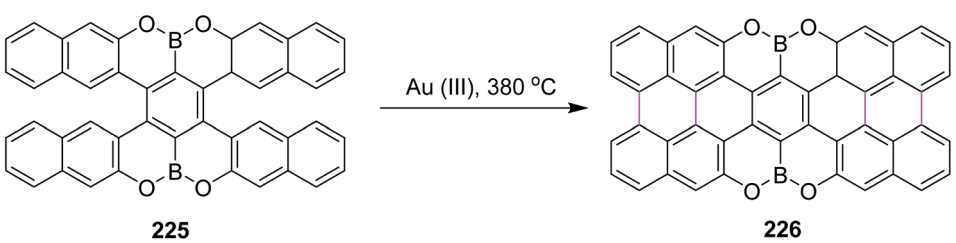

Scheme 96 Synthetic route to the peri-hexacene derivative on gold surface.

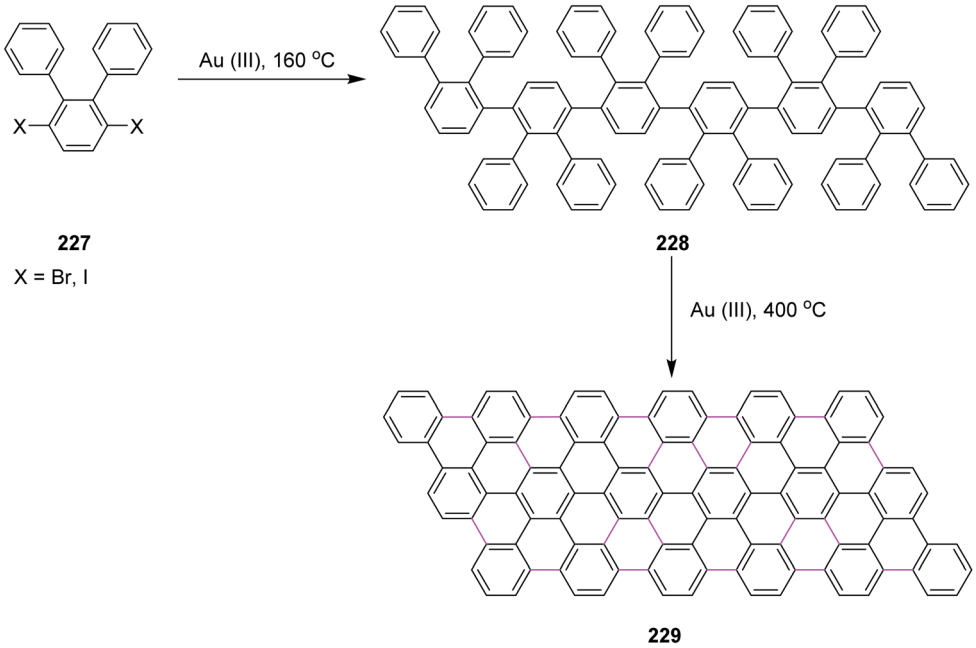

Scheme 97 On-surface growth dynamics of graphene nanoribbons.

halogen functionalization (Br or I) of the molecular precursors **227** (Scheme 97).[130] The researchers showed that the use of di-iodinated monomers fosters the growth of longer graphene nanoribbons (average length of 45 nm) due to a larger separation of the polymerization and cyclodehydrogenation temperatures for the conversion of **228** into **229**. The reaction was thermally activated on Au(111) and proceeds *via* two steps (with $T_1 < T_2$), involving aryl–aryl coupling (after dehalogenation) and cyclodehydrogenation.

In 2019, Pena and co-workers synthesized the trigonal porous nanographenes **231** on gold surface, combining the solution chemistry and surface chemistry under the Scholl reaction. They constructed inter-blade and intra-blade C–C bonds for annular π-extension of PAHs. They implemented on-surface cyclodehydrogenation on the gold surface at elevated temperatures (Scheme 98). They initially used other typical oxidants such as DDQ and $Pd(PPh_3)_4$ but did not get satisfactory results due to incomplete cyclization. The complete cyclization of PAH **230** was realized in the presence of a gold catalyst at enhanced annealing temperature and 3 new C–C bonds **231** were formed.[131]

In 2019, Feng and co-workers introduced a process for the synthesis of non-planar porous nanographenes. They implemented on-surface synthetic methodology for the construction of C–C bonds between the aryl rings upon heating on a gold surface. Notably, this type of cyclization of porous compounds **232** is not possible to carry out in solution; therefore, the reaction was carried out *via* surface chemistry. The well-developed non-planar nanographenes **233** were constructed by annealing the PAHs **232** on the gold surface (Scheme 99).[132]

In 2020, Torres and co-workers introduced a new protocol for the construction of π-extended boron-dipyrromethene (BODIPY) derivatives **235** such as by gold-catalyzed

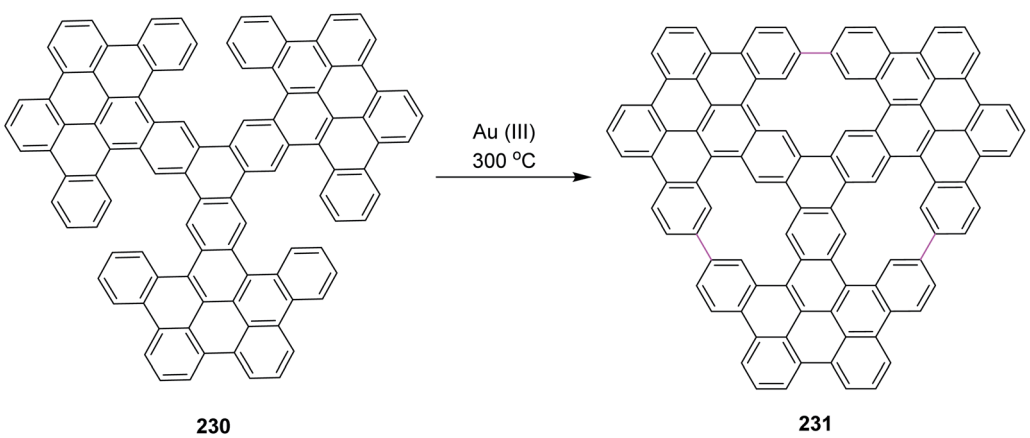

Scheme 98 Trigonal porous nanographene synthesis.

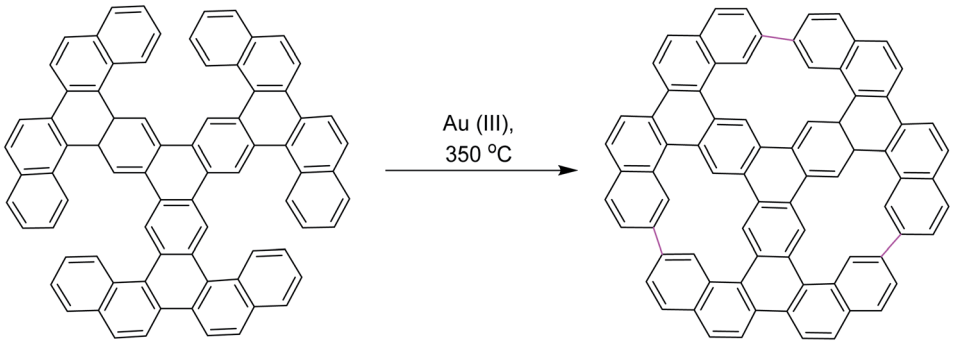

232 233

Scheme 99 Non-planar porous nanographene synthesis.

cycloisomerization. The reaction was carried out under mild Scholl conditions, which provided excellent yields of **235** in a short time. The resulting product was formed regioselectively and formed to be kinetically and thermodynamically stable (Scheme 100). Gold showed high affinity for the π-bonds of alkynes **234** and constructed various η^2-alkyne complexes. These complexes further reacted with different heteroatom- or carbon-based nucleophiles under mild reaction conditions.[133]

In 2021, Itami and co-workers published their most recent work on gold-catalyzed heptagon-containing molecular nanocarbons. The synthetic methodology behind their work was Scholl cyclization involving the on-surface synthesis of azulene-embedded nanocarbons **237**. The cyclodehydrogenation of PAHs **236** resulted in the formation of giant nanographenes (Scheme 101). They established a novel pathway for the construction of abnormal 5–7 defects in N-doped nanographene by the on-surface cyclodehydrogenation reaction. The reaction pathway consisted of many intermediate states but the fundamental step, where the final product combining the azulene motifs was formed, occurred on the Au(111) surface.[134]

Overall, it is concluded that $AuCl_3$ proves to be a better oxidant due to its excellent oxidizing capacity as compared to all the abovementioned oxidants. Its reduction potential value is +1.50 V.

6. Comparative summary of various reagents used in the Scholl reaction

Thus far, we have discussed in detail the implementations, merits, and demerits of various reagents used in the Scholl reaction. Herein, we will briefly compare these reagents with one another. With time and more demand for improved conditions, reagents have been modified gradually from the simplest reagent system comprising $AlCl_3$ (proposed by Scholl) to the most advanced recent oxidizing reagent systems utilizing gold and electrochemistry. Each reagent system has some benefits as well as drawbacks associated with it and the choice of the reagent system is dictated by the synthetic target. For example, copper salts are prominent due to their better yields, low cost, easy availability, and less or non-toxic properties. Iron chloride is eco-friendly, plays the dual role of oxidant and Lewis acid, and provides excellent yields. Moreover, it is non-hazardous and provides a lesser number of side products. Similarly, DDQ is readily available, cost effective, and provides high yield. It offers pure and highly selective products. Molybdenum pentachloride offers a facile and efficient route, which provides high yields of symmetrical, regioselective, and twisted isomers of nanographenes. PIFA provides excellent yield and eliminates any pre-activation of the monomers. It is useful for heteroatomic binary coupling under mild oxidation conditions, providing a less toxic and direct synthetic pathway. Palladium complexes give selective arylations of sterically congested substrates, providing high yields as well. Finally, though still the most valuable, electrochemical oxidation and gold are the utmost advanced reagent systems; they involve surface chemistry, eliminating the complex and extensive solution systems, is less hazardous, quick, and provides pure products. The higher reduction potential of various oxidants used in the Scholl reactions indicate that these are the best oxidizing agents and

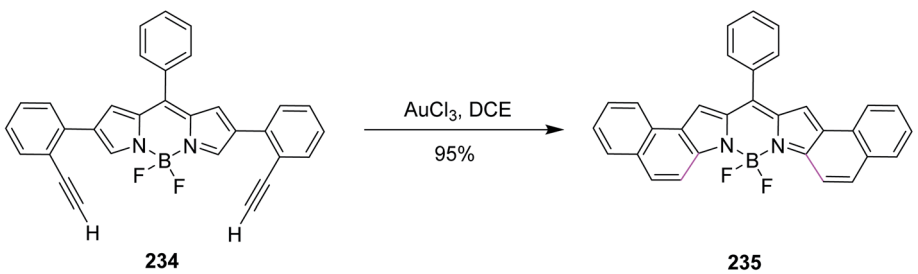

234 235

Scheme 100 Synthesis of π-extended BODIPYs.

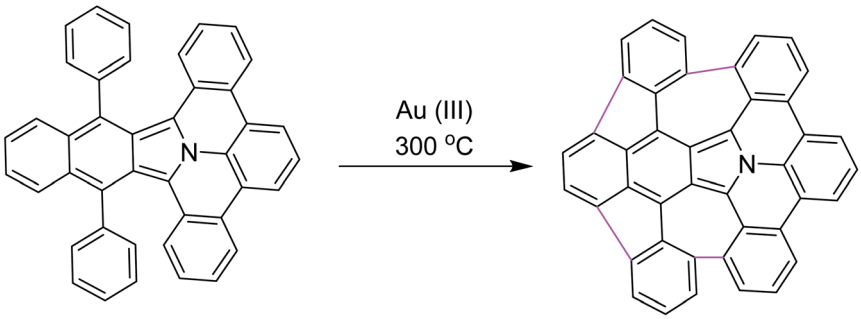

236 237

Scheme 101 Synthesis of molecular nanographenes.

thus have the potential to dehydrogenase the aromatics. For example, the reduction potential of various metals/reagents is in the following order, *i.e.*, $Pd^{2+} > Mn^{2+} > Au^{3+} > Ag^{2+} > I^{-} >$ DDQ $> Cu^{2+} > Co^{2+} > Tl^{3+} > Fe^{3+} > Al^{3+} > Mo^{2+}$ (+0.951 V > +1.54 V > +1.50 V > +0.80 V > +0.54 V > +0.50 V > +0.34 V > −0.28 V > −0.34 V > −0.409 V > −1.667 V > −1.75 V). This information reveals that the metals such as Ag, Cu, Fe, and Mn, and DDQ reagent have high affinity for hydrogen removal. They ensure complete cyclization to provide extended nanographenes. Moreover, many of the structures that are accessible by intramolecular oxidative coupling, in particular, large planar and curved PAHs, would be nearly impossible to synthesize using other methods for forming biaryl bonds because of the required pre-functionalization. Although a variety of valuable reactants are being developed for oxidative coupling, intramolecular oxidative coupling is dominated by two oxidants, namely, $FeCl_3$ and DDQ/acid (Rathore conditions). These two reagents have been used by the Müllen, Itami, Miao, and Wu groups for the preparation of the most spectacular PAH molecules to date, including nanographenes and nanobelts. Overall, it is concluded that the oxidants $AlCl_3$, $FeCl_3$, DDQ, and Au(111) have stronger oxidizing capacity as compared to the other various reagents. The electrochemical deposition method substantially simplifies the film-forming process and produces high-quality thin PAH films with a controlled thickness and doping level. Notably, these PAHs self-assemble to form discrete nanofibers with a defined molecular alignment. This discovery offers a new method to align insoluble polycyclic aromatic materials with strong π–π interactions into thin films. The latter hold promises for further incorporation into photovoltaic cells and field-effect transistors. Thus far, we have compared the merits of each reagent system, although there are certainly some shortcomings associated with them as well. These have been already discussed in our sequential development of the reagent system.

7. Conclusion and future perspectives

Over the years, tremendous knowledge has been collected regarding the dehydrogenative inter and intramolecular C–C coupling of aromatic compounds. These economically advantageous processes attract warranted attention as the ultimate method for the formation of complex biaryl units. Electron-rich and electron-neutral compounds/moieties can both react to form one or more carbon–carbon single bonds. The presentation of various aspects of oxidation leading to the formation of aryl–aryl linkages has allowed us to state the hypothesis that depending on the structure of the substrates, two mechanisms must be considered. The fact that this process can be mediated by both a strong Lewis acid at high temperature and by mild oxidants under mild conditions has caused certain confusion in recent years. Therefore, we propose to call this process dehydrogenative aromatic coupling when the mechanism is unclear. We also propose to reserve the name "Scholl reaction" only for those cases when non-oxidizing Brønsted or Lewis acids are used to perform the reaction (with or without the use of an additional oxidant). Moreover, we have explained above that the Scholl reaction can occur in many cases with substrates having low oxidation potentials but are still able to provide the final products in good yield. To conclude, we have described some advanced synthetic methods, employing the Scholl reaction in the development of planar and non-planar nanographenes. Among all the methods, cyclodehydrogenation *via* on-surface gold catalysis appears to be advanced and efficient to push multiple dehydrogenations, and thus needs to be explored further in future. Furthermore, a great deal of additional effort, particularly focusing on electrochemically-mediated oxidative aromatic coupling, experiments with Brønsted acids, and computational studies, is needed to clarify the mechanisms of these processes. We hope that this review, in addition to providing and organizing the overview of the topic, will serve as a catalyst to spark further studies.

Abbreviations

APEX	Annulative *p*-extension
BIC	Bicyclic
BODIPY	Boron dipyrromethenes
CPME	Cyclopentyl methyl ether
CV	Cyclic voltammetry
DCE	1,2-Dichloroethane
DCM	Dichloromethane
DDQ	2,3-Dichloro-5,6-dicyano-1,4-benzoquinone

DFT	Density functional theory
GNRs	Graphene nanoribbons
HBC	Hexabenzocoronene
HFIP	Hexafluoroisopropanol
HITAB	Hydroxy(tosyloxy)iodobenzene
HPB	Hexaphenylbenzene
MALDI	Matrix-assisted laser desorption ionization
MOPs	Microporous organic polymers
NCS	*N*-Chlorosuccinimide
NIR	Near infrared
OFETs	Organic field-effect transistors
PAHs	Polycyclic aromatic hydrocarbons
PIDA	Phenyliodine(III) diacetate
PIFA	(Bis(trifluoroacetoxy)iodo)benzene
PPA	Polyphosphoric acid
POF	Porous organic framework
TTFA	Thenoyltrifluoroacetone
TBTQ	Tribenzotriquinacene
TMSBr	Trimethylsilyl bromide
TFA	Trifluoroacetic acid

Conflicts of interest

There are no conflicts to declare.

Acknowledgements

The authors would like to extend their sincere appreciation to Taif University Researchers Supporting Project number (TURSP-2020/312), Taif University, Taif, Saudi Arabia. The authors are also highly grateful to the Higher Education Commission of Pakistan (HEC) for providing financial assistance under Project No. (NRPU-6484). The authors are highly thankful to Prof. Dr Dietmar Kuck, Department of Chemistry, Bielefeld University, Germany for his kind help in proof-reading and editing this review.

References

1 L. Chen, Y. Hernandez, X. Feng and K. Müllen, *Angew. Chem., Int. Ed.*, 2012, **51**, 7640–7654.
2 J. Zhao, C. He, R. Yang, Z. Shi, M. Cheng, W. Yang, G. Xie, D. Wang, D. Shi and G. Zhang, *Appl. Phys. Lett.*, 2012, **101**, 063112.
3 L. Zhi and K. Müllen, *J. Mater. Chem.*, 2008, **18**, 1472–1484.
4 X.-Y. Wang, X. Yao, A. Narita and K. Müllen, *Acc. Chem. Res.*, 2019, **52**, 2491–2505.
5 K. Müllen and J. P. Rabe, *Acc. Chem. Res.*, 2008, **41**, 511–520.
6 M. C. Drummer, V. Singh, N. Gupta, J. L. Gesiorski, R. B. Weerasooriya and K. D. Glusac, *Photosynth. Res.*, 2021, 1–22.
7 P. Blake, P. D. Brimicombe, R. R. Nair, T. J. Booth, D. Jiang, F. Schedin, L. A. Ponomarenko, S. V. Morozov, H. F. Gleeson and E. W. Hill, *Nano Lett.*, 2008, **8**, 1704–1708.
8 R. Rieger and K. Müllen, *J. Phys. Org. Chem.*, 2010, **23**, 315–325.
9 C. Lee, X. Wei, J. W. Kysar and J. Hone, *Science*, 2008, **321**, 385–388.
10 M. Quernheim, F. E. Golling, W. Zhang, M. Wagner, H. J. Räder, T. Nishiuchi and K. Müllen, *Angew. Chem., Int. Ed.*, 2015, **54**, 10341–10346.
11 M. Grzybowski, K. Skonieczny, H. Butenschoen and D. T. Gryko, *Angew. Chem., Int. Ed.*, 2013, **52**, 9900–9930.
12 R. Scholl and C. Seer, *Justus Liebigs Ann. Chem.*, 1912, **394**, 111–177.
13 E. Faggi, R. M. Sebastián, R. Pleixats, A. Vallribera, A. Shafir, A. Rodríguez-Gimeno and C. Ramirez de Arellano, *J. Am. Chem. Soc.*, 2010, **132**, 17980–17982.
14 M. L. Rahman, G. Hegde, M. M. Yusoff, M. N. F. A. Malek, H. T. Srinivasa and S. Kumar, *New J. Chem.*, 2013, **37**(8), 2460–2467.
15 T. M. Swager and B. Koo, *Synfacts*, 2014, **10**, 0581.
16 Y. Yang, L. Yuan, B. Shan, Z. Liu and Q. Miao, *Chem.–Eur. J.*, 2016, **22**, 18620–18627.
17 A. Balaban and C. Nenitzescu, *Friedel-Crafts Relat. React.*, 1964, **2**, 979–1047.
18 K. S. Novoselov, A. K. Geim, S. V. Morozov, D. Jiang, Y. Zhang, S. V. Dubonos, I. V. Grigorieva and A. A. Firsov, *Science*, 2004, **306**, 666–669.
19 A. K. Geim and K. S. Novoselov, in *Nanoscience and technology: a collection of reviews from nature journals*, World Scientific, 2010, pp. 11–19.
20 (*a*) X. Dou, X. Yang, G. J. Bodwell, M. Wagner, V. Enkelmann and K. Müllen, *Org. Lett.*, 2007, **9**, 2485–2488; (*b*) C. Shen, G. Zhang, Y. Ding, N. Yang, F. Gan, J. Crassous and H. Qiu, *Nat. Commun.*, 2021, **12**, 1–8; (*c*) Z. Qiu, S. Asako, Y. Hu, C.-W. Ju, T. Liu, L. Rondin, D. Schollmeyer, J.-S. b. Lauret, K. Müllen and A. Narita, *J. Am. Chem. Soc.*, 2020, **142**, 14814–14819; (*d*) M. Krzeszewski, K. Sahara, Y. M. Poronik, T. Kubo and D. T. Gryko, *Org. Lett.*, 2018, **20**, 1517–1520; (*e*) X. Zhang, Z. Xu, W. Si, K. Oniwa, M. Bao, Y. Yamamoto and T. Jin, *Nat. Commun.*, 2017, **8**, 1–8; (*f*) A. Pradhan, P. Dechambenoit, H. Bock and F. Durola, *J. Org. Chem.*, 2013, **78**, 2266–2274.
21 D. J. Jones, B. Purushothaman, S. Ji, A. B. Holmes and W. W. Wong, *Chem. Commun.*, 2012, **48**, 8066–8068.
22 X. Feng, W. Pisula and K. Müllen, *Pure Appl. Chem.*, 2009, **81**, 2203–2224.
23 (*a*) G. Baddeley and J. Kenner, *J. Chem. Soc.*, 1935, 303–309; (*b*) G. Baddeley, *J. Chem. Soc.*, 1950, 994–997.
24 M. Grzybowski, B. Sadowski, H. Butenschön and D. T. Gryko, *Angew. Chem., Int. Ed.*, 2020, **59**, 2998–3027.
25 B. T. King, J. Kroulík, C. R. Robertson, P. Rempala, C. L. Hilton, J. D. Korinek and L. M. Gortari, *J. Org. Chem.*, 2007, **72**, 2279–2288.
26 L. Zhai, R. Shukla, S. H. Wadumethrige and R. Rathore, *J. Org. Chem.*, 2010, **75**, 4748–4760.
27 P. Rempala, J. Kroulík and B. T. King, *J. Am. Chem. Soc.*, 2004, **126**, 15002–15003.
28 (*a*) J. Wu, W. Pisula and K. Müllen, *Chem. Rev.*, 2007, **107**, 718–747; (*b*) K. Müllen, *ACS Nano*, 2014, **8**, 6531–6541; (*c*) L. Chen, Y. Hernandez, X. Feng and K. Müllen, *Angew. Chem., Int. Ed.*, 2012, **51**, 7640–7654; (*d*) X. Yan and

L.-s. Li, *J. Mater. Chem.*, 2011, **21**, 3295–3300; (*e*) K. K. Baldridge and J. S. Siegel, *Angew. Chem., Int. Ed.*, 2013, **52**, 5436–5438; (*f*) M. Ball, Y. Zhong, Y. Wu, C. Schenck, F. Ng, M. Steigerwald, S. Xiao and C. Nuckolls, *Acc. Chem. Res.*, 2015, **48**, 267–276; (*g*) W. W. Wong, J. Subbiah, S. R. Puniredd, B. Purushothaman, W. Pisula, N. Kirby, K. Müllen, D. J. Jones and A. B. Holmes, *J. Mater. Chem.*, 2012, **22**, 21131–21137; (*h*) Y. Morita, S. Suzuki, K. Sato and T. Takui, *Nat. Chem.*, 2011, **3**, 197; (*i*) Z. Sun, Z. Zeng and J. Wu, *Chem.–Asian J.*, 2013, **8**, 2894–2904.

29 L. Zhai, R. Shukla and R. Rathore, *Org. Lett.*, 2009, **11**, 3474–3477.

30 (*a*) A. Ronlan, O. Hammerich and V. D. Parker, *J. Am. Chem. Soc.*, 1973, **95**, 7132–7138; (*b*) A. Ronlan and V. D. Parker, *J. Org. Chem.*, 1974, **39**, 1014–1016; (*c*) R. Rathore and J. K. Kochi, *J. Org. Chem.*, 1995, **60**, 7479–7490.

31 R. Scholl and J. Mansfeld, *Ber. Dtsch. Chem. Ges. A*, 1910, **43**, 1734–1746.

32 R. Scholl, C. Seer and R. Weitzenböck, *Ber. Dtsch. Chem. Ges. A*, 1910, **43**, 2202–2209.

33 F. Wiener and W. Mieg, *CA*, 1941, **35**, 1240.

34 P. Kovacic and A. Kyriakis, *Tetrahedron Lett.*, 1962, **3**, 467–469.

35 H. Vollmann, *Justus Liebigs Ann. Chem.*, 1963, **669**, 22–44.

36 R. Scholl and C. Seer, *J. Org. Chem.*, 1971, **36**, 2053.

37 A. Wick, *Helv. Chim. Acta*, 1971, **54**, 769–782.

38 M. Hovorka, J. Günterova and J. Zavada, *Tetrahedron Lett.*, 1990, **31**, 413–416.

39 M. Smrčina, M. Lorenc, V. Hanus, P. Sedmera and P. Kocovsky, *J. Org. Chem.*, 1992, **57**, 1917–1920.

40 M. Smrčina, S. Vyskocil, B. Maca, M. Polasek, T. A. Claxton, A. P. Abbott and P. Kocovsky, *J. Org. Chem.*, 1994, **59**, 2156–2163.

41 M. Müller, H. Mauermann-Düll, M. Wagner, V. Enkelmann and K. Müllen, *Angew. Chem., Int. Ed.*, 1995, **107**, 1751–1754.

42 C. D. Simpson, J. D. Brand, A. J. Berresheim, L. Przybilla, H. J. Räder and K. Müllen, *Chem.–Eur. J.*, 2002, **8**, 1424–1429.

43 Y. Avlasevich, C. Kohl and K. Müllen, *J. Mater. Chem.*, 2006, **16**, 1053–1057.

44 P. Rempala, J. Kroulík and B. T. King, *J. Org. Chem.*, 2006, **71**, 5067–5081.

45 C. Jiao and J. Wu, *Curr. Org. Chem.*, 2010, **14**, 2145–2168.

46 F. Cataldo, O. Ursini, G. Angelini and S. Iglesias-Groth, *Fullerenes, Nanotubes, Carbon Nanostruct.*, 2011, **19**, 713–725.

47 (*a*) E. U. Mughal and D. Kuck, *Chem. Commun.*, 2012, **48**, 8880–8882; (*b*) E. U. Mughal, B. Neumann, H. G. Stammler and D. Kuck, *Eur. J. Org. Chem.*, 2014, 7469–7480.

48 S. Pola, C.-H. Kuo, W.-T. Peng, M. M. Islam, I. Chao and Y.-T. Tao, *Chem. Mater.*, 2012, **24**, 2566–2571.

49 M. S. Markoulides, C. Venturini, D. Neumeyer and A. Gourdon, *New J. Chem.*, 2015, **39**, 6498–6503.

50 Y. N. Oded, S. Pogodin and I. Agranat, *J. Org. Chem.*, 2016, **81**, 11389–11393.

51 Z. He, T. Wang, Y. Xu, M. Zhou, W. Yu, B. Shi and K. Huang, *J. Phys. Chem. C*, 2018, **122**, 8933–8940.

52 I. Agranat, Y. N. Oded, T. Mala'bi, S. Pogodin and S. Cohen, *Struct. Chem.*, 2019, **30**, 1579–1610.

53 P. C. Solórzano, M. T. Baumgartner, M. Puiatti and L. B. Jimenez, *RSC Adv.*, 2020, **10**, 21974–21985.

54 J. Wang, C. Wang, H. Wang, B. Jin, P. Zhang, L. Li and S. Miao, *Microporous Mesoporous Mater.*, 2021, **310**, 110596.

55 H. Naarmann, M. Hanack and R. Mattmer, *Synthesis*, 1994, 477–478.

56 G. Cooke, V. Sage and T. Richomme, *Synth. Commun.*, 1999, **29**, 1767–1771.

57 R. C. Borner, N. Boden, R. J. Bushby, R. Borner, A. N. Cammidge, R. Bushby, A. Cammidge and M. Jesudason, *Liq. Cryst.*, 2006, **33**, 1439–1448.

58 W. Bai and J. Lin, *Synth. Commun.*, 2011, **41**, 903–906.

59 X.-L. Li, J.-H. Huang and L.-M. Yang, *Org. Lett.*, 2011, **13**, 4950–4953.

60 M. Takase, T. Narita, W. Fujita, M. S. Asano, T. Nishinaga, H. Benten, K. Yoza and K. Müllen, *J. Am. Chem. Soc.*, 2013, **135**, 8031–8040.

61 A. Narita, X. Feng, Y. Hernandez, S. A. Jensen, M. Bonn, H. Yang, I. A. Verzhbitskiy, C. Casiraghi, M. R. Hansen and A. H. Koch, *Nat. Chem.*, 2014, **6**, 126–132.

62 T. Wöhrle, J. Kirres, M. Kaller, M. Mansueto, S. Tussetschläger and S. Laschat, *J. Org. Chem.*, 2014, **79**, 10143–10152.

63 A. N. Lakshminarayana, J. Chang, J. Luo, B. Zheng, K.-W. Huang and C. Chi, *Chem. Commun.*, 2015, **51**, 3604–3607.

64 M. Quernheim, F. E. Golling, W. Zhang, M. Wagner, H. J. Räder, T. Nishiuchi and K. Müllen, *Angew. Chem., Int. Ed.*, 2015, **54**, 10341–10346.

65 Q. Ye, Z. Zhang, Z. M. Png, W. T. Neo, T. Lin, H. Zeng, H. Xu and J. Xu, *J. Org. Chem.*, 2016, **81**, 9219–9226.

66 M. Murata, A. Wakamiya and Y. Murata, *Angew. Chem., Int. Ed.*, 2017, **129**, 5164–5168.

67 S. Grätz, D. Beyer, V. Tkachova, S. Hellmann, R. Berger, X. Feng and L. Borchardt, *Chem. Commun.*, 2018, **54**, 5307–5310.

68 N. K. Saha, N. K. Mitra, K. F. Johnson and B. L. Merner, *Org. Lett.*, 2018, **20**, 6855–6858.

69 J. Urieta-Mora, M. Krug, W. Alex, J. Perles, I. Fernández, A. Molina-Ontoria, D. M. Guldi and N. Martín, *J. Am. Chem. Soc.*, 2019, **142**, 4162–4172.

70 L. Zhai, R. Shukla and R. Rathore, *Org. Lett.*, 2009, **11**, 3474–3477.

71 D. J. Jones, B. Purushothaman, S. Ji, A. B. Holmes and W. W. Wong, *Chem. Commun.*, 2012, **48**, 8066–8068.

72 K. Kawasumi, Q. Zhang, Y. Segawa, L. T. Scott and K. Itami, *Nat. Chem.*, 2013, **5**, 739–744.

73 F. Schlütter, T. Nishiuchi, V. Enkelmann and K. Müllen, *Angew. Chem., Int. Ed.*, 2014, **126**, 1564–1568.

74 K. Y. Cheung, X. Xu and Q. Miao, *J. Am. Chem. Soc.*, 2015, **137**, 3910–3914.

75 D. Reinhard, F. Rominger and M. Mastalerz, *J. Org. Chem.*, 2015, **80**, 9342–9348.

76 J. Liu, S. Osella, J. Ma, R. Berger, D. Beljonne, D. Schollmeyer, X. Feng and K. Müllen, *J. Am. Chem. Soc.*, 2016, **138**, 8364–8367.
77 H.-W. Ip, C.-F. Ng, H.-F. Chow and D. Kuck, *J. Am. Chem. Soc.*, 2016, **138**, 13778–13781.
78 W. S. Wong, C. F. Ng, D. Kuck and H. F. Chow, *Angew. Chem., Int. Ed.*, 2017, **56**, 12356–12360.
79 S. Nobusue, K. Fujita and Y. Tobe, *Org. Lett.*, 2017, **19**, 3227–3230.
80 Y. Hu, X. Y. Wang, P. X. Peng, X. C. Wang, X. Y. Cao, X. Feng, K. Müllen and A. Narita, *Angew. Chem., Int. Ed.*, 2017, **56**, 3374–3378.
81 M. Ajayakumar, Y. Fu, J. Ma, F. Hennersdorf, H. Komber, J. J. Weigand, A. Alfonsov, A. A. Popov, R. Berger and J. Liu, *J. Am. Chem. Soc.*, 2018, **140**, 6240–6244.
82 L. He, C. F. Ng, Y. Li, Z. Liu, D. Kuck and H. F. Chow, *Angew. Chem., Int. Ed.*, 2018, **57**, 13635–13639.
83 K. M. Magiera, V. Aryal and W. A. Chalifoux, *Org. Biomol. Chem.*, 2020, **18**, 2372–2386.
84 Y. Han, Z. Xue, G. Li, Y. Gu, Y. Ni, S. Dong and C. Chi, *Angew. Chem., Int. Ed.*, 2020, **132**, 9111–9116.
85 J. Ma, Y. Fu, E. Dmitrieva, F. Liu, H. Komber, F. Hennersdorf, A. A. Popov, J. J. Weigand, J. Liu and X. Feng, *Angew. Chem., Int. Ed.*, 2020, **132**, 5686–5691.
86 Y. Zou, Y. Han, S. Wu, X. Hou, C. H. E. Chow and J. Wu, *Angew. Chem., Int. Ed.*, 2021, **60**(32), 17654–17663.
87 (*a*) Z. Xia, S. H. Pun, H. Chen and Q. Miao, *Angew. Chem., Int. Ed.*, 2021, **133**, 10399–10406; (*b*) K. Y. Cheung, S. Gui, C. Deng, H. Liang, Z. Xia, Z. Liu, L. Chi and Q. Miao, *Chem*, 2019, **5**, 838–847.
88 H.-W. Ip, Y. Li, D. Kuck and H.-F. Chow, *J. Org. Chem.*, 2021, **86**, 5546–5551.
89 S. Kumar and M. Manickam, *Chem. Commun.*, 1997, 1615–1666.
90 B. Kramer and S. R. Waldvogel, *Angew. Chem., Int. Ed.*, 2004, **116**, 2501–2503.
91 A. Spurg, G. Schnakenburg and S. R. Waldvogel, *Chem.–Eur. J.*, 2009, **15**, 13313–13317.
92 K. Hackeloer, G. Schnakenburg and S. R. Waldvogel, *Org. Lett.*, 2011, **13**, 916–919.
93 S. Tadano, Y. Mukaeda and H. Ishikawa, *Angew. Chem., Int. Ed.*, 2013, **125**, 8148–8152.
94 E. M. Boyd and J. Sperry, *Org. Lett.*, 2015, **17**, 1344–1346.
95 T. Fujikawa, N. Mitoma, A. Wakamiya, A. Saeki, Y. Segawa and K. Itami, *Org. Biomol. Chem.*, 2017, **15**, 4697–4703.
96 S. B. Beil, P. Franzmann, T. Müller, M. M. Hielscher, T. Prenzel, D. Pollok, N. Beiser, D. Schollmeyer and S. R. Waldvogel, *Electrochim. Acta*, 2019, **302**, 310–315.
97 T. Takada, M. Arisawa, M. Gyoten, R. Hamada, H. Tohma and Y. Kita, *J. Org. Chem.*, 1998, **63**, 7698–7706.
98 H. Tohma, M. Iwata, T. Maegawa, Y. Kiyono, A. Maruyama and Y. Kita, *Org. Biomol. Chem.*, 2003, **1**, 1647–1649.
99 T. Dohi, K. Morimoto, A. Maruyama and Y. Kita, *Org. Lett.*, 2006, **8**, 2007–2010.
100 T. Dohi, K. Morimoto, C. Ogawa, H. Fujioka and Y. Kita, *Chem. Pharm. Bull.*, 2009, **57**, 710–713.
101 W. Guo, E. Faggi, R. M. Sebastián, A. Vallribera, R. Pleixats and A. Shafir, *J. Org. Chem.*, 2013, **78**, 8169–8175.
102 A. A. Van Loon, M. K. Holton, C. R. Downey, T. M. White, C. E. Rolph, S. R. Bruening, G. Li, K. M. Delaney, S. J. Pelkey and E. T. Pelkey, *J. Org. Chem.*, 2014, **79**, 8049–8058.
103 C. Depken, F. Krätzschmar and A. Breder, *Org. Chem. Front.*, 2016, **3**, 314–318.
104 N. J. Truax, F. Banales Mejia, D. O. Kwansare, M. M. Lafferty, M. H. Kean and E. T. Pelkey, *J. Org. Chem.*, 2016, **81**, 6808–6815.
105 Z. Jia, T. Jiu, Y. Li and Y. Li, *Mater. Chem. Front.*, 2017, **1**, 2261–2264.
106 Z. Yang, F.-C. Qiu, J. Gao, Z.-W. Li and B.-T. Guan, *Org. Lett.*, 2015, **17**, 4316–4319.
107 K. Ozaki, K. Murai, W. Matsuoka, K. Kawasumi, H. Ito and K. Itami, *Angew. Chem., Int. Ed.*, 2017, **129**, 1381–1384.
108 H. Ito, K. Ozaki and K. Itami, *Angew. Chem., Int. Ed.*, 2017, **56**, 11144–11164.
109 S. Maddala, S. Mallick and P. Venkatakrishnan, *J. Org. Chem.*, 2017, **82**, 8958–8972.
110 A. McKillop, A. G. Turrell, D. W. Young and E. C. Taylor, *J. Am. Chem. Soc.*, 1980, **102**, 6504–6512.
111 B. Mohr, V. Enkelmann and G. Wegner, *J. Org. Chem.*, 1994, **59**, 635–638.
112 J. D. Debad, J. C. Morris, V. Lynch, P. Magnus and A. J. Bard, *J. Am. Chem. Soc.*, 1996, **118**, 2374–2379.
113 R. Rathore, A. Kumar, S. V. Lindeman and J. K. Kochi, *J. Org. Chem.*, 1998, **63**, 5847–5856.
114 S. Kumar and S. K. Varshney, *Liq. Cryst.*, 1999, **26**, 1841–1843.
115 S. Kumar and S. K. Varshney, *Synthesis*, 2001, **1**, 0305–0311.
116 T. Dohi, Y. Minamitsuji, A. Maruyama, S. Hirose and Y. Kita, *Org. Lett.*, 2008, **10**, 3559–3562.
117 Z.-H. Shan, J. Liu, L.-M. Xu, Y.-F. Tang, J.-H. Chen and Z. Yang, *Org. Lett.*, 2012, **14**, 3712–3715.
118 K. Wang, Y. Hu, Z. Li, M. Wu, Z. Liu, B. Su, A. Yu, Y. Liu and Q. Wang, *Synthesis*, 2010, **10**, 1083–1090.
119 K. Morimoto, N. Yamaoka, C. Ogawa, T. Nakae, H. Fujioka, T. Dohi and Y. Kita, *Org. Lett.*, 2010, **12**, 3804–3807.
120 A. K. Budniak, M. Masny, K. Prezelj, M. Grzeszkiewicz, J. Gawraczyński, Ł. Dobrzycki, M. K. Cyrański, W. Koźmiński, Z. Mazej and K. J. Fijałkowski, *New J. Chem.*, 2017, **41**, 10742–10749.
121 S. Grätz, M. Oltermann, C. G. Vogt and L. Borchardt, *ACS Sustainable Chem. Eng.*, 2020, **8**, 7569–7573.
122 (*a*) D. A. Evrard, *Studies toward a biomimetic oxidative macrocyclization approach to the synthesis of the vancomycin family of antibiotics*, Harvard University, 1994; (*b*) R. Rathore and J. K. Kochi, *J. Org. Chem.*, 1995, **60**, 7479–7490.
123 C. Zeng, B. Wang, H. Zhang, M. Sun, L. Huang, Y. Gu, Z. Qiu, K. Müllen, C. Gu and Y. Ma, *J. Am. Chem. Soc.*, 2021, **143**, 2682–2687.
124 H. A. Wegner, *Chimia*, 2009, **63**, 44–48.

125 J. Cai, P. Ruffieux, R. Jaafar, M. Bieri, T. Braun, S. Blankenburg, M. Muoth, A. P. Seitsonen, M. Saleh and X. Feng, *Nature*, 2010, **466**, 470–473.

126 P. Ruffieux, S. Wang, B. Yang, C. Sánchez-Sánchez, J. Liu, T. Dienel, L. Talirz, P. Shinde, C. A. Pignedoli and D. Passerone, *Nature*, 2016, **531**, 489–492.

127 C. Sanchez-Sanchez, A. Nicolaï, F. Rossel, J. Cai, J. Liu, X. Feng, K. Müllen, P. Ruffieux, R. Fasel and V. Meunier, *J. Am. Chem. Soc.*, 2017, **139**, 17617–17623.

128 J. Liu, R. Berger, K. Müllen and X. Feng, *From Polyphenylenes to Nanographenes and Graphene Nanoribbons*, 2017, pp. 1–32.

129 X.-Y. Wang, T. Dienel, M. Di Giovannantonio, G. B. Barin, N. Kharche, O. Deniz, J. I. Urgel, R. Widmer, S. Stolz, L. H. De Lima, M. Muntwiler, M. Tommasini, V. Meunier, P. Ruffiuex, X. Feng, R. Fasel, K. Mullen and A. Narita, *J. Am. Chem. Soc.*, 2017, **139**, 4671–4674.

130 M. Di Giovannantonio, O. Deniz, J. I. Urgel, R. Widmer, T. Dienel, S. Stolz, C. S. Sánchez, M. Muntwiler, T. Dumslaff, R. Berger, R. Berger, A. Narita, X. Feng, K. Mullen, P. Ruffiuex and R. Fasel, *ACS Nano*, 2018, **12**, 74–81.

131 R. Zuzak, I. Pozo, M. Engelund, A. Garcia-Lekue, M. Vilas-Varela, J. M. Alonso, M. Szymonski, E. Guitián, D. Pérez, S. Godlewski and D. Peña, *Chem. Sci.*, 2019, **10**, 10143–10148.

132 K. Xu, J. I. Urgel, K. Eimre, M. Di Giovannantonio, A. Keerthi, H. Komber, S. Wang, A. Narita, R. Berger, P. Ruffieux, C. A. Pignedoli, J. Liu, K. Müllen, R. Fasel and X. Feng, *J. Am. Chem. Soc.*, 2019, **141**, 7726–7730.

133 J. Labella, G. Durán-Sampedro, M. V. Martínez-Díaz and T. Torres, *Chem. Sci.*, 2020, **11**, 10778–10785.

134 C. Chaolumen, I. A. Stepek, K. E. Yamada, H. Ito and K. Itami, *Angew. Chem., Int. Ed.*, 2021, **133**, 2–27.